VOLTAGE CONTROL OF A PHOTOVOLTAIC CONNECTED POWER GRID

BY

MOHAMMED KHALEEL AHMED

A Thesis Presented to the

DEANSHIP OF GRADUATE STUDIES

KING FAHD UNIVERSITY OF PETROLEUM & MINERALS

DHAHRAN, SAUDI ARABIA

In Partial Fulfillment of the
Requirements for the Degree of

MASTER OF SCIENCE

In

ELECTRICAL ENGINEERING

APRIL 2012

KING FAHD UNIVERSITY OF PETROLEUM AND MINERALS

DHAHRAN 31261, SAUDI ARABIA

DEANSHIP OF GRADUATE STUDIES

This thesis, written by **MOHAMMED KHALEEL AHMED** under the direction of his thesis advisor and approved by his thesis committee members, has been presented to and accepted by the Dean of Graduate Studies, in partial fulfillment of the requirements of degree of **MASTER OF SCIENCE IN ELECTRICAL ENGINEERING**

Thesis Committee

Dr. Ibrahim M. El-Amin (Advisor)
Professor, EE Dept.

Dr. Ali Ahmad Al-Shaikhi
Department Chairman

Dr. Mohammad Ali Y Abido (Member)
Professor, EE Dept.

Dr. Salam A. Zummo
Dean of Graduate Studies

Dr. Ali Al-Awwami (Member)
Assistant Professor, EE Dept.

29/5/12

Date

أَعُوْذُ بِاللهِ مِنَ الشَّيْطَانِ الرَّجِيْمِ

بِسْمِ اللهِ الرَّحْمٰنِ الرَّحِيْمِ

اِقْرَاْ بِاسْمِ رَبِّكَ الَّذِيْ خَلَقَ ۝ خَلَقَ الْاِنْسَانَ مِنْ عَلَقٍ ۝ اِقْرَاْ وَرَبُّكَ الْاَكْرَمُ ۝
الَّذِيْ عَلَّمَ بِالْقَلَمِ ۝ عَلَّمَ الْاِنْسَانَ مَا لَمْ يَعْلَمْ ۝

"1. Read! In the Name of Your Lord, who has created (all that exists), 2. has created man from a clot (a piece of thick coagulated blood). 3. Read! and Your Lord is the Most Generous, 4. who has taught (the writing) by the pen, 5. has taught man that which He knew not."

.... Al Quran 96:1-5

—This is the first revelation which was revealed on Prophet Muhammad (peace be upon him) by Allaah, in the cave of Hira in Makkah, on 10th August, 610 CE.

Dedicated To

My beloved Parents, Brother and Sisters

Acknowledgements

All the praise is for Allaah, the one and the only God, the Lord of the worlds. Peace and blessings be upon the greatest human being that ever walked this earth, the last and the final Prophet, Muhammad (peace be upon him), and upon his children, wives and companions. I start by thanking Allaah for all He has provided me and this time it's a master's degree, which I had always desired pursuing.

I would like to thank my parents, Mr. and Mrs. Mohammed Farooq Ali, from the bottom of my heart for their immense patience and the motivation they had given me. My brother Mohammed Aqueel Ahmed and sisters, too share the same acknowledgements for their support. It would not be wrong to say that they have worked more than me, in making me what I am today. I also thank my maternal uncle Mohammed Ahmed and my maternal grandmother, who have always been a great support for me and my family. I ask Allaah to reward all of them the best in this world and the hereafter, aameen.

I thank the Saudi Arabian government for giving me a chance to study in KFUPM and also providing all the facilities to pursue the same. I thank the chairman of EE Department Dr. Ali Al-Shaikhi for his guidance and support.

I, owe indelible favors of, and thank, my advisor Dr. Ibrahim Al-Amin for his guidance as a thesis advisor and as a course instructor. He has been quite patient and supportive through-out my thesis work. I also thank the other members of my thesis committee viz. Dr. Mohammad Ali Abido and Dr. Ali Al-Awami. I would always carry what I have learnt from them. I also thank all the other teachers who taught me in the university.

This acknowledgement would definitely be incomplete without mentioning two of the greatest educationists whom I came across as a child. I thank Mohammad L. A. Khan Kaleem, who motivated me from an early childhood and Mir Wajid Ali Aejaz who has always been a moral support. I also thank all the teachers who taught me in schools, junior college and engineering college.

I would like to express thanks to my senior Mir Shahed Ali, who helped me in doing the thesis and also made his work available to me. Last but not the least; I thank the Indian community brothers of KFUPM who have been extremely supportive in all the aspects of life during my stay in Saudi Arabia. I would specially like to mention the following brothers who are a great moral support.

AbdurRahman Aravind
Mohammed AbdulMalik
Mohammed AbdulAzeem
Mohammed AbdulMubeen

Finishing my thesis work would have been more difficult had I not received help from the following brothers.

Mohammed Touseef Hussain
Ghufran Ahmed
Mohammed AbdulHai
Sameer Hussain Arastu
Mohammed Akber Ali

جزاكم الله خيرا

Table of contents

Table of contents vii

List of Figures xii

List of Tables xvii

THESIS ABSTRACT (ENGLISH) xviii

ملخص الأطروحة (عربي) xix

Nomenclature xx

CHAPTER 1 1

INTRODUCTION 1

1.1 Introduction to Distributed Generation System (DG) 1

1.2 Development of a PV Connected Microgrid 2

1.3 Thesis Motivation 3

1.4 Thesis Objectives 4

1.5 Thesis Organization 5

CHAPTER 2 7

LITERATURE SURVEY 7

2.1 The PV Cell 7

2.1.1 The Physics of a PV Cell 7

2.1.2 Ideal PV Cell 7

2.1.3 Practical PV Cell 8

2.1.4 Mathematical Formulation of a PV Cell 9

2.2 The Photovoltaic Module 11

2.2.1 Types of Photovoltaic Cells 12

2.3 Making of Large PV Arrays 13

2.3.1 Voltage and Amperage Boost Up 13

2.3.2 Solar Tracker 14

2.4 Problems incurred in PV Modules 15

2.5 Problems incurred in PV Connected Power Grids 16

CHAPTER 3 21

SYSTEM MODELING 21

3.1 System Description 21

3.2 System Components 21

3.3 Development of PV Generation System 21

3.3.1 Adjusting the Model 23

3.3.2 Maximum Power Point Tracking (MPPT) 24

3.4 Power Conditioning Unit 26

3.4.1 DC-DC Converter 27

3.4.2 Theory of Operation 27

3.4.3 Battery 31

3.4.4 DC-AC Converter 31

3.4.5 Phase Locked Loop (PLL) 32

3.5 Grid Synchronization 32

3.6 Modeling a DG system involving PV generator and loads 34

3.7 Harmonic interaction between the DG inverters and the grid 36

3.7.1 Measuring the Harmonic Content 36

3.7.2 Total Harmonic Distortion 37

CHAPTER 4 38

STEADY STATE ANALYSIS 38

4.1 PV System Characteristics 38

4.1.1 I-V Characteristics of a PV Array 38

4.1.2 P-V Characteristics of a PV Array 41

4.2 The Grid System 42

4.3 Voltage Profile with PV System Disconnected 43

4.4 Voltage profile at varying PV Power Penetrations 43

4.5 Harmonic Analysis 44

4.6 Three Phase Harmonic Filter 50

4.7 Variation of Load at PCC 52

CHAPTER 5 54

VOLTAGE CONTROL 54

5.1 Voltage Control by Switching Methodology 54

5.1.1 Switching Transients 56

5.2 Solar Tracker Voltage Control Method 57

5.2.1 Necessity of a PI Controller 58

5.2.2 Solar Tracker Dynamics 62

5.3 Voltage control using DC-DC Converter 63

CHAPTER 6 65

FAULT ANALYSIS 65

6.1 Three-Phase Fault Analysis 65

6.1.1 Fault at Bus-7 65

6.1.2 Fault at Bus-6 70

6.1.3 Fault at Bus-2 75

6.2 Single Phase Faults 78

6.2.1 Fault at bus-7 79

6.2.2 Fault at Bus-6 92

6.2.3 Fault at Bus-2 105

CHAPTER 7 118

7.1 Conclusion 118

7.2 Future Work 119

APPENDIX 120

Simulink Models 120

System Parameters 124

REFERENCES 126

List of Figures

Figure 2.1 Characteristics of an ideal PV cell 8

Figure 2.2: Practical PV Cell 8

Figure 2.3: Combination of Nser series PV modules and Npar parallel PV modules connected to form a PV Array 13

Figure 2.4: Solar Tracker at different times of the day 15

Figure 3.1: The formation of a PV array from a single PV cell 22

Figure 3.2: Current Voltage Characteristics of a PV Cell 25

Figure 3.3: MPPT and the DC-DC Converter Unit System 26

Figure 3.4: Power Conditioning Unit 27

Figure 3.5: Working of a DC-DC Converter 28

Figure 3.6: Block Diagram of DC-DC Converter System 29

Figure 3.7: Inverter Grid Synchronization 33

Figure 3.8: Single Line Diagram of DG system 35

Figure 3.9: Differences between Linear and Non-Linear Loads [28] 36

Figure 4.1: I-V characteristics of KCT 200GT array at different temperatures 39

Figure 4.2: I-V characteristics of KCT 200GT array at different irradiations 40

Figure 4.3 P-V characteristics of KCT 200GT array at different temperatures 41

Figure 4.4 P-V characteristics of KCT 200GT array at different irradiations 42

Figure 4.5: Voltage waveform at bus-1 with a PV power penetration of 30 kW 45

Figure 4.6: Voltage waveform at bus-2 with a PV power penetration of 30 kW 45

Figure 4.7: Voltage waveform at bus-3 with a PV power penetration of 30 kW 46

Figure 4.8: Voltage waveform at bus-4 with a PV power penetration of 30 kW 46

Figure 4.9: Voltage waveform at bus-5 with a PV power penetration of 30 kW 47

Figure 4.10: Voltage waveform at bus-6 with a PV power penetration of 30 kW 47

Figure 4.11: Voltage waveform at bus-7 with a PV power penetration of 30 kW 48

Figure 4.12: Voltage level at PCC with different levels of loading conditions 52
Figure 5.1: Voltage control methodology using switch for the power grid 55
Figure 5.2: Voltage profile of showing the switching transients 57
Figure 5.3: Working of a Solar Tracker 59
Figure 5.4: Voltage control methodology using solar tracker for the power grid 60
Figure 5.5: Voltage Control System 60
Figure 5.6: Solar Tracker Angle Dynamics 62
Figure 5.7: Voltage control using DC-DC converter 63
Figure 6.1: Voltage at Bus-7 when a 3-phase fault occurs at Bus-7 66
Figure 6.2: Voltage at Bus-2 when a 3-phase fault occurs at Bus-7 67
Figure 6.3: Voltage at Bus-3 when a 3-phase fault occurs at Bus-7 68
Figure 6.4: Voltage at Bus-4 when a 3-phase fault occurs at Bus-7 69
Figure 6.5: Voltage at Bus-5 when a 3-phase fault occurs at Bus-7 69
Figure 6.6: Voltage at Bus-6 when a 3-phase fault occurs at Bus-7 70
Figure 6.7: Voltage at Bus-6 when a 3-phase fault occurs at Bus-6 71
Figure 6.8: Voltage at Bus-2 when a 3-phase fault occurs at Bus-6 72
Figure 6.9: Voltage at Bus-3 when a 3-phase fault occurs at Bus-6 73
Figure 6.10: Voltage at Bus-4 when a 3-phase fault occurs at Bus-6 73
Figure 6.11: Voltage at Bus-5 when a 3-phase fault occurs at Bus-6 74
Figure 6.12: Voltage at Bus-7 when a 3-phase fault occurs at Bus-6 74
Figure 6.13: Voltage at Bus-2 when a 3-phase fault occurs at Bus-2 75
Figure 6.14: Voltage at Bus-3 when a 3-phase fault occurs at Bus-2 76
Figure 6.15: Voltage at Bus-4 when a 3-phase fault occurs at Bus-2 76
Figure 6.16: Voltage at Bus-5 when a 3-phase fault occurs at Bus-2 77
Figure 6.17: Voltage at Bus-6 when a 3-phase fault occurs at Bus-2 77
Figure 6.18: Voltage at Bus-7 when a 3-phase fault occurs at Bus-2 78

Figure 6.19: Voltage at Phase-A of Bus-7 when a Single-phase fault occurs at Phase-A of Bus-7.....79
Figure 6.20: Voltage at Phase-B of Bus-7 when a Single-phase fault occurs at Phase-A of Bus-7.....80
Figure 6.21: Voltage at Phase-C of Bus-7 when a Single-phase fault occurs at Phase-A of Bus-7.....80
Figure 6.22: Voltage at Phase-A of Bus-2 when a Single-phase fault occurs at Phase-A of Bus-7.....82
Figure 6.23: Voltage at Phase-B of Bus-2 when a Single-phase fault occurs at Phase-A of Bus-7.....82
Figure 6.24: Voltage at Phase-C of Bus-2 when a Single-phase fault occurs at Phase-A of Bus-7.....83
Figure 6.25: Voltage at Phase-A of Bus-3 when a Single-phase fault occurs at Phase-A of Bus-7.....84
Figure 6.26: Voltage at Phase-B of Bus-3 when a Single-phase fault occurs at Phase-A of Bus-7.....84
Figure 6.27: Voltage at Phase-C of Bus-3 when a Single-phase fault occurs at Phase-A of Bus-7.....85
Figure 6.28: Voltage at Phase-A of Bus-4 when a Single-phase fault occurs at Phase-A of Bus-7.....86
Figure 6.29: Voltage at Phase-B of Bus-4 when a Single-phase fault occurs at Phase-A of Bus-7.....86
Figure 6.30: Voltage at Phase-C of Bus-4 when a Single-phase fault occurs at Phase-A of Bus-7.....87
Figure 6.31: Voltage at Phase-A of Bus-5 when a Single-phase fault occurs at Phase-A of Bus-7.....88
Figure 6.32: Voltage at Phase-B of Bus-5 when a Single-phase fault occurs at Phase-A of Bus-7.....88
Figure 6.33: Voltage at Phase-C of Bus-5 when a Single-phase fault occurs at Phase-A of Bus-7.....89
Figure 6.34: Voltage at Phase-A of Bus-6 when a Single-phase fault occurs at Phase-A of Bus-7.....90
Figure 6.35: Voltage at Phase-B of Bus-6 when a Single-phase fault occurs at Phase-A of Bus-7.....90
Figure 6.36: Voltage at Phase-C of Bus-6 when a Single-phase fault occurs at Phase-A of Bus-7.....91
Figure 6.37: Voltage at Phase-A of Bus-6 when a Single-phase fault occurs at Phase-A of Bus-6.....92
Figure 6.38: Voltage at Phase-B of Bus-6 when a Single-phase fault occurs at Phase-A of Bus-6.....93
Figure 6.39: Voltage at Phase-C of Bus-6 when a Single-phase fault occurs at Phase-A of Bus-6.....93
Figure 6.40: Voltage at Phase-A of Bus-2 when a Single-phase fault occurs at Phase-A of Bus-6.....95
Figure 6.41: Voltage at Phase-B of Bus-2 when a Single-phase fault occurs at Phase-A of Bus-6.....95
Figure 6.42: Voltage at Phase-C of Bus-2 when a Single-phase fault occurs at Phase-A of Bus-6.....96
Figure 6.43: Voltage at Phase-A of Bus-3 when a Single-phase fault occurs at Phase-A of Bus-6.....97
Figure 6.44: Voltage at Phase-B of Bus-3 when a Single-phase fault occurs at Phase-A of Bus-6.....97

Figure 6.45: Voltage at Phase-C of Bus-3 when a Single-phase fault occurs at Phase-A of Bus-6 98
Figure 6.46: Voltage at Phase-A of Bus-4 when a Single-phase fault occurs at Phase-A of Bus-6 99
Figure 6.47: Voltage at Phase-B of Bus-4 when a Single-phase fault occurs at Phase-A of Bus-6 99
Figure 6.48: Voltage at Phase-C of Bus-4 when a Single-phase fault occurs at Phase-A of Bus-6 100
Figure 6.49: Voltage at Phase-A of Bus-5 when a Single-phase fault occurs at Phase-A of Bus-6 101
Figure 6.50: Voltage at Phase-B of Bus-5 when a Single-phase fault occurs at Phase-A of Bus-6 101
Figure 6.51: Voltage at Phase-C of Bus-5 when a Single-phase fault occurs at Phase-A of Bus-6 102
Figure 6.52: Voltage at Phase-A of Bus-7 when a Single-phase fault occurs at Phase-A of Bus-6 103
Figure 6.53: Voltage at Phase-B of Bus-7 when a Single-phase fault occurs at Phase-A of Bus-6 103
Figure 6.54: Voltage at Phase-C of Bus-7 when a Single-phase fault occurs at Phase-A of Bus-6 104
Figure 6.55: Voltage at Phase-A of Bus-2 when a Single-phase fault occurs at Phase-A of Bus-2 105
Figure 6.56: Voltage at Phase-B of Bus-2 when a Single-phase fault occurs at Phase-A of Bus-2 106
Figure 6.57: Voltage at Phase-C of Bus-2 when a Single-phase fault occurs at Phase-A of Bus-2 106
Figure 6.58: Voltage at Phase-A of Bus-3 when a Single-phase fault occurs at Phase-A of Bus-2 108
Figure 6.59: Voltage at Phase-B of Bus-3 when a Single-phase fault occurs at Phase-A of Bus-2 108
Figure 6.60: Voltage at Phase-C of Bus-3 when a Single-phase fault occurs at Phase-A of Bus-2 109
Figure 6.61: Voltage at Phase-A of Bus-4 when a Single-phase fault occurs at Phase-A of Bus-2 110
Figure 6.62: Voltage at Phase-B of Bus-4 when a Single-phase fault occurs at Phase-A of Bus-2 110
Figure 6.63: Voltage at Phase-C of Bus-4 when a Single-phase fault occurs at Phase-A of Bus-2 111
Figure 6.64: Voltage at Phase-A of Bus-5 when a Single-phase fault occurs at Phase-A of Bus-2 112
Figure 6.65: Voltage at Phase-B of Bus-5 when a Single-phase fault occurs at Phase-A of Bus-2 112
Figure 6.66: Voltage at Phase-C of Bus-5 when a Single-phase fault occurs at Phase-A of Bus-2 113
Figure 6.67: Voltage at Phase-A of Bus-6 when a Single-phase fault occurs at Phase-A of Bus-2 114
Figure 6.68: Voltage at Phase-B of Bus-6 when a Single-phase fault occurs at Phase-A of Bus-2 114
Figure 6.69: Voltage at Phase-C of Bus-6 when a Single-phase fault occurs at Phase-A of Bus-2 115
Figure 6.70: Voltage at Phase-A of Bus-7 when a Single-phase fault occurs at Phase-A of Bus-2 116

Figure 6.71: Voltage at Phase-B of Bus-7 when a Single-phase fault occurs at Phase-A of Bus-2 116

Figure 6.72: Voltage at Phase-C of Bus-7 when a Single-phase fault occurs at Phase-A of Bus-2 117

List of Tables

Table 2.1: Parameters of KCT 200GT Solar Array at Nominal Operating Conditions [2] 12

Table 4.1: Voltage profile at different buses with PV system disconnected 43

Table 4.2: Voltage profile at different buses in pu for different levels of PV penetration 44

Table 4.3: Harmonic Content at bus 6 & 7 for a PV penetration of 90kW & 110 kW 49

Table 4.4: Harmonic Content at bus 6 & 7 for a PV penetration of 90kW & 110 kW 51

Table 5.1: Voltage profile at different buses in pu for different levels of PV penetration with switch voltage control methodology 56

Table 5.2: Voltage profile at different buses in pu for different levels of PV penetration with solar tracker voltage control methodology 61

Table 5.3: Voltage profile at different buses in pu for different levels of PV penetration with DC-DC converter based voltage control methodology 64

THESIS ABSTRACT (ENGLISH)

Name: MOHAMMED KHALEEL AHMED

Title: VOLTAGE CONTROL OF A PHOTOVOLTAIC CONNECTED POWER GRID

Degree: MASTER OF SCIENCE

Major Field: ELECTRICAL ENGINEERING

The demand and consumption in the fossil fuels have risen exponentially over the years resulting in increased pollution and creating the possibility of exhaustion of non-renewable energy resources which are in use today. This has led the world to focus on renewable sources of energy systems. The wind and photovoltaic (PV) power generation systems are the best renewable energy resources with promising prospects. With the advent of renewable energy resources an entirely new concept of distributed generation (DG) has been developed in the past few decades. However the integration of DG systems is associated with a number of technical problems like overvoltage, flicker, DC injection etc. The prominent of these problems is the over voltage problem. This work deals with the designing of three voltage control methodologies for a PV connected DG system. Firstly a detailed modeling of a PV generating system has been carried out. The developed PV system is then integrated to a 7-bus power grid system forming a microgrid. The voltage problems due to increased penetration of PV have been studied. Three voltage control methodologies have been designed to overcome the problem of overvoltage. The first method proposed is by implementing a control system involving a switching protection which can disconnect the PV system in the case of overvoltage and vice versa. The second method of controlling the voltage is by changing the inclination of PV panels. Thirdly, voltage control is achieved by controlling the duty cycle of the DC-DC converter. The effects of connecting a PV to the microgrid system on the load handling capacity and on the fault scenarios have also been studied.

MASTER OF SCIENCE DEGREE

KING FAHD UNIVERSITY OF PETROLEUM AND MINERALS

Dhahran, Saudi Arabia.

2012.

ملخص الأطروحة (عربي)

الاسم: **محمد خليل احمد**

عنوان الأطروحة: **التحكم بجهد الخلايا الضوئية المربوطة مع شبكة الكهرباء**

الدرجة: **ماجستير في العلوم الهندسية**

التخصص: **الهندسة الكهربائية**

سنة التخرج: **٢٠١٢**

إنّ الطلبَ والإستهلاكَ المتزايدين للوقود المستخرجِ يُؤدّيانِ إلى التلوثِ المتزايدِ ويَخْلقانِ إمكانيةَ نفاد مصادرِ الطاقة غير المتجدّدةَ . هذا السبب قادَ العالمَ للتَركيز على أنظمةِ مصادرِ الطاقة القابلة للتجديدِ مثل طاقة الريحَ و الطاقة الشمسية وهما أفضل مصادرِ الطاقة المتجدّدةِ الوَاعْدة. المولدات الموزعة مفهوم جديد في انظمة توليد الطاقة في العقود الأخيرة الماضية ولكن هذه المولدات الموزعة تسبب بعض المشاكل في نوعية الطاقة المغذاة من الشبكة.

هذه الدراسة تقوم على تَصميم ثلاث طرق للتحكم والسيطرة للخلايا الشمسية والمولدات الموزعة, أولاً عمل نظام مكافئ للخلايا الضوئية ومن ثم ربطه مع نظام مكون من سبعة مغذيات وهذا النظام بمثابة شبكة دقيقة وتم دراسة مشاكل الفولطية في الشبكة القياسية هذه.

الطريقة الأولى المقترحة للتحكم في الجهد الكهربي بتنفيذ نظام مراقبة ينطوي تبديل تلقائي الذي يمكن قطع النظام PV في حالة فوق فولتية والعكس بالعكس. الطريقة الثانية للتحكم في الجهد الكهربي بتغيير ميل لوحات PV.الطريقة الثالثة للتحكم في الجهد الكهربي بالتحكم بدورة العمل لمحول DC-DC. وتمت دراسة أيضا تأثيرها على نظام ميكروجيرد في التحميل والتعامل مع القدرات وعلى السيناريوهات خطأ الاتصال PV-

ماجستير في العلوم الهندسية

جامعة الملك فهد للبترول والمعادن

الظهران، المملكة العربية السعودية

٢٠١٢

Nomenclature

PV	Photovoltaic
DG	Distributed Generation
pu	Per Unit
PCC	Point of Common Coupling
MPP	Maximum Power Point
MPPT	Maximum Power Point Technique
PCU	Point of Common Coupling
PI	Proportional Integral
PR	Proportional Resonant
PID	Proportional Integral Derivative
PWM	Pulse Width Modulation
PLL	Phase Locked Loop
CCM	Continuous Conduction Mode
DCM	Discontinuous Conduction Mode
MW_p	Mega-Watt Peak

I_D	Diode current
V_t	Thermal Voltage of a given solar cell
I_0	Reverse Saturation / Leakage Current of the diode
q	Electron charge
k	Boltzmann constant
$I_{0,n}$	Nominal Saturation Current
a	Diode Ideality Constant
T	Actual Temperature of the Cell
T_n	Nominal Temperature
$I_{pv,n}$	Light-generated Current at the nominal condition
K_I	Short-circuit Current/Temperature Coefficient
ΔT	Difference between Actual and Nominal Temperature
G	Irradiation on the panel surface
G_n	Nominal Irradiation
T [K]	Temperature of the *p-n* Junction
I_p	Current Through shunt resistance R_p
R_s	Series Resistance
R_p	Parallel Resistance
I_{pv}	Current Generated by the incident light
N_s	Number of Cells in one Module
N_{ser}	Number of PV Modules Connected in Series
N_{par}	Number of PV Modules Connected in Parallel
THD	Total Harmonic Distortion

N_{ss}	Number of arrays connected in series
N_{pp}	Number of arrays connected in parallel
eV	Electron Volt

CHAPTER 1

INTRODUCTION

1.1 Introduction to Distributed Generation System (DG)

Electrical energy is the most used form of energy by human beings. Due to this, the demand in the fossil fuel has risen exponentially over the years, leading to increased consumption of fossil fuels. The increased combustion of fossil fuels in order to produce electrical energy has not only increased pollution but also resulted in the possibility of exhaustion of non-renewable energy resources which are in used today. These non-renewable sources are bound to be exhausted in the future at some time or the other. This has led the world to focus on renewable sources of energy which can be used for generating electricity. The main renewable sources which can be used for generating electrical energy are wind and photovoltaic (PV) power generation. In a deregulated system, the power generation, besides taking place at the power stations in large quantities, also takes place at the distribution level typically by renewable energy resources like wind and photovoltaic (PV) systems. This brings up an entirely new concept which was hitherto unknown until very recently. In this type of generation, a small scale generation is located at the distribution end and even at the load centers. These small scale generators are integrated with the utility to facilitate power transfer. Such a power system involving generation at the distribution level is called Distributed Generation (DG).

The usage of PV technology for power generation has increased exponentially in the past few decades. The incorporation of PV into the gird system has created new

planning and operation challenges. The challenges range from modeling, equipment selection, to implementation. Therefore there is a need of exploring this area of renewable generation. In this work, a PV connected power distribution system is studied. The impact of different levels of PV power penetrations on distribution system is studied in details.

1.2 Development of a PV Connected Microgrid

A PV generation system generates electrical energy by converting solar irradiation into electricity. In a PV generation system, electricity is produced in solar cells by the conversion of the incident solar irradiation into electrical energy. A solar cell is a photosensitive semiconductor device fabricated in thin layers. When solar electromagnetic radiations are incident on it, electricity is produced by photovoltaic effect. As only 2 W power is produced by a solar cell at a voltage of 1.5 V, these cells are connected in series in order to obtain a useful amount of output. This combination is called an elementary PV module. A PV module contains a number of solar cells connected in series. Each module is designed to produce a defined electrical power. A PV array is a combination of a number of PV modules connected in series and in parallel according to the power requirement.

As a PV generation system requires many supporting devices like converters, inverters etc., for grid connection, a number of problems came into existence in a PV connected microgrid.

This work is related to the impact of integration of PV generation system on DG system for different levels of PV power penetration. To study the impact of PV generation system, a distributed power system with loads at different buses would be

considered. A 7-bus system would be tested in which a PV generator and loads would be incorporated at different buses [1].

1.3 Thesis Motivation

Distributed generation involves renewable sources of electrical energy usually wind and photovoltaic generation. Distributed generators which are usually located near the load ends create power quality problems. The prominent of which is the voltage rise at the point of common coupling (PCC) [1]. This is usually observed at light loadings.

At the normal conditions the bus voltages are within the limits. However, as the penetration of the PV increases the voltage at PCC and at the buses near PCC, increases. This problem has to be dealt with for a satisfactory performance of a PV System.

The literature review in the topic shows that limited work has been carried out in order to control the gird voltage at PCC. This thesis proposes to study the voltage profile at the PCC between a PV and a distribution network. This is done through simulation and modeling. Three control methodologies have been proposed to deal with the problem of increase in the voltage at PCC and in the buses situated near to it.

1.4 Thesis Objectives

This work focuses on modeling of a DG involving PV generator and loads. The thesis objectives are:

1. To develop a standalone photovoltaic generator model.
2. To develop a system for maximum power point tracking (MPPT) system.
3. To develop a distributed generation model involving multiple buses and loads.
4. To integrate and synchronize the photovoltaic system with the grid.
5. To study the impact of different levels of PV penetration into the grid from the point of view of voltage at point of common coupling (PCC) and the buses located near to the PCC.
6. To develop control methodologies in order to control voltage at PCC of the grid.
7. To analyze the effectiveness of the proposed control methodologies.
8. To study the harmonic impact of PV power integration at the PCC and to design a three phase harmonic filter to overcome the problem of harmonics.
9. To study the fault analysis by applying fault on different buses of the grid system.

1.5 Thesis Organization

This thesis is organized in a total of 7 chapters. The content of each of these chapters is explained below.

Chapter 1: This chapter consists of the introduction of the thesis work, and a brief description of important systems is explained. Then the thesis motivation and objectives are stated.

Chapter 2: In this chapter, a detailed literature review is presented. Literary descriptions of PV cell, PV module and PV array are explained in details. The formation of a PV array from the elementary PV cells has also been discussed. Finally, the formation of a DG system and the problems incurred in a typical DG system has been presented.

Chapter 3: Chapter three presents detailed modeling of various system components like PV generation system, power conditioning unit, DC-DC converter unit, inverter, grid synchronizing unit etc. A comprehensive description of development of a PV connected DG system is presented. Other important concepts like harmonic etc. have also been presented.

Chapter 4: In this chapter, PV generating system characteristics have been presented and simulations have been carried out. The developed system is simulated with and without the PV generating system connected. Harmonic analysis has been carried out to find out the impact of increased PV penetrations. A three phase harmonic filter has been designed to overcome the harmonic problems. Lastly, the voltage profile at the point of common coupling (PCC) is analyzed by varying load at the PCC.

Chapter 5: This chapter has been dedicated to the voltage control methodologies. Three different voltage control methodologies have been presented in this chapter.

Chapter 6: In this chapter, fault analysis of the system has been studied. The system is simulated for different fault scenarios at different buses. The analysis has been carried out with and without PV system connected to the power grid. A comparative study of the fault current has been carried in order to determine the effect of PV system during the fault conditions.

Chapter 7: In this chapter, thesis conclusion and future works are presented.

CHAPTER 2

LITERATURE SURVEY

2.1 The PV Cell

2.1.1 The Physics of a PV Cell

A Solar cell is a photosensitive semiconductor device fabricated in thin layers. When solar electromagnetic radiations are incident on it, electricity is produced by photovoltaic effect. When the PV cell is exposed to sunlight, charge carriers are produced which create an electric current if the circuit is closed. Charges are generated when the incident energy of the photon is sufficient enough (having energy more than the band gap energy of the electron) to displace the covalent electron of the semiconductor. Due to this, an internal electric field is created. This internal electric field results in separation of oppositely charged charge carriers. The motion of these charge carriers creates a current, referred as photocurrent. A PV cell essentially exhibits non-linear characteristics, as it can be imagined as a combination of a current source in parallel with an ideal diode [1, 2].

2.1.2 Ideal PV Cell

An ideal PV cell is the one in which there is no presence of the series and the shunt resistances. An ideal PV cell can be assumed to be a constant current source. Figure 2.1 shows the characteristics of an ideal PV cell [3].

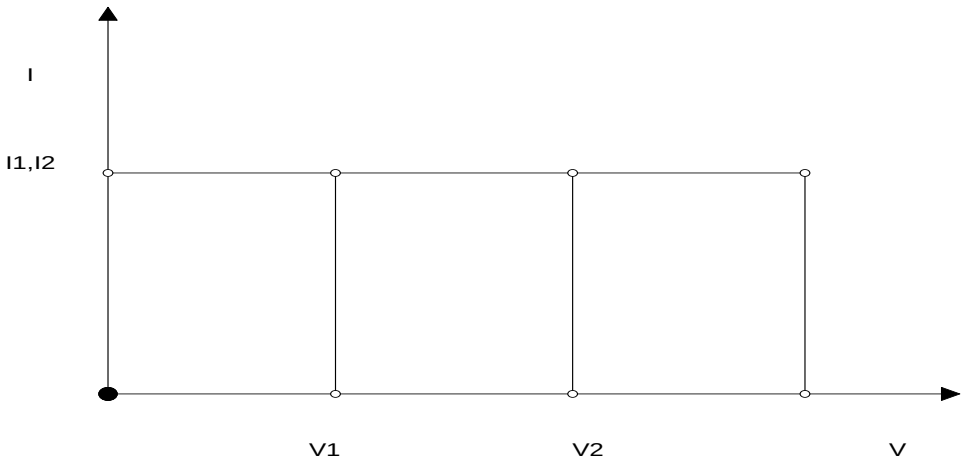

Figure 2.1 Characteristics of an ideal PV cell

2.1.3 Practical PV Cell

In reality a PV cell does have series and parallel resistances. For accurate measurements, these series and parallel resistances should be taken into consideration. The series resistance is assumed to be in series with the load. The circuit of a practical PV cell can be thought of as a current source with a series resistance R_s and a parallel resistance R_p connected to it [2]. The parameters R_s and R_p are usually assumed to be 0 and ∞ respectively. For obtaining high accuracy the exact values of R_s and R_p are found out using experimental data.

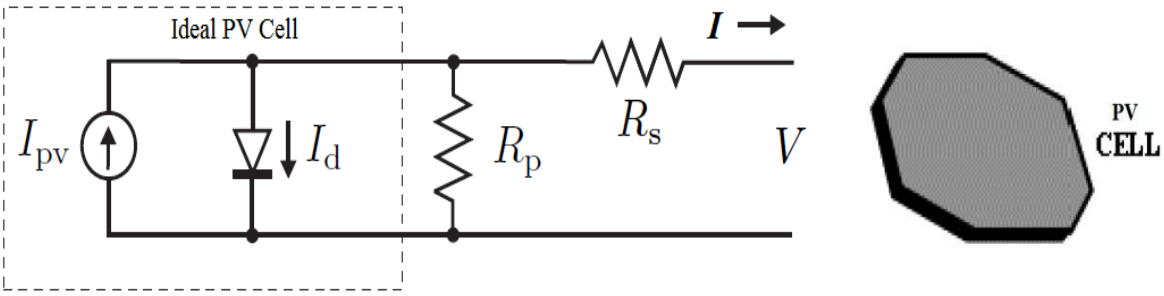

Figure 2.2: Practical PV Cell

2.1.4 Mathematical Formulation of a PV Cell

A practical PV cell behaves like a current source connected in parallel to a diode with a series and a shunt resistance connected to it. The equation of a semiconductor diode current is given by [2]:

$$I_d = I_0 \left[e^{\left(\frac{V+R_S I}{V_t a}\right)} - 1 \right] \quad (2.1)$$

Where:

- I_d is the diode current
- V_t is the thermal voltage of the cell given by $V_t = \frac{kT}{q}$
- I_0 is the reverse saturation or leakage current of the diode
- q=1.60217646× 10^{-19}C is the electron charge
- k=1.3806503× 10^{-23} J/K is the Boltzmann constant

In the above equation, the term I_0 corresponds to the reverse saturation or leakage current of a semiconductor diode. It is expressed as:

$$I_0 = I_{0,n} \left(\frac{T_n}{T}\right)^3 e^{\left[\frac{qE_g}{ak}\left(\frac{1}{T_n} - \frac{1}{T}\right)\right]} \quad (2.2)$$

Where:

- $I_{0,n}$ is the nominal saturation current
- $E_g \approx 1.12\ eV$
- a is the diode ideality constant (usually in between 1.0 and 1.5)
- T is the actual temperature
- T_n is the nominal temperature

The current generated by a PV cell, when it is irradiated by incident solar radiation, is given by:

$$I_{pv} = \left(I_{pv,n} + K_I \Delta T\right) \frac{G}{G_n} \quad (2.3)$$

Where:

- $I_{pv,n}$ is the is the light-generated current at the nominal condition (usually 25 ◦C and 1000 W/m^2)
- K_I is the short-circuit current/temperature coefficient
- $\Delta T = T - T_n$ is the difference between the actual and the nominal temperature.
- G $[W/m^2]$ is the irradiation on the device surface
- $G_n$is the nominal irradiation, which is 1000 W/m^2
- T [K] is the temperature of the *p-n* junction.

Also using KCL in the loop shown in circuit of Figure 2.2, the current through the shunt resistance R_p is given by:

$$I_p = \frac{V + R_S I}{R_p} \quad (2.4)$$

Where:

- I_p is the current through shunt resistance R_p
- R_s is the resistance of the series resistance
- R_p is the resistance of the parallel resistance

The mathematical equation of a practical PV cell can be given as: [2]:

$$I = I_{pv} - I_d - I_p \quad (2.5)$$

Where:

- I_{pv} is the current generated by the incident light given in (2.3)
- I_d is the diode current given by (2.1)
- I_p is the current through shunt resistance R_p given in (2.4)

In the above equation substituting the respective values of I_{pv}, I_d and I_p:

$$I = \left(I_{pv,n} + K_I \Delta T\right) \frac{G}{G_n} - I_0 \left[e^{\left(\frac{V+R_S I}{V_t a}\right)} - 1\right] - \frac{V+R_S I}{R_p} \quad (2.6)$$

This equation is usually written as:

$$I = I_{pv} - I_0 \left[e^{\left(\frac{V+R_S I}{V_t a}\right)} - 1\right] - \frac{V+R_S I}{R_p} \quad (2.7)$$

2.2 The Photovoltaic Module

Generally manufacturers produce solar modules which are a combination, generally series, of a number of PV cells with the addition of bypass and blocking diodes components. This combination is to bring the voltage and amperage to practical values. This combination is called an elementary PV module [3]. In this work, the PV generator model considered is KCT 200GT PV Array. The rated output of the module is 200.143 W at the rated voltage of 26.3 V and rated current of 7.61 A at the maximum power point.

One module consists of a 54 solar PV cells connected in series. Table 2.1 shows the complete characteristics of the module used [2].

Table 2.1: Parameters of KCT 200GT Solar Array at Nominal Operating Conditions [2]

Parameter	I_{mpp}	V_{mpp}	P_{mpp}	I_{sc}	V_{oc}	I_0	I_{pv}	a	R_p	R_s
Value	7.61A	26.3V	200.143W	8.21A	32.9V	$9.825 \times 10^{-8}\ A$	8.214 A	1.3	415.4 Ω	0.221 Ω

Extending the equation of a PV cell to a PV module, where there are a number of PV cells connected in series, equation (2.8) is obtained. It should be noticed that the only difference between the current equation of a PV cell and a PV module is in the term V_t which is the thermal voltage. In the case of a PV cell, the thermal voltage is given by $V_t = \frac{kT}{q}$ whereas in the case of a PV module the thermal voltage is given by $V_t = \frac{N_s kT}{q}$, where N_s is the number of cells in the module.

$$I = I_{pv} - I_0 \left[e^{\left(\frac{V+R_S I}{V_t a}\right)} - 1 \right] - \frac{V+R_S I}{R_p} \qquad (2.8)$$

2.2.1 Types of Photovoltaic Cells

A number of PV cells have been developed in recent times, from materials ranging from semiconductors to organic substances. However, the following two types of PV cells are used most. They are:

- Polycrystalline Silicon PV Cell
- Amorphous Silicon PV Cell

2.3 Making of Large PV Arrays

A number of elementary PV modules are connected in series and parallel combination to give still higher amount of currents and power. This is called a PV array. In short, a series combination of a number of PV cells makes a PV module. And a number of PV modules connected in series and parallel combination is called a PV Array [4].

2.3.1 Voltage and Amperage Boost Up

In order to obtain a required output voltage and current, a number of PV modules are connected series and in parallel. The net output current of the PV array is equal to the product of number of PV modules connected in parallel and the current rating of one PV module. The net output voltage of the PV array is equal to the product of number of PV modules connected in series and the voltage rating of one PV module. Figure 2.3 shows an array of several (N_{ser}) series and several (N_{par}) parallel identical PV modules connected in series and parallel combination to form a PV array. The output voltage as well as current are increased proportionately to $N_{ser}$and N_{par} respectively. The equivalent series and parallel resistances depend on the number of series and parallel connections of the elementary module as shown in figure [4].

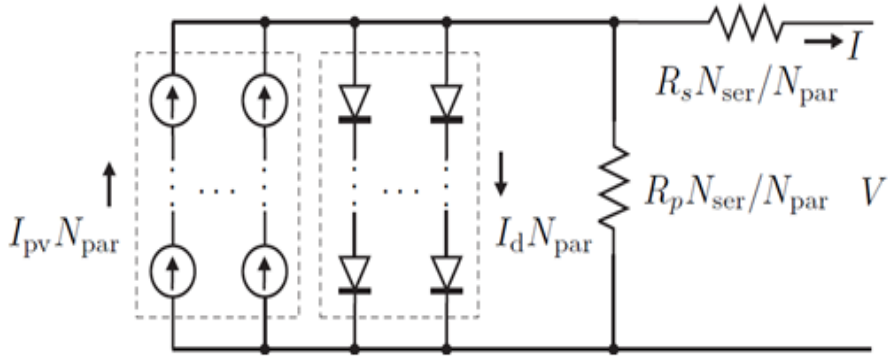

Figure 2.3: Combination of N_{ser} series PV modules and N_{par} parallel PV modules connected to form a PV Array

Notice that N_s and N_{ser} are different terms. N_s is the number of series elementary PV cells which form the elementary PV module, where as N_{ser} is the number of PV modules connected in series to form the array.

2.3.2 Solar Tracker

Due to the continuous rotation and revolution of earth around the sun, the angle of incidence of solar irradiation at a given place on earth changes continuously throughout the day. At a given place on earth, the solar irradiation is highest at the noon time as at that time, the sun is directly above on that surface. In other words the angle of elevation of the solar rays at that point of time is 90^0 with respect to the horizontal plane.

The energy trapped by solar panel is highest during the noon when the angle is 90^0. As the time passes, the elevation angle starts changing. The incident irradiation on the panels decreases resulting in the reduction of generated power.

In order to capture the maximum irradiation at all the day times, it is necessary for the array to orient itself according to the movement of the sun such that at any given instant of time the elevation angle of sun with respect to the PV panel is 90^0 [5]. To achieve this, solar trackers are used. Solar Trackers of PV panels are the devices which are used for the orientation of panels. PV panels are mounted on solar trackers. The trackers change the angle of panels continuously in order to arrange the panel such that the angle of elevation of the solar rays with respect to the panel is always at 90^0. Figure 2.4 shows the orientation of PV panel by a solar tracker at different times of the day.

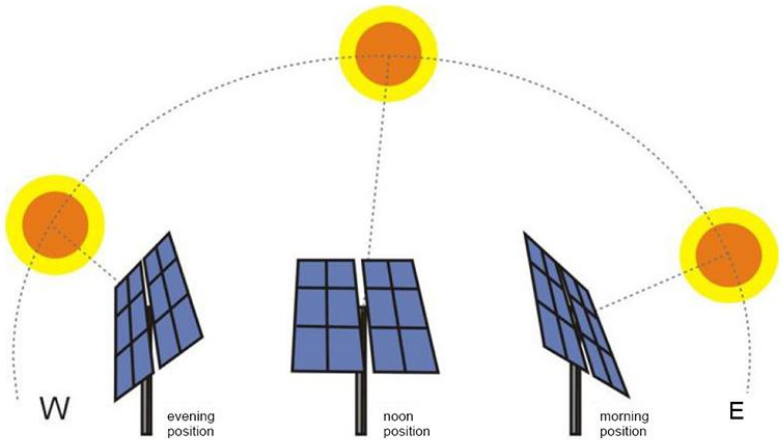

Figure 2.4: Solar Tracker at different times of the day

Using the solar trackers, the amount of energy trapped in the photovoltaic panel increases.

2.4 Problems incurred in PV Modules

In an ideal condition, all the PV cells should behave identically if they are exposed to same illumination, irrespective of the location and number of modules. Practically not all the cells behave identically. This is due to the inherent differences at the micro level created during the manufacturing processes. In some cases even when all the cells are illuminated identically, they don't produce the same amount of power. When a number of cells don't produce current, an open circuit situation is created which may result in the overheating of the module. If a PV module undergoes overheating for a long duration then the entire PV panel may have to be replaced. The electrical irregularities and the cell breakdown can be avoided by using proper circuit components. One of the common solutions applied is using of diodes.

2.5 Problems incurred in PV Connected Power Grids

When the power systems were built, there was no concept of power generation at the distribution level. There was no consideration of any incorporation of generating units besides central generating entities. As there has been an exponential increase in the penetration of PV in the utility systems, interconnection of PV to the grid is associated with many technical problems [6].

A classification of these problems was summarized in [6]. Almost all the DG systems face the problem of voltage rise and harmonic distortions. The author also discusses that the dynamic stability of a DG system increases with the increased penetration of DG. Large number of DG units decreases the magnitude of power angle deviations. Nevertheless the oscillatory stability of a system decreases with the integration of DG. Oscillatory instability is usually due to inadequate damping of electromagnetic oscillations.

The different types and benefits of PV, interconnection issues of PV clustered systems, are discussed in [7].The paper also discusses, the solution for the above mentioned problems with reference to the "IEEE Std. 929, Recommended Practice for Utility Interface of Photovoltaic Systems."

A detailed modeling of a clustered PV connected grid sytem has been carried out in [8]. On the basis of practical experience and data, the main power quality issues observed at the point of common coupling are voltage variation, current and voltage harmonics, islanding protection, increase in short circuit capacity. These problems have been observed in the DG installation sites of Gunma, Japan and Freiburg, Germany etc [8]. It was observed that as the PV penetration increases the voltage at PCC would rise.

This increase in the voltage is prominent in case of light loads. It was also observed that when the PV power penetration into the grid was low, the harmonic content in the voltage was low. When the PV penetration was increased gradually, the harmonic content also increased proportionately. The major technical issues which were observed are, increase in reactive power requirements, flicker, over current, anti-islanding, stress on distribution system. The paper also discussed the over voltage at the PCC due to reverse flow of current. The authors also suggested the corresponding solutions to the technical issues.

The power quality problems associated with PV inverters of a DG are discussed in [9]. The paper mainly dealt the harmonic Interference of Inverters with the grid. A detailed design of a DG system was carried. The network contained a number of inverters. The effect of large numbers of inverters on the quality of power was discussed in details, power quality was studied by applying different inverter topologies and different network topologies. Different control strategies were tried in each case to minimize power quality distortions. The power quality phenomenon were studied and analyzed by experimental implementation and a number of simulations. It was found that the inverter topology had a great impact on the power quality of a grid. The series and parallel resonances which occur in a grid due to the frequency interaction between the network and the grid were also modeled and analyzed.

A similar but detailed impedance based harmonic analysis is carried out in [10]. In this paper a relatively new method of modeling harmonic interactions between the grid and the DG inverter has been carried out. It was proposed that the main reason for these harmonic interactions was the impedance network's quasi-resonance which takes place between the effective inverter impedance and the grid impedance as seen from the

inverter. In this paper, a new design criteria for grid connected inverters has been suggested which can be used as an additional design criteria. The proposed models can be used to forecast power quality problems during the designing stage of a DG system containing a number of power inverters. Firstly a detailed impedance model of a single inverter connected to the grid has been carried out. The design is extended to the case of a grid containing a number of inverters. A dual loop control for inverter design using proportional, integral (PI) and proportional resonant (PR) controllers has also been proposed. It was found that using dual loop control minimized the harmonic interaction between the grid and the inverter.

A practical case study was carried out in order to study the impact of 100 kW PV generation on the DG system is carried out in [11]. The power quality parameters like voltage swell, harmonic content, flicker, voltage etc. were measured and compared with the EN50160 standard.

An urban DG system is analyzed by integrating a number of PV generators to the system in [12]. The maximum number of PV systems and so the maximum PV penetration that can installed to the system was discussed. The problems due to the increase in PV penetration on a practical clustered DG system in the city of Torino, Italy were then analyzed and discussed.

A comprehensive analysis of a clustered DG system was done by S. Favuzza and others in [13]. The paper proposed the impact of different types of PV plants on an urban power grid based on the results of many experimental analyses. Different power quality parameters like voltage variations, current distortion, flicker, power factor etc. were

measured. The measured parameters were compared with the standards specified by IEEE.

The integration of PV with the utility also has the effects on the protective device coordination. The protection of a power system forms an extremely important aspect of power industry. The behavior of protective devices in the presence of DG systems is discussed in detail in [14]. The protective system is designed assuming a radial system; but in a DG system some part of the system no longer remains radial. The impact of distributed generation on the protective device coordination like fuse to fuse, fuse-closure, relay to relay, relay to circuit breaker were discussed in detail. The analysis also shows the available margins in the protective device coordination which can be utilized.

In [15], the author discusses the losses in the power output of a PV system due to over voltage of the distributed line. A detailed performance analysis of a grid connected clustered PV generation system is carried out. This paper discusses in detail the factors responsible for the overvoltage viz. light loads, increased PV penetration. In the paper, the influence of variation in load and increased penetration of PV system are studied. It was found that the decreased in the load during a weekend resulted in the voltage raise of 2 V near the PCC.

The power loss in a PV connected microgrid due to the voltage rise at PCC was discussed in detail in [16]. The analysis was carried out on a clustered PV system consisting of 553 residential PV systems with a PV capacity of 2.1 MW each. Only a small number of PVs were found to undergo powerless. Other system outputs such as harmonics etc. also contributed to the power loss. In this analysis a voltage control

strategy was proposed. The power conditioning unit (PCU) was used to regulate the power. This method is not efficient as it involved a high power loss in switching.

It is observed that the problems associated with the clustered DG systems have been discussed in detail in many papers. The main problems associated with the PV connected DGs is that of the voltage rise at the PCC, current and voltage harmonics. Out of the above mentioned technical issues associated with DG integration with the grid, the most important issue to be dealt with is the overvoltage issue since it has a major impact on the system performance.

Most of the work done in this area only discusses about the voltage rise issue and the methods to control the voltage but very little work has actually been analyzed in order to overcome the major problem of voltage rise. There is a shortage of modeling in order to control the DG voltage at the PCC. This thesis addresses this issue and proposes simulation model to study the system performance. Three voltage control methodologies have been proposed in order to control the voltages at the PCC.

CHAPTER 3

SYSTEM MODELING

3.1 System Description

This chapter deals with the modeling of the system. The system consists of the six major subsystems. They are The PV Generator System, DC-DC Converter, Battery, DC-AC Converter, Inverter Grid Synchronization unit, and the microgrid system. Additional subsystems of voltage control switch and solar tracker PI controller are implemented for voltage control. In this chapter the description and working of each sub-system are presented. The modeling of voltage control systems will be presented in the subsequent chapter.

3.2 System Components

The PV connected grid system can be divided into a number of subsystems. The subsystems are the PV generation system, DC-link, battery, inverter, phase lock loop (PLL), inverter grid synchronization unit, distribution system. In the following section the modeling of subsystems are explained in detail.

3.3 Development of PV Generation System

In the modeling of a PV system, the following assumptions are made regarding a PV module.

1. Series connection of solar cells multiplies the voltage capacity of a PV module.
2. It is assumed that every cell's behavior is identical under a given set of environmental parameters.
3. The bypass and the isolation diodes are assumed to be identical.

A PV module is a combination of a number of elementary PV cells connected in series, usually rated between 50 W to 500 W. In the practical applications where PV generation systems are involved, the generation requirement is much higher than this range, and in most of the cases it is in kilowatts. On the other hand the voltage and current handling capacities of a PV module is much smaller than that required in practical applications. Therefore in order obtain a proper set of voltage, current and power ratings, a number of PV modules are connected in series and in parallel to obtain the required power, voltage and amperage. A number of elementary PV modules are connected in series and parallel combination to give still higher amount of currents and power. When a number of PV modules are connected in series and/or in parallel, a PV array is formed. The output voltage as well as current are increased proportionately by N_{ser} and N_{par} times respectively. The equivalent series and parallel resistances depend on the number of series and parallel connections of the elementary module.

Figure 3.1 shows the formation of a PV array from elementary PV modules. It can be seen that the PV array is a combination of 3 parallel strings of 4 PV modules connected in series.

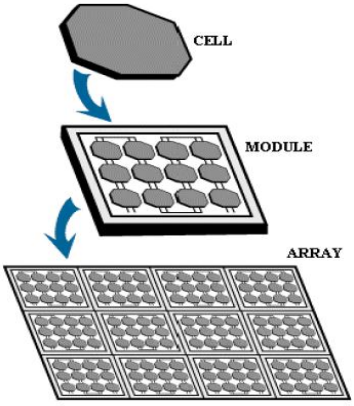

Figure 3.1: The formation of a PV array from a single PV cell

For any given array formed by $N_{ser} \times N_{par}$ identical modules the following equivalent I-V equation is valid:

$$I = I_{pv}N_{par} - I_0 N_{par}\left[e^{\left(\frac{V+R_S\left(\frac{N_{ser}}{N_{par}}\right)I}{V_t a N_{ser}}\right)} - 1\right] - \frac{V+R_S\left(\frac{N_{ser}}{N_{par}}\right)I}{R_p\left(\frac{N_{ser}}{N_{par}}\right)} \quad (3.1)$$

Where:

- N_{ser} is the number of PV modules connected in series
- N_{par} is the number of PV modules connected in parallel

For a PV array having elementary PV modules only in series, $N_{par} = 1$. For a PV array having elementary PV modules only in parallel $N_{ser} = 1$. In case of a single PV module $N_{ser} = N_{par} = 1$ [2, 4].

3.3.1 Adjusting the Model

Usually R_p and R_s are assumed to be ∞ and 0 respectively. To maintain accuracy the exact values of R_p and R_s are found out using the experimental data using the condition:

$$P_{max,m} = P_{max,e} \quad (3.2)$$

There is only one pair $\{R_p, R_s\}$ which satisfies equation (3.2)

Therefore substituting the values, the following relation is obtained:

$$V_{mp}I_{mp} = P_{max,e} \quad (3.3)$$

Substituting the value of current from (2.7):

$$V_{mp}\left\{I_{pv} - I_0\left[e^{\left(\frac{V_{mp}+R_S I_{mp}}{V_t a}\right)} - 1\right] - \frac{V_{mp}+R_S I_{mp}}{R_p}\right\} = P_{max,e} \quad (3.4)$$

$$R_p = \frac{V_{mp}\left(V_{mp}+I_{mp}R_s\right)}{\left\{V_{mp}I_{pv} - V_{mp}I_0 e^{\left(\frac{V_{mp}+R_S I_{mp}}{V_t a}\right)} + V_{mp}I_0 - P_{max,e}\right\}} \quad (3.5)$$

Above equation states that, for every value of R_s there is a corresponding value of R_p that makes the mathematical I-V curve cross the experimental peak power at (V_{mp}, I_{mp}) point.

Increasing the iteration starting from $R_s = 0$ until the mathematical curve coincides with the experimental one, the corresponding values of an $\{R_p, R_s\}$ pair which give the maximum power are obtained, such that:

$$P_{max,m} = P_{max,e} = V_{mp}I_{mp} \quad (3.6)$$

The values obtained are $R_s = 0.2273$ and $R_p = 540.551$

The subsystem block of PV generation system has been shown in the appendix section. The function of each block of the system is also explained.

3.3.2 Maximum Power Point Tracking (MPPT)

Power Output from a PV is dependent on incident radiation, cell temperature, array open circuit voltage and load connected to it. However the major factor is incident radiation. The cell temperature has small/negligible effect on the power output. The major impact is because of incident radiation. As the incident radiation keeps on changing throughout a day, the operating points also changes. A typical V-I characteristics of a PV cell is as

shown in the Figure 3.2. When a load R is connected to the PV, the corresponding slope $1/R$ is drawn. It can be seen that for a given radiation there is only one value of load (R) that will produce maximum power. Therefore for a given radiation there is only one value of load (R_{opt}) that will produce maximum power. But if irradiation changes then that maximum power point will also change. As the irradiance keeps on changing and is not constant, so there is always a need of a tracking mechanism in PV generators that needs to match the operating point to the maximum power point [1].

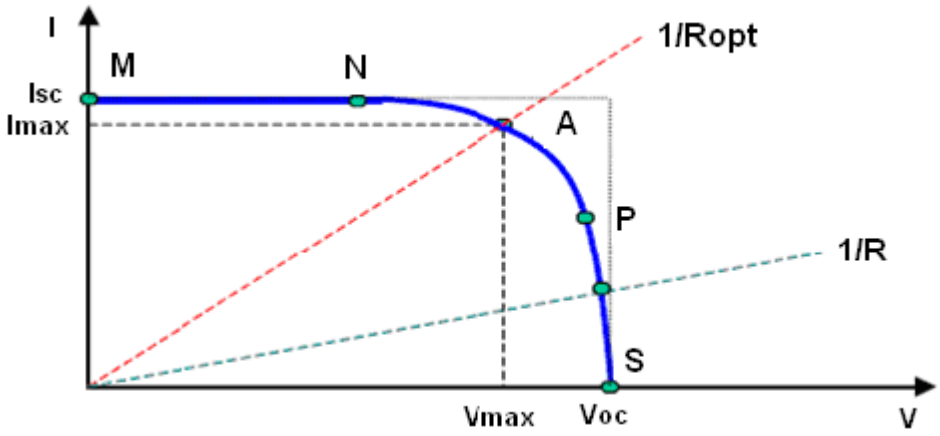

Figure 3.2: Current Voltage Characteristics of a PV Cell

A number of MPPT techniques have been developed and implemented. Mostly used MPPT techniques are constant voltage MPPT, Perturb and Observe MPPT and Incremental Conductance MPPT. It was shown that from the practical application point of view, Perturb and Observe MPPT is most appropriate for usage [17].

In constant voltage MPPT system, it is assumed that the MPPT point occurs at .75 and hence only current needs to be tracked as the voltage is kept constant [18].

In this work a controller based MPPT technique has been used. Figure 3.3 shows the configuration of the MPPT technique used in this work.

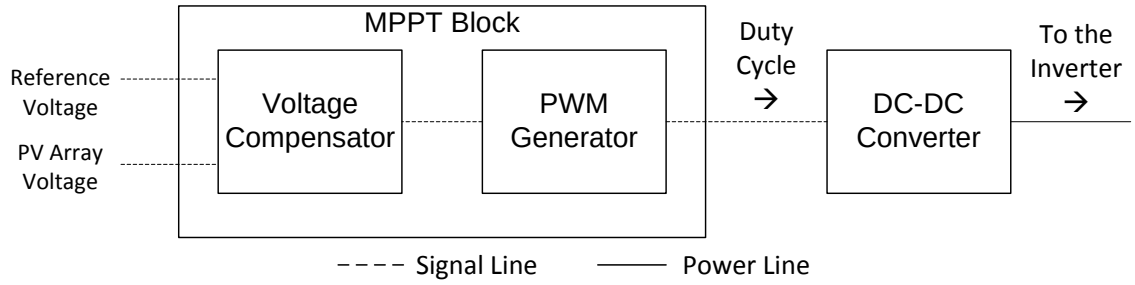

Figure 3.3: MPPT and the DC-DC Converter Unit System

The voltage compensator consists of a PI controller designed to control the DC-DC converter such that the PV array works at the maximum power point. The controller equation used in the compensator is:

$$C(s) = 1 + \frac{500}{s} \qquad (3.7)$$

3.4 Power Conditioning Unit

A PV Generating System which produces DC electricity cannot be directly connected to a grid or to a load; the power has to be processed through a system which can generate a uniform and a smooth AC power from the generated varying DC power. This functionality is fulfilled by a power conditioning unit. A power conditioning unit usually consists of a number of components. A typical connection of a PV generation system with the grid consists of the following components in the power conditioning unit. A detailed description of each of the component would be presented here. The power conditioning unit usually consists of the methodology for MPPT. The power conditioning unit also consists of the DC-DC converter which usually consists of a controlled diode

and an inductor in series [17, 19]. Figure 3.4 shows the block diagram of the DC power conditioning unit.

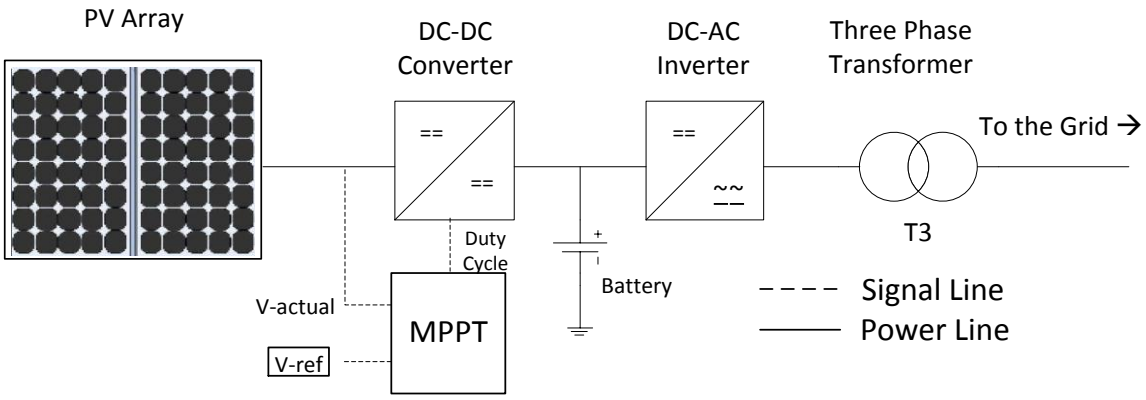

Figure 3.4: Power Conditioning Unit

3.4.1 DC-DC Converter

A DC-DC converter is used to step up or step down the DC voltage developed in the PV. It acts as an interface between the PV array and the load or the grid. It maintains the required DC voltage level by controlling the duty cycle. There are two basic topologies of a DC-DC converter viz. buck converter and boost converter. Other configurations also exist but they are also derived from these two topologies.

3.4.2 Theory of Operation

A DC-DC converter operates in two modes viz. continuous conduction mode (CCM) and discontinuous conduction mode (DCM). During the commutation if the current through the inductor does not fall to zero then the converter is said to operate in CCM. If the current falls to zero in during a cycle then, the converter is said to operate in DCM. In this work CCM of the DC-DC converter is considered.

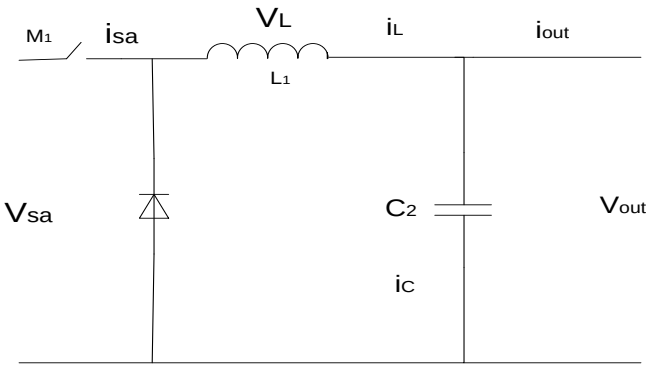

Figure 3.5: Working of a DC-DC Converter

It is assumed that the output voltage V_{sa} of the converter is ripple free although practically there is a small presence of ripples [20]. The output capacitor has enough ratings to assume that the output ripple under 3 %. The buck converter is operated in continuous conduction mode. The electrical circuit of a buck converter is shown in Figure 3.5.

The operation of the converter is divided into two modes, when the switch M_1 is closed and when switch M_1 is opened. If the switch M_1 is closed inductor supplies the output power whereas the diode is reversed biased. At this stage the inductor current increases at the rate given by (3.8).

$$\frac{di_L}{dt} = \frac{v_L}{L_1} = \frac{v_{sa} - v_{out}}{L_1}, 0 \leq t \leq \delta T \qquad (3.8)$$

If the switch M_1 is opened the output current continues to operate through diode and the diode is forward biased. In this mode the inductor current is decreased at the rate given by (3.9).

$$\frac{di_L}{dt} = \frac{v_L}{L_1} = \frac{-v_{out}}{L_1}, \delta T \leq t \leq T \qquad (3.9)$$

The circuit parameters are such that the inductor continues to conduct until the switch is closed for the next operation cycle. The average value V_{out} is given by (3.10).

$$v_{out} = \frac{1}{T}\int_0^T v_{out}(t) = \frac{1}{T}\int_0^{\delta T} v_{sa}(t) = v_{sa}\delta \qquad (3.10)$$

This gives:

$$v_{out} = v_{sa}\delta \qquad (3.11)$$

In (3.11) the term $'\delta'$ is the duty cycle of the converter. Its value remains between 0 and 1 for a buck converter.

When an MPPT algorithm is combined with DC-DC converter then the DC-DC converter also operates the DC link at MPP. Figure 3.6 shows the block diagram of DC-DC converter utilized for operating the system at MPP.

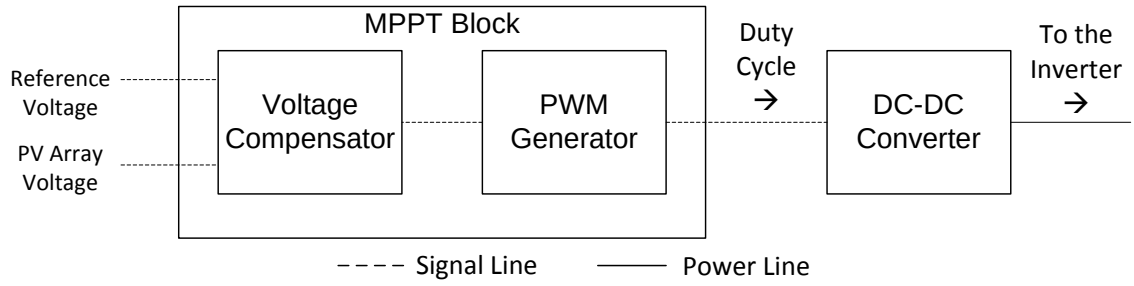

Figure 3.6: Block Diagram of DC-DC Converter System

The reference voltage and the PV array voltage are compared in the voltage compensator, using a PI controller, and the processed signal is fed to the pulse width modulator (PWM) which gives the control signals to the DC-DC converter switch. The duty cycle of the PWM generator is changed according to the need and the PWM generator controls the firing angle of the DC-DC converter. The voltage compensator consists of a PI controller in order to generate appropriate control signals for PWM

generator. The general control equations for the integral and proportional controllers are respectively:

$$I = K_I . \int_0^t E(t)dt \quad (3.12)$$

$$\mathrm{P} = K_p . E(t) \quad (3.13)$$

Where:

- P represents the proportional output
- I represents the integral output
- K_I represents the integral constant
- K_p represents the proportional constant
- $E(t)$ represents the error signal

There are a number of methods have been listed in the literature for tuning the parameters K_p and K_I . The most common of these methods are:

- Ziegler–Nichols
- Cohen-Coon
- Manual Tuning
- Software Based Methods

The control equation of the DC voltage compensator of the DC converter used for this work, in frequency domain, is given by (3.14). Manual tuning has been used to configure the parameters K_p and K_I.

$$C(s) = 1 + \frac{500}{s} \quad (3.14)$$

The rated of output power of one PV module is 200.143 W at a rated voltage of 26.3 V. The block diagram of the DC link is shown in the appendix section.

3.4.3 Battery

A DC link can either be a capacitor or a battery. It is required for many reasons like providing support by providing some extra capacity to the system when the system is weak. Amongst the common battery technologies, Lithium-Ion (Li-ion) batteries are mostly used to work as a battery. There has been a lot of research going on the Li-Ion technology and it is widely adopted in most of the batteries used for portable devices like cell phones etc. [20].

3.4.4 DC-AC Converter

A DC-AC Inverter is an essential part of a DG system. Its main purpose is to convert the DC current to AC current. It bonds the DC part of the system to the AC part of the system which is the grid system. It usually utilizes of IGBT / MOSFET transistors for their on and off operations. Its primary function is to convert the DC signal into AC. Usually the produced AC current is either single phase or three phase. The firing signals to the inverter are usually produced by a Pulse Width Modulation (PWM) generator. The AC voltage produced by DC-AC converter can be set constant to a particular phase angle or can be controlled by changing the firing angle of the PWM generator.

When controlled PWM signals are generated, it can be current controlled or voltage controlled. When the PV system is connected to the grid through an inverter, the grid controls the magnitudes of amplitude and frequency of the inverter output voltage and the inverter is said to be operating in current control mode. In standalone modes, as there is only one source of power, the inverter is controlled by voltage and is said to operate in voltage control mode [17, 19].

The firing angles of an inverter are generally produced by a PWM generator. The inverter system used here is a 3-phase 3-arm inverter of IGBT switches. It converts the DC signal to a 3 phase AC signal. The gating signals to the inverter are fed from a PWM modulator. The reference signal to the PWM modulator is given by a PLL circuit. The carrier frequency of the inverter used in this system is 2000 Hz. The synchronization of the inverter with the grid will be explained in detail in the coming sections.

3.4.5 Phase Locked Loop (PLL)

A phase lock loop is used in order to detect the frequency and phase of the grid voltage. The measured values of frequency and phase are then fed to the PWM gate controller. The PWM gate controller generates the required pulse for the inverter such that it remains in phase with the grid. The frequency measured by the PLL can also be used for frequency control [17, 21].

3.5 Grid Synchronization

To obtain a uniform power supply from the PV generator system, the PV inverter should work in congruency with the grid i.e., the inverter should produce amplitude and phase values of the voltage identical to that of the grid. Controlling the inverter such that it always produces voltage identical to the grid voltage is called Synchronization. The inverter synchronization with the grid system is carried out by the controlled gate signals which are fed to the inverter. These signals are generated by a controller which is fed voltage phase angle of the grid using a phase lock loop (PLL) to generate and control the gate signals to obtain stable and synchronized inverter output [19, 22]. To synchronize an inverter with the grid, the phase and the frequency values of the grid voltage should be

detected. This is achieved by the PLL unit. The inverter is now synchronized by controlling it to work at the same phase and frequency.

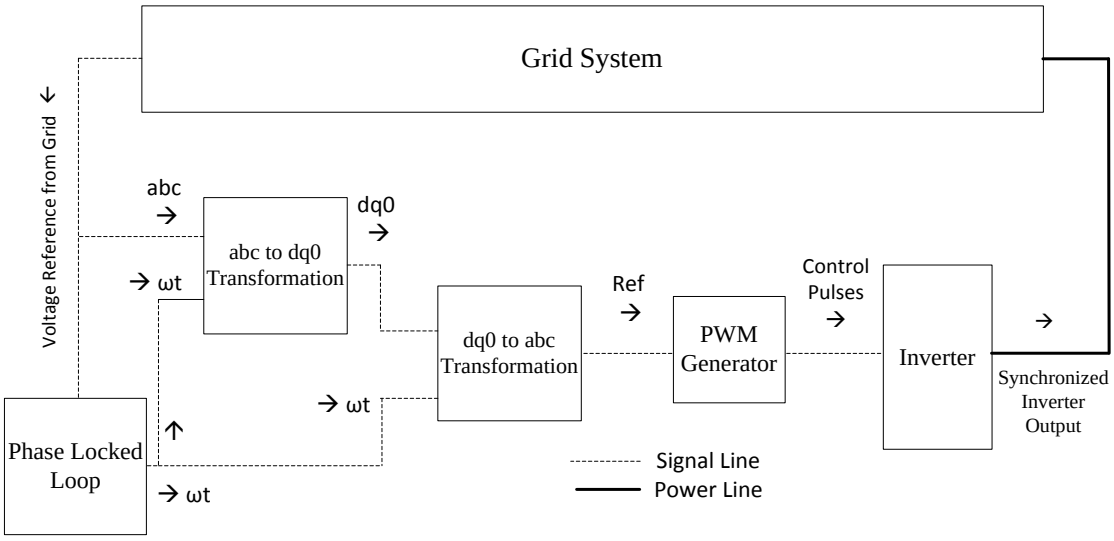

Figure 3.7: Inverter Grid Synchronization

As shown in the Figure 3.7 the synchronization of the inverter involves different components functionalities to accomplish. The voltage reference signal from the gird is fed into the PLL system which detects the phase of the grid voltage. From the grid reference voltage, the 'abc to dq0' transformation block gets the vector 'abc.' The phase angle of the grid voltage is then given to 'abc to dq0' transformation block. Now the 'dq0' signal and the phase signal are fed into a 'dq0 to abc' transformation which gives the reference three phase signal 'abc' to the PWM generator. The PWM generator generates the controlled reference pulses for the inverter gates such that the inverter remains in synchronism with the grid. The simulink block diagram of the inverter grid synchronization unit is shown in the appendix section.

3.6 Modeling a DG system involving PV generator and loads

After developing a standalone PV generator, a distributed generator system involving PV generator and loads at different buses will be developed. A 7-bus system will be tested in which PV generator will be incorporated near the load end [1]. The buses would also include loads.

To analyze the effect of PV penetration on a power grid, a DG system is implemented. It's a distribution system wherein PV power generation takes place on the roof tops of the houses. The generated PV power is then fed to the grid through transformer. The grid produces power at a voltage of 69 kV. This voltage is stepped down to 11.4 kV and transferred to the loads. This voltage is further stepped down to incorporate the domestic low voltage load where PV generation also takes place. The generated PV is fed to the grid system. The ratings of the general components of the grid system have been tabulated in the appendix section. Figure 3.8 shows the single line diagram of the system.

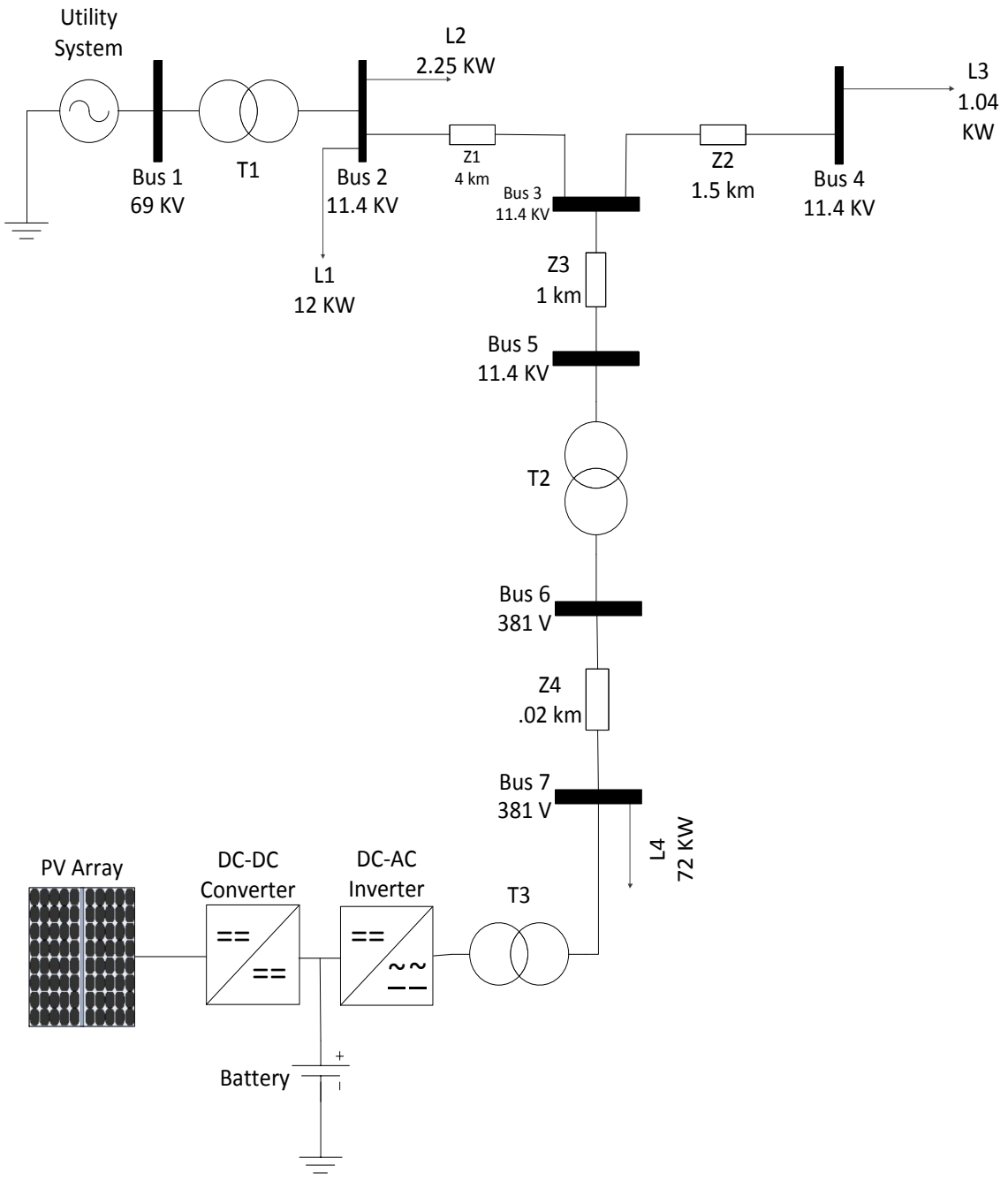

Figure 3.8: Single Line Diagram of DG system

3.7 Harmonic interaction between the DG inverters and the grid

A power system is made to work at a frequency of 50Hz or 60 Hz. Due to the presence of non-linear loads the power system frequency is polluted. This is because these loads draw currents and/or voltages with frequencies which are multiples of the actual frequency. These types of higher unwanted frequencies are called Power System Harmonics [23-25]. Harmonics are very prominent in the case of distributed generation. They create distortions in the grid current due to the presence of PV converters, which are nonlinear devices.

In the case of distributed generation where there are large number of PV converters installed, there are high problems of harmonics, voltage distortions and network resonances [9, 26].

Power System Harmonics is one of the major problems faced in the case of distributed generation (DG) of power. The harmonic interactions may worsen in the case of large number of inverters deeply penetrated in the distribution system [27].

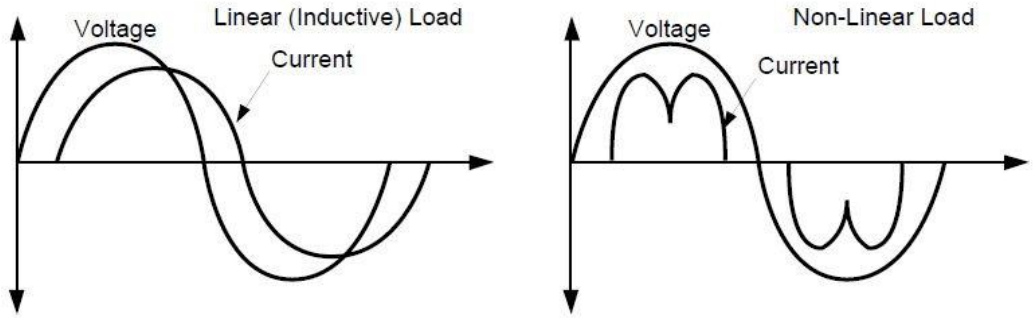

Figure 3.9: Differences between Linear and Non-Linear Loads [28]

3.7.1 Measuring the Harmonic Content

Fourier analysis shows that any non-sinusoidal waveform can be expressed in a series as a combination of DC component and, sine and cosine components, with a fundamental

frequency and multiples of fundamental frequency, called harmonics. As the output of an inverter has the positive and the negative half cycles symmetrical with respect to Y axis and as there is no DC component, the cosine terms and the constant a_0 become zero, the inverter wave form can be expressed by (3.15) (3.15)where the coefficients represent the order of harmonics.

$$V = V_{1m}Sin\ \omega t + V_{3m}Sin\ 3\omega t + V_{5m}Sin\ 5\omega t + \dots\dots\dots + V_{nm}Sin\ n\omega t \quad (3.15)$$

3.7.2 Total Harmonic Distortion

To measure the extent of harmonic components present in a signal, a measure called Total Harmonic Distortion (THD) is used. It gives the total value of harmonic content as a fraction of the fundamental harmonic. It is given by:

$$THD = \frac{\sqrt{V_{RMS}^2 - V_{1RMS}^2}}{V_{1RMS}} \quad (3.16)$$

Where:

- V_{RMS} is the RMS value of the total of all the orders
- V_{1RMS} is the RMS value of the fundamental order

V_{RMS} in (3.16) is given by:

$$V_{RMS} = \sqrt{V_1^2 + V_2^2 + \cdots\dots\dots\dots\dots + V_n^2} \quad (3.17)$$

CHAPTER 4

STEADY STATE ANALYSIS

4.1 PV System Characteristics

The incident radiation keeps on changing throughout a day, therefore the operating points also changes. A typical V-I characteristics of a PV cell is as show in Figure 3.2. In this thesis, KCT 200GT module has been used for the simulation purposes. The rated output power of one module is 200.143 W. An array of 8 modules has been simulated giving a total output of 1601.144 W of power. Figure 4.1 shows the PV generating system developed for the analysis.

4.1.1 I-V Characteristics of a PV Array

The I-V and P-V characteristics of KCT 200GT module has been simulated in this thesis to show its characteristics. The rated output power of a KCT 200GT array is 200.143 W.

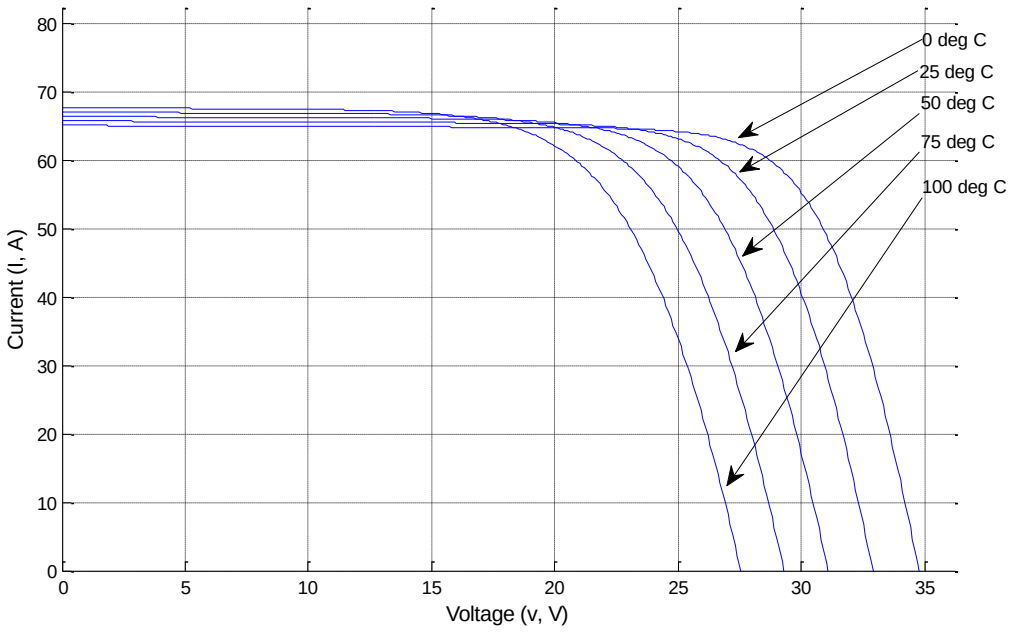

Figure 4.1: I-V characteristics of KCT 200GT array at different temperatures

Figure 4.1 shows the I-V characteristics of KCT 200GT array at different temperatures. The temperature has been varied from 0^0C to 100^0C in the steps of 25^0C. As shown in the figure, it is observed when the temperature is high, the value of current is also high but at the same time; it drops early i.e. at a lower voltage.

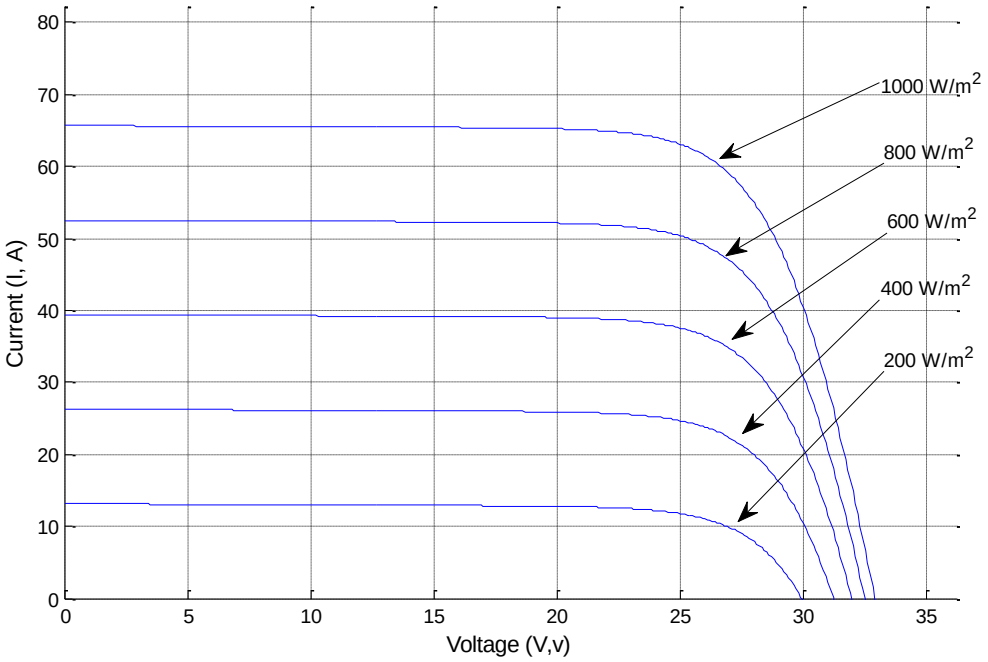

Figure 4.2: I-V characteristics of KCT 200GT array at different irradiations

Figure 4.2 shows the I-V characteristics of KCT 200GT array at different solar irradiations. The irradiation has been varied from 200 $^{W}/_{m^2}$ to 1000 $^{W}/_{m^2}$. As shown in the figure, it is observed that as the irradiation increases, the value of current also increases. An irradiation of 1000 $^{W}/_{m^2}$ is usually assumed in most of the cases.

4.1.2 P-V Characteristics of a PV Array

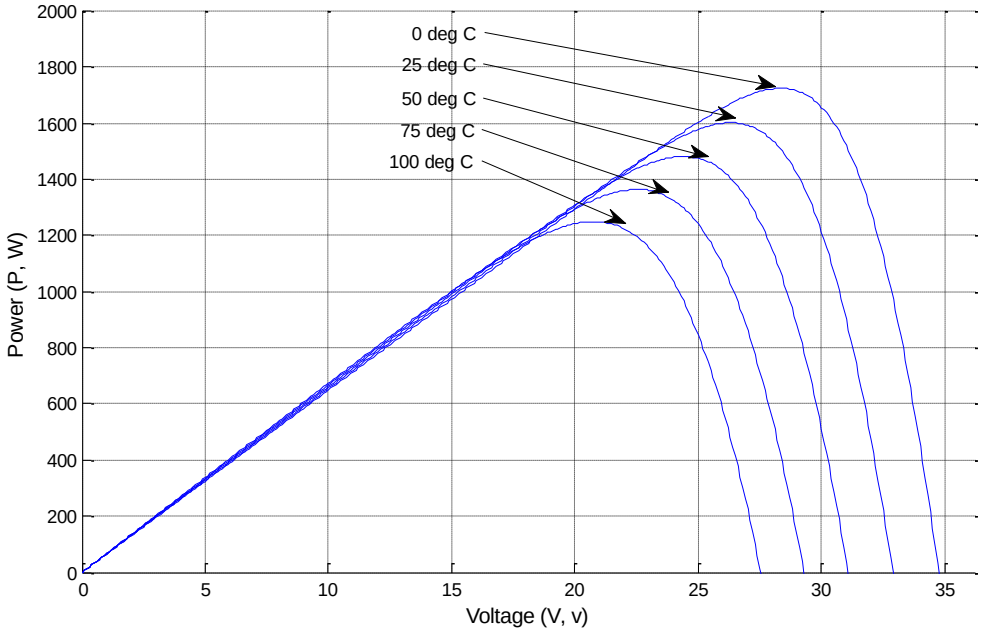

Figure 4.3 P-V characteristics of KCT 200GT array at different temperatures

Figure 4.3 shows the P-V characteristics of KCT 200GT array at different temperatures. The temperature has been varied from 0^0C to 100^0C in the steps of 25^0C. It can be seen that the output power increases as the temperature decreases. As an array of 8 modules, with 200.143 W rating of each module, has been simulated, it can be seen that at nominal temperature of $25^0\ C$ the power reaches 1600 W.

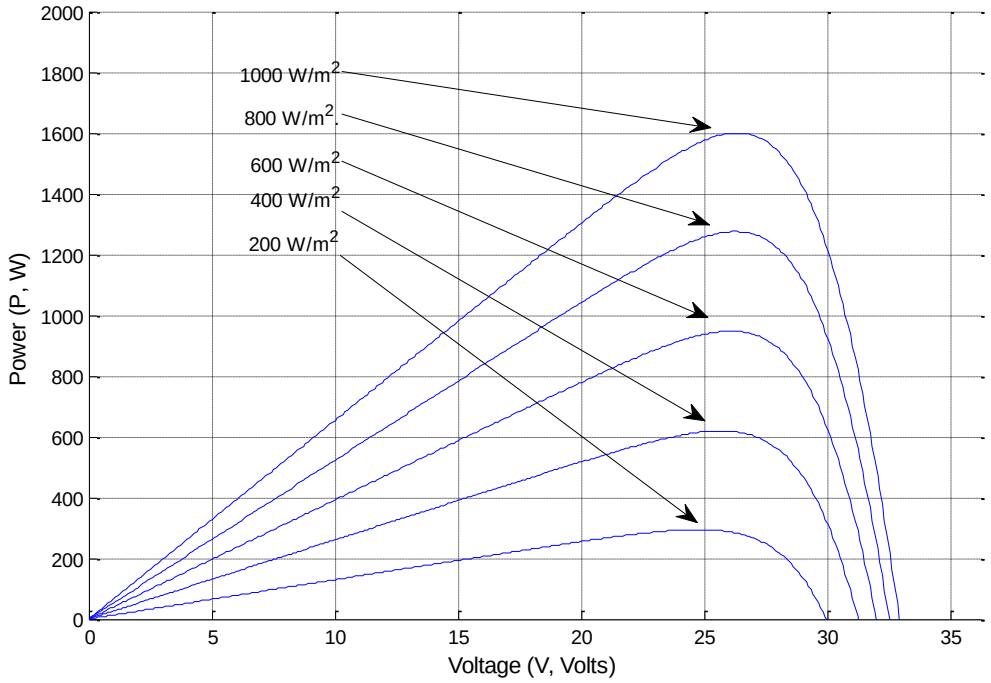

Figure 4.4 P-V characteristics of KCT 200GT array at different irradiations

Figure 4.4 shows the P-V characteristics of KCT 200GT array at different irradiations. The irradiation has been varied from 200 $^{W}/_{m^2}$ to 1000 $^{W}/_{m^2}$. It can be seen that the output power increases as the irradiation increases. As an array of 8 modules, with 200.143 W rating of each module, has been simulated, it can be seen that at nominal irradiation of 1000 $^{W}/_{m^2}$ the power reaches 1600 W.

4.2 The Grid System

Firstly the grid system has been simulated by disconnecting the PV system in order to know the behavior of the grid system without the PV generation system. Then to analyze the influence of connecting PV generation system on the grid, the grid is simulated with PV system connected. The complete system model is shown in the appendix.

4.3 Voltage Profile with PV System Disconnected

Table 4.1 shows the voltage profiles of different buses in pu obtained when the only grid system was simulated without connecting the PV generation system at normal loading conditions.

Table 4.1: Voltage profile at different buses with PV system disconnected

Bus No.	Voltage in pu
1	1
2	0.9999
3	0.9997
4	0.9997
5	0.9994
6	0.9915
7	0.9883

From Table 4.1 it can be observed that the voltages at all the buses are within the limits of 0.95 to 1.05 per unit.

4.4 Voltage profile at varying PV Power Penetrations

The PV generator system is connected to the power grid system and its impacts on the bus system have been studied in detail. For a detailed analysis, the PV penetration has been increased from 30 kW to 110 kW by increasing the number of arrays in each case. The following are the results for different scenarios.

Table 4.2: Voltage profile at different buses in pu for different levels of PV penetration

PV Power (kW)	Bus-1	Bus-2	Bus-3	Bus-4	Bus-5	Bus-6	Bus-7
30	1.000	0.999	0.998	0.998	0.997	0.995	1.000
50	1.000	1.001	1.004	1.004	1.004	1.027	1.042
70	1.000	1.001	1.003	1.004	1.004	1.027	1.045
90	1.000	1.001	1.004	1.005	1.005	1.034	1.051
110	1.000	1.001	1.005	1.005	1.006	1.035	1.052

From Table 4.2, the following observations are made:

1. As the PV penetration increases the voltage also increases.
2. At one level of penetration, the voltage at bus-7 crossed the limit of 1.05 pu. This is when the penetration from PV is 90 kW or greater.
3. The results indicate that if the penetration level of a renewable source of generation increases, the voltage at different buses of the microgrid system also increases with a significant increase at the PCC.
4. In a grid system if the voltage at a particular bus is low due to an increased load at that bus, then a PV generation system can be connected to that bus in order to compensate for the decrease in the voltage.

If the increase in the voltage, at one level of penetration, crosses the allowable limit which is 1.05 pu, it may cause problems such as overvoltage. In the next chapter, three methods are proposed to address the problem, have been discussed.

4.5 Harmonic Analysis

Figure 4.5 to Figure 4.11 show the voltage waveforms of bus 1 to 7 for a PV penetration of 30 kW.

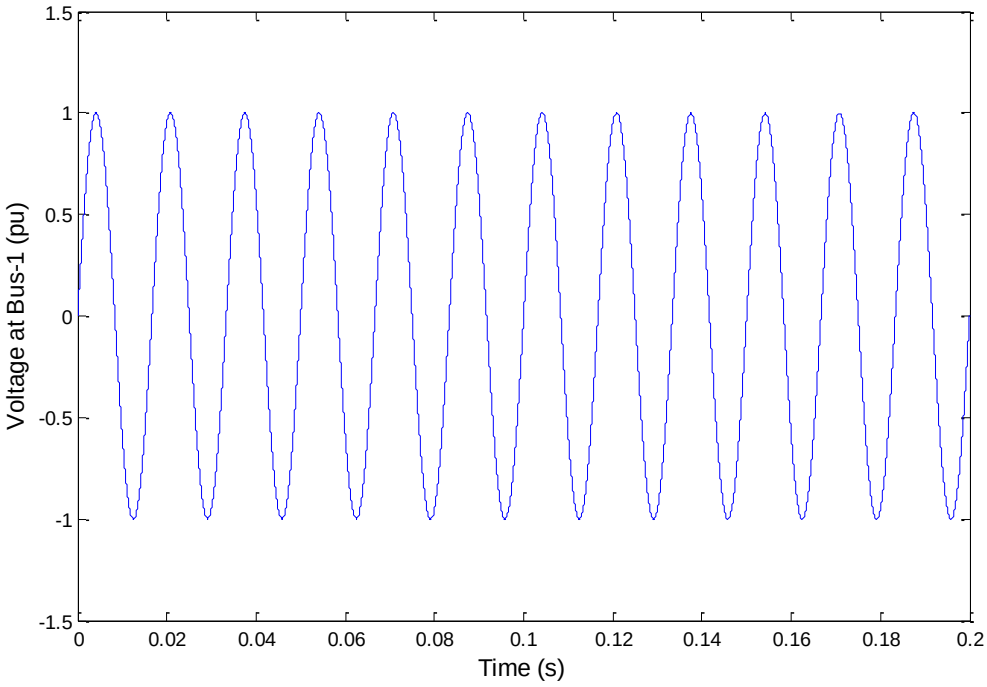

Figure 4.5: Voltage waveform at bus-1 with a PV power penetration of 30 kW

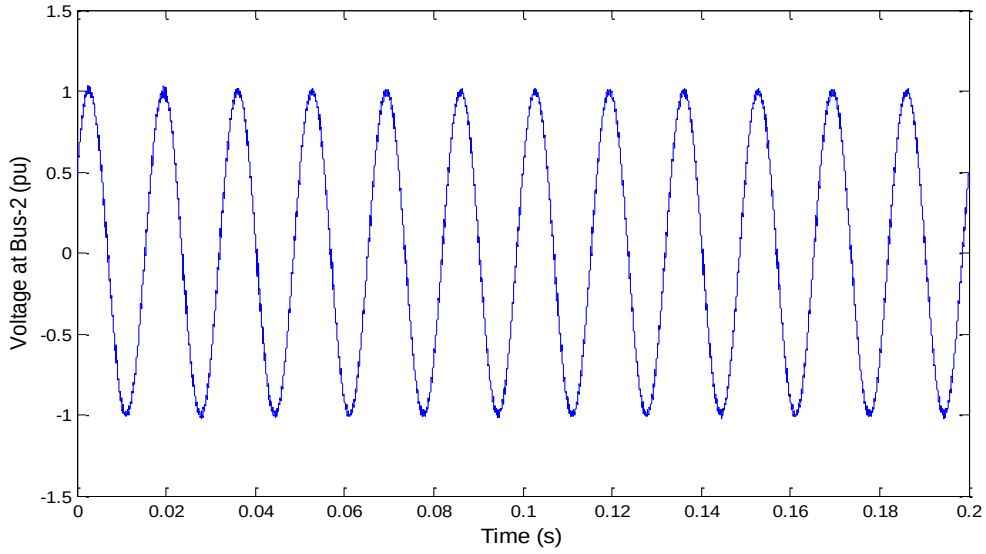

Figure 4.6: Voltage waveform at bus-2 with a PV power penetration of 30 kW

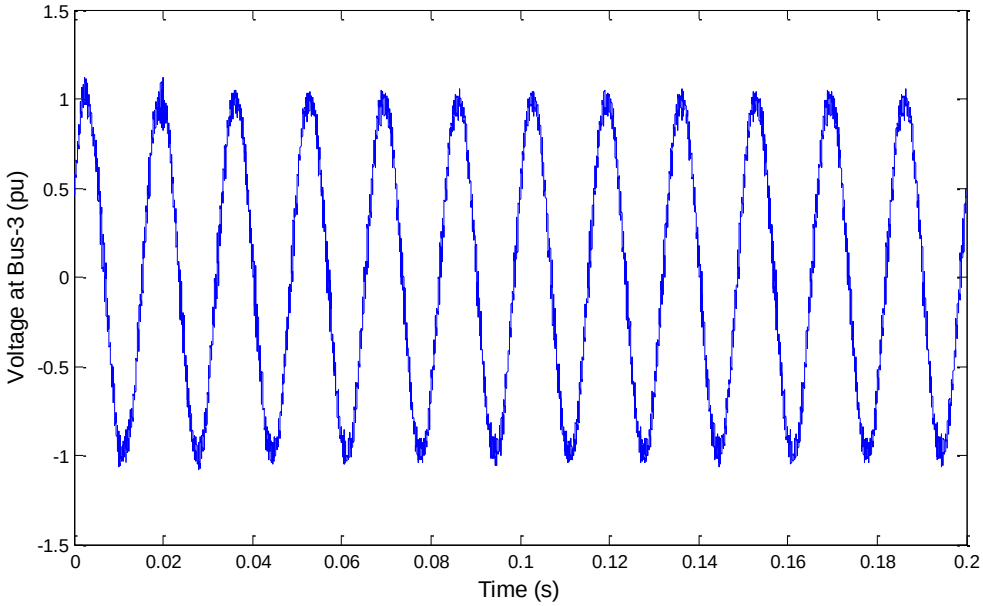

Figure 4.7: Voltage waveform at bus-3 with a PV power penetration of 30 kW

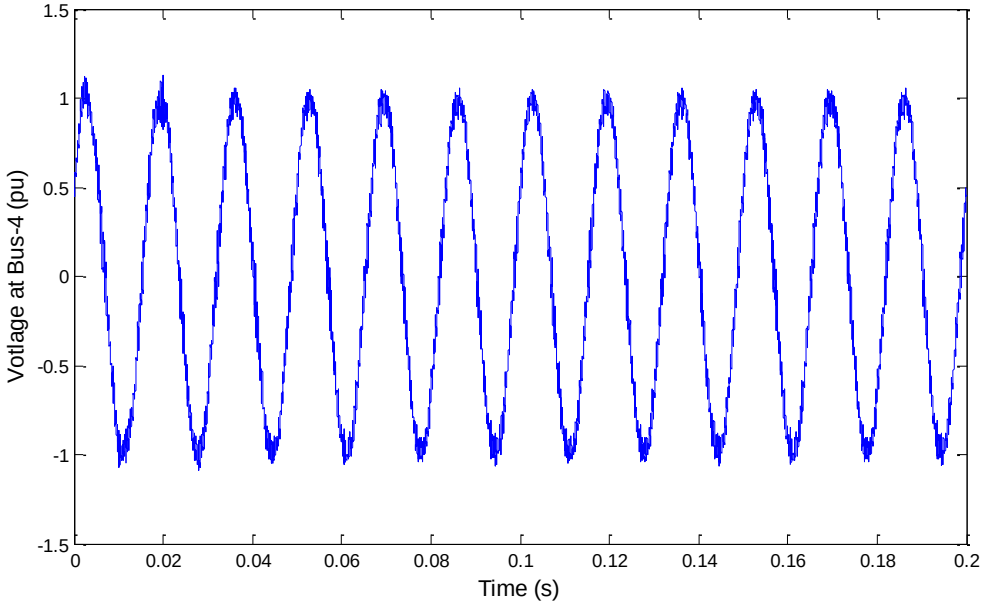

Figure 4.8: Voltage waveform at bus-4 with a PV power penetration of 30 kW

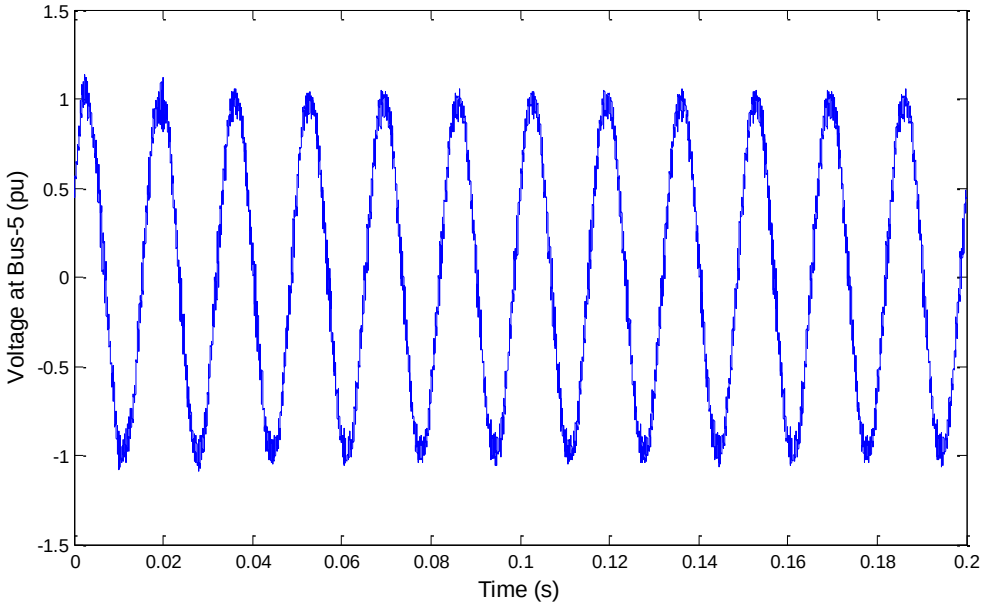

Figure 4.9: Voltage waveform at bus-5 with a PV power penetration of 30 kW

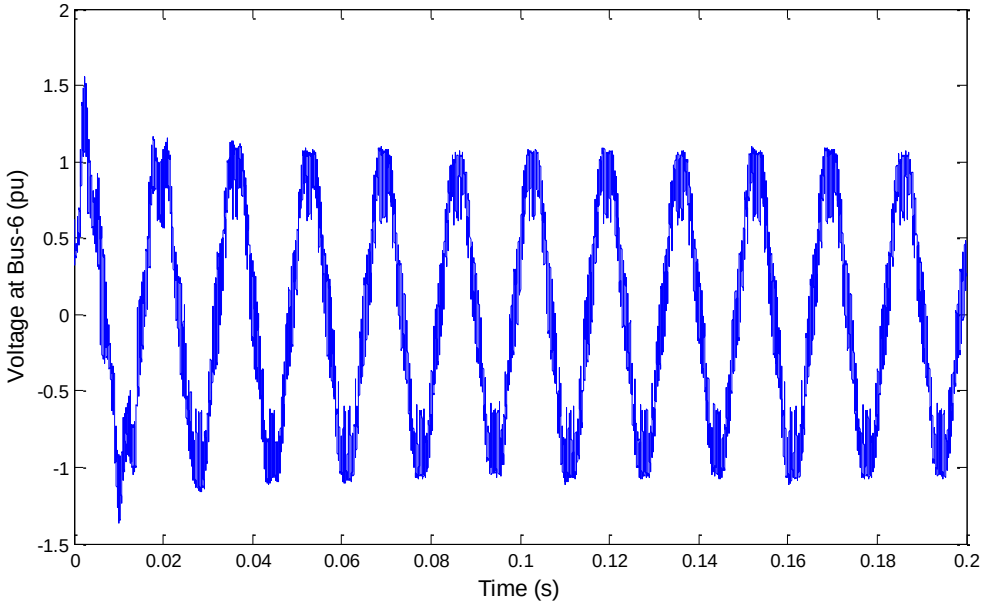

Figure 4.10: Voltage waveform at bus-6 with a PV power penetration of 30 kW

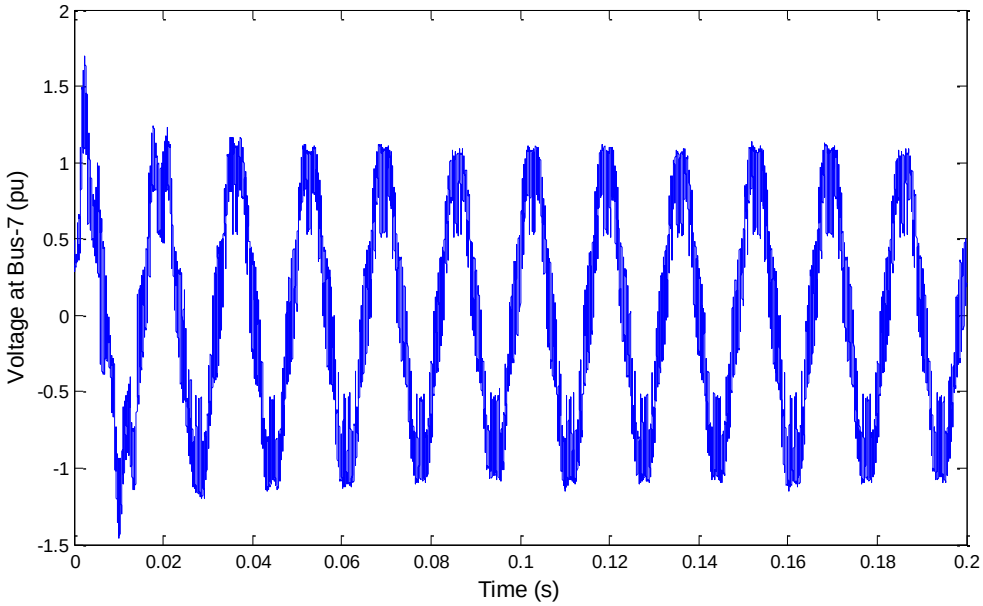

Figure 4.11: Voltage waveform at bus-7 with a PV power penetration of 30 kW

From Figure 4.5 to Figure 4.11, it can be observed that the voltage at buses 6 & 7 has higher harmonic content. For determining the harmonic content present at PCC (bus-7) and bus-6, Fourier analysis is performed on the voltage output for two different penetrations of PV powers. Table 4.3 shows the result of the analysis.

Table 4.3: Harmonic Content at bus 6 & 7 for a PV penetration of 90kW & 110 kW

Order	90 kw		110 kw	
	Harmonic Content in per unit			
	Bus-6	**Bus-7**	**Bus-6**	**Bus-7**
Fundamental	1.007	1.0068	1.07	1.009
2	0.0075	0.007	0.005	0.01
3	0.006	0.0045	0.006	0.007
4	0.007	0.006	0.007	0.008
5	**0.084**	**0.065**	**0.07**	**0.08**
6	0.008	0.006	0.007	0.01
7	**0.036**	**0.028**	**0.03**	**0.04**
8	0.009	0.008	0.0085	0.0095
9	0.006	0.005	0.0055	0.0065
10	0.007	0.005	0.0055	0.0075
11	**0.014**	**0.011**	**0.012**	**0.015**
12	0.007	0.005	0.006	0.008
13	**0.0075**	**0.0065**	**0.008**	**0.01**
THD %	10.4	13.3	10.5	13.2

From Table 4.3, following observations can be made:

1. In the voltage waveforms, 5^{th}, 7^{th}, 11^{th} & 13^{th} (in bold figures in the table) harmonic have considerable values. The other harmonics are negligible.
2. The harmonic content is higher when PV power penetration is higher.
3. Bus-7 has higher harmonic content than bus-6. This is due to the fact that the PV system is connected to bus-7.

4. The total harmonic distortion (THD) value of is also calculated. It is found higher in the case of higher power penetration. Also, the voltage at bus-7 has higher value of THD than the voltage at bus-6.

4.6 Three Phase Harmonic Filter

In the previous section it was observed that the system contained large harmonic content at all the buses. Harmonic phenomena are more prominently found at bus-6 and bus-7. The harmonics are due to the presence of non-linear devices like the converters. To overcome this, a three phase harmonic filter is designed.

A second order filter has been used to mitigate the harmonics present in the system. A second order filter provides good attenuation at an economic cost. It comprises of two inductors L_1, L_2 and a capacitor C. The value of inductor L_1 which is on the inverter side is calculated for a ripple of 10 to 15 % of the rated current. Inductor L_2 is computed as $L_2 = 0.8\, L_1$. Inductor L_1 is given the relation:

$$L_1 = \frac{V_g}{2\sqrt{6}\, f_s i_{r,p}} \qquad (4.1)$$

Where:

- V_g is the grid voltage (rms)
- f_s is the inverter switching frequency

The filter capacitance C is calculated according to the relation $C \leq 0.05\, C_b$, where C_b is the base capacitance given by $C_b = \frac{1}{\omega_n Z_b}$. The term $Z_b$is the base impedance of the system given by the relation [29]:

$$Z_b = \frac{V_{g,ll}^2}{P_n}$$

Where

- $V_{g,ll}$ is the grid line voltage (rms)
- P_n is the rated power of the inverter

Having designed filter the grid system is again simulated for a PV power penetration of 90 kW and 110 kW; Figure 4.4 shows the harmonic spectrum is obtained when the Fourier analysis is performed.

Table 4.4: Harmonic Content at bus 6 & 7 for a PV penetration of 90kW & 110 kW

Order	90 kW		110 kw	
	Harmonic Content in per unit			
	Bus-6	Bus-7	Bus-6	Bus-7
1	0.9909	0.9878	0.9908	0.9877
2	2.50E-05	3.60E-05	4.00E-05	5.00E-05
3	1.50E-05	2.30E-05	2.00E-05	2.75E-05
4	1.00E-05	1.50E-05	1.50E-05	5.00E-05
5	8.00E-06	1.20E-05	1.10E-05	1.50E-05
6	6.00E-06	1.00E-05	9.00E-06	1.25E-05
7	5.00E-06	8.50E-05	8.00E-06	1.00E-05
8	5.00E-06	7.50E-06	7.00E-06	9.00E-06
9	4.00E-06	6.50E-06	6.00E-06	8.00E-06
10	4.00E-06	6.00E-06	5.00E-06	7.00E-06
11	4.00E-06	5.50E-06	4.50E-06	6.00E-06
12	3.00E-06	5.00E-06	4.50E-06	6.00E-06
13	3.00E-06	4.50E-06	4.00E-06	6.00E-06
THD %	0.014	.005	0.012	.001

From Table 4.4 it can be observed that all the harmonic values from order 2 onwards have reduced to negligible values. The THD in both the cases is lower than 1 %.

4.7 Variation of Load at PCC

In order to see the effect of connecting PV generation system at bus-7 (PCC), the load connected at bus-7 is varied from 120 kW to 400 kW. And the simulations are carried for the grid system with PV system connected, but keeping the PV power penetration constant.

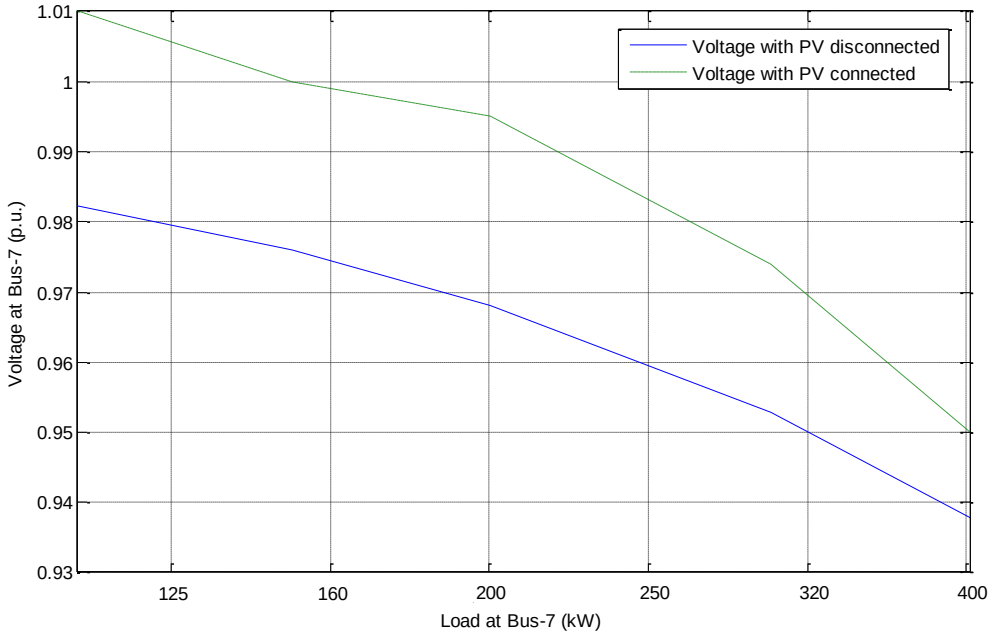

Figure 4.12: Voltage level at PCC with different levels of loading conditions

It can be inferred from the graphs that when the PV system was disconnected from the grid, the voltage level dropped to 0.95 pu at a load of 320 kW. Whereas in the second scenario when the PV system was connected to the grid system, the voltage at the same load is 0.97 pu, higher than the limit of 0.95 pu. It can also be seen from the graph that even when the load was increased to 400 kW, the voltage profile in the case when the

PV system is connected to the grid, does not fall beyond 0.95 pu. This analysis implies that in a power system when the voltage at a bus is reduced due to increased loads at the bus, a PV system can be installed in order to improve the voltage profile.

CHAPTER 5

VOLTAGE CONTROL

In the previous chapter, the PV connected microgrid system was simulated for different levels of PV penetration. It was observed that the increase in the PV penetration had a prominent impact at the PCC, which is bus-7. The per unit value of voltage at most of the buses increased as the PV penetration into the grid was increased. It was also observed that the voltage at bus-7 exceeded the voltage limit of 1.05 pu. In this chapter two voltage control methodologies have been proposed in order to control the voltage of the buses with special emphasis on voltage at bus-7, in the scenario of increased PV penetrations.

5.1 Voltage Control by Switching Methodology

A voltage control methodology has been presented in order to control the voltage with increased value of PV penetration. In this method, the voltage at PCC i.e. at bus-7 is measured and sent to the control system. The control system analyzes the obtained voltage measurement of bus-7 and processes its action. The control logic is relatively simple. When the voltage increases beyond 1.05 pu, the control system disconnects the PV generation system from the grid. On the other hand if the voltage falls below 0.95 pu, the control system reconnects the PV generating system to the grid. The following block diagram shows the control methodology of this technique.

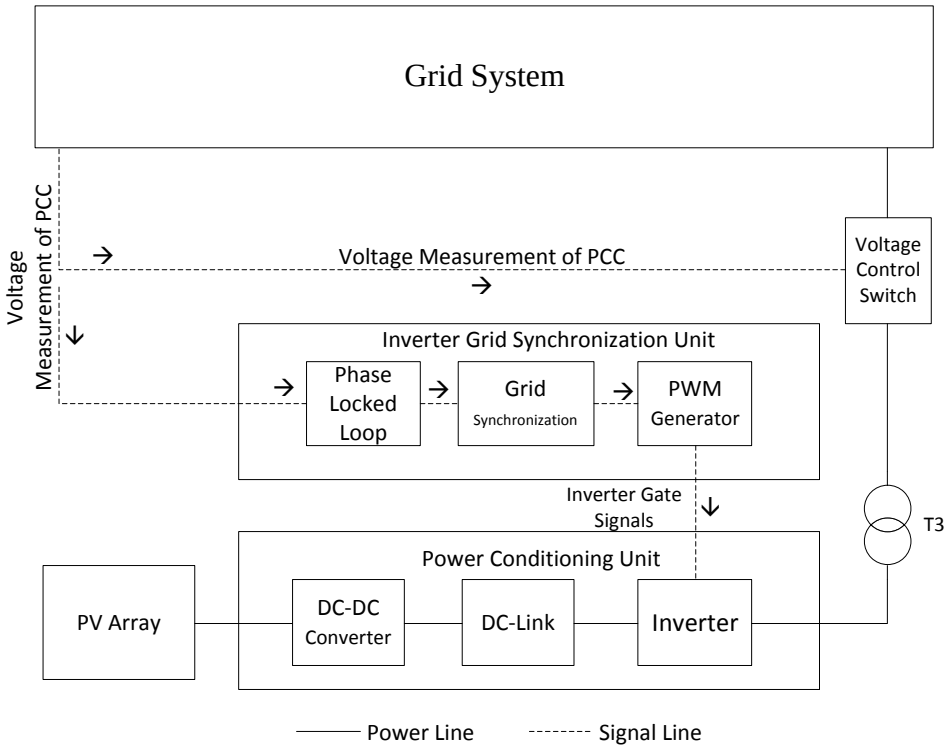

Figure 5.1: Voltage control methodology using switch for the power grid

The voltage control system compares the measured voltage at PCC with the standard values of 0.95 pu and 1.05 pu. If the voltage at PCC is found to be lower than 0.95 pu then the control system reconnects the PV generating system to the grid. When the voltage exceeds the upper limit of 1.05 pu, the control system disconnects the PV generating system from the microgrid.

The distribution system is tested again for different levels of PV penetration. This time, the voltage control system has been included to analyze its effectiveness in maintaining a voltage level near to 1.00 pu. For a detailed analysis, the PV penetration has been increased from 30 kW to 110 kW. The following are the results for different scenarios. The PV penetration has been varied from 30 kW to 110 kW.

Table 5.1: Voltage profile at different buses in pu for different levels of PV penetration with switch voltage control methodology

PV Power (kW)	Bus-1	Bus-2	Bus-3	Bus-4	Bus-5	Bus-6	Bus-7
30	1.000	1.000	1.000	1.000	1.001	1.006	1.011
50	1.000	1.000	1.000	1.000	1.001	1.004	1.011
70	1.000	1.000	1.001	1.001	1.001	1.004	1.010
90	1.000	1.000	1.001	1.002	1.000	1.005	1.010
110	1.000	1.000	1.001	1.002	1.001	1.005	1.010

Table 5.1 shows the bus voltage profiles at different PV penetrations when the switching voltage control is applied. The following observations are made:

1. It can be observed that the voltage profile has improved in this case and is much below 1.05 pu.
2. When the switching-based voltage control system was employed, the voltage level at none of the buses has exceeded the upper voltage limit of 1.05 pu. The highest voltage is only 1.01 pu which is well below the upper voltage limit of 1.05 pu.

Nevertheless in this control methodology, the PV generation system remains either connected to the system or completely disconnected to the system. A drawback of this method is that the switching operation creates switching pulses which can impose detrimental effects on the grid system. The switch based voltage control model of the grid has been shown in the appendix section.

5.1.1 Switching Transients

Switching of power system devices often creates switching transients. Controlling the voltage using the switch creates switching transients. Figure 5.2 shows the switching

transients showing the voltage waveform for a PV penetration of 110 kW. It can be observed from the figure that at time $t = 0.157\ s$, a transient takes place.

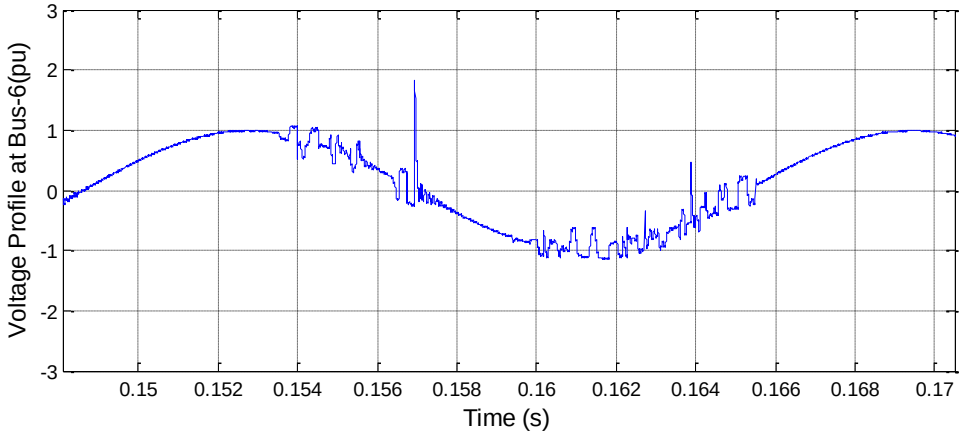

Figure 5.2: Voltage profile of showing the switching transients

5.2 Solar Tracker Voltage Control Method

In this section a voltage control methodology has been presented in order to control the voltage with increased value of PV power penetration. In this method, the voltage at PCC i.e. at bus-7 is measured and sent to the control system. The control system analyzes the voltage measurements of bus-7 and processes its action. The control logic is to control the angle of incidence between the PV panel and the incident solar irradiation. Any change in the angle of irradiation causes a corresponding change in the PV power.

When the voltage increases beyond 1.00 pu, the control system detects the increase in the voltage and compares the current voltage value with the reference value, which is set at 1.00 pu. The control system now gives out a control signal such that the error between the current value of the voltage and the reference value of the voltage is reduced. On the other hand when the voltage falls below 1.00 pu, the control system gives the appropriate signal to the solar tracker such that it aligns itself to collect

maximum irradiation. This will lead to increased power generation which would in turn increases the voltage. Figure 5.4 shows the control methodology of this technique.

The effective incident solar radiation on a PV panel is given by:

$$G = G_n Cos\ \theta$$

Where:

- θ is the angle between the incident radiation and the normal perpendicular to the panel
- G is the effective solar irradiation
- G_n is the normal solar irradiation when $\theta = 0^0$

5.2.1 Necessity of a PI Controller

A solar tracker always orient the panel load such that at any given instant of time of the day, maximum irradiation is incident on the PV panels. If the solar panel can be controlled to orient such that the incident irradiation can be changed according to the requirement, the generated PV power can also be varied according to the requirement. The PV power generation can be controlled in order to maintain 1.00 pu voltage at PCC. When the voltage at PCC is greater than 1.00 pu, the PV power penetration should be decreased. This can be achieved by decreasing the angle between the solar array and the S incident, θ as shown in Figure 5.3. Similarly when it is required to increase the PV generation power, the angle θ should be increased until the requirement is met.

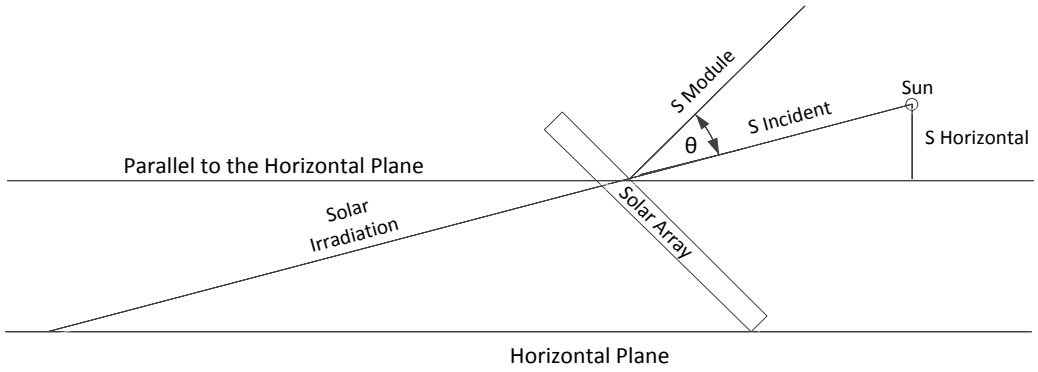

Figure 5.3: Working of a Solar Tracker

In order to orient the tracker, a controller is required which can control the angle of the solar tracker in order to give it appropriate instructions such that the voltage at PCC is maintained at 1.00 pu.

To accomplish the control action of the solar tracker, a PI controller is used in this work, which can orient the PV panel mounted on it according to the control requirements. The proportional and integral elements of a PI controller are given by (5.1) and (5.2) respectively.

$$\mathrm{P} = K_p . E(t) \qquad (5.1)$$

$$I = K_I . \int_0^t E(t)dt \qquad (5.2)$$

The control function used in this work for the solar tracker orientation control is given by (5.3), manual tuning has been used to configure the parameters K_p and K_I:

$$C(s) = 500 + \frac{10}{s} \qquad (5.3)$$

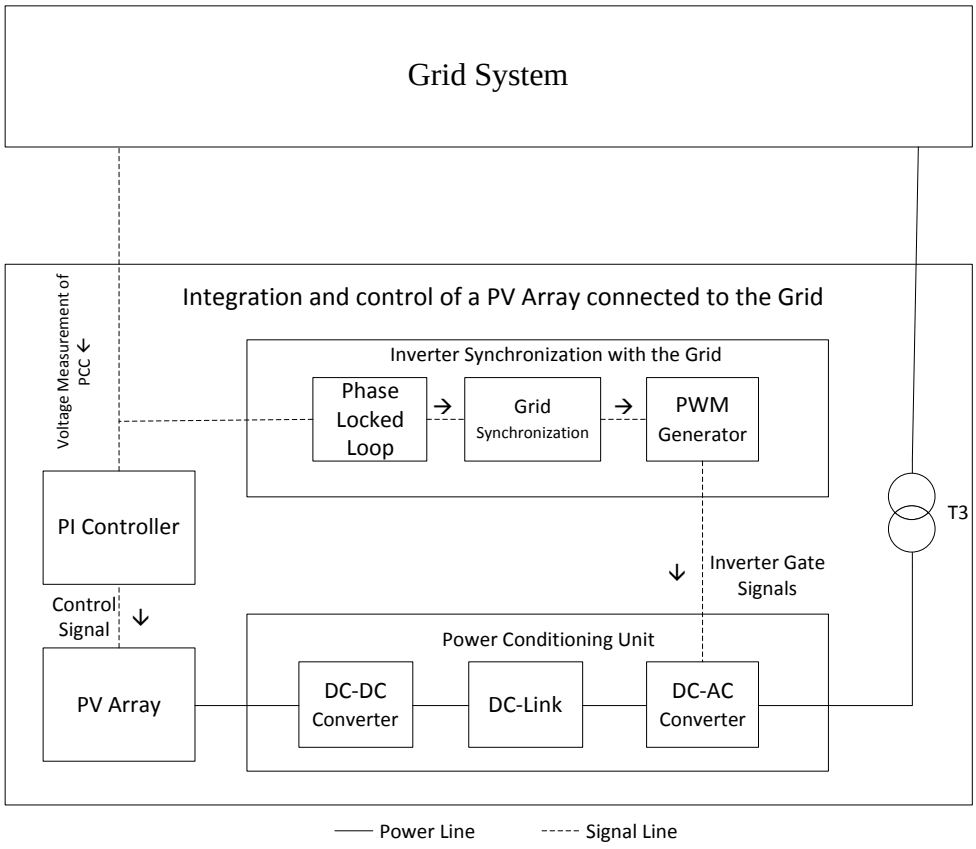

Figure 5.4: Voltage control methodology using solar tracker for the power grid

The voltage controller's functionality is explained in Figure 5.5.

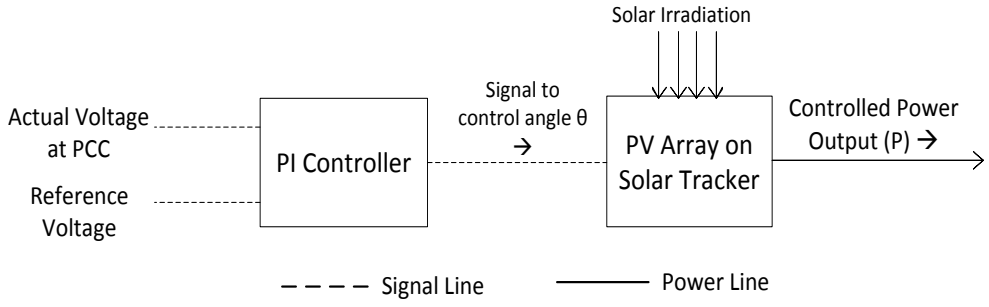

Figure 5.5: Voltage Control System

The power grid system is tested again for different levels of PV penetration. This time, the solar tracker voltage control system has been included to analyze its effectiveness in maintaining a voltage level near to 1.00 pu. For a detailed analysis, the PV penetration has been increased from 30 kW to 110 kW. The following are the results for different scenarios. The PV penetration has been varied from 30 kW to 110 kW.

Table 5.2: Voltage profile at different buses in pu for different levels of PV penetration with solar tracker voltage control methodology

PV Power	Bus-1	Bus-2	Bus-3	Bus-4	Bus-5	Bus-6	Bus-7
30 kW	1.000	0.999	0.998	0.998	0.997	0.998	1.000
50 kW	1.000	0.999	0.999	0.998	0.998	0.998	1.000
70 kW	1.000	1.000	0.999	0.999	0.998	0.998	1.000
90 kW	1.000	1.000	1.000	0.999	0.998	1.001	1.010
110 kW	1.000	0.999	0.999	0.998	0.998	0.998	1.000

Table 5.2 shows the bus voltage profile with solar tracker voltage control method for different PV power penetrations. The following observations are made:

1. It can be seen that the voltage level is well maintained even at the PCC which is bus-7.
2. It can be observed that the above results are better than both the previous cases, when switch based control methodology is applied (Table 5.1) and when no voltage control is applied (Table 4.2).
3. Using this technique voltage is dynamically controlled with higher precession when compared to the previous control method, closer to 1.00 pu.
4. It can also be noticed that voltage levels at all buses are near to the value of 1.00 pu. From the results it can be concluded that even when the penetration level of PV generation system is high, the voltage at bus-7 (PCC) and bus-6 was much below 1.05 pu.

Nevertheless this control methodology is a bit expensive, as it necessitates solar tracker and its control components, and complex, as it requires expertise to be installed.

5.2.2 Solar Tracker Dynamics

The solar tracker is controlled by a PI controller. The controller's elevation is varied with respect to time. Figure 5.6 shows the variation of solar tracker angle with respect to time. The solar tracker is governed by the PI controller given by equation (5.4).

$$C(s) = 500 + \frac{10}{s} \qquad (5.4)$$

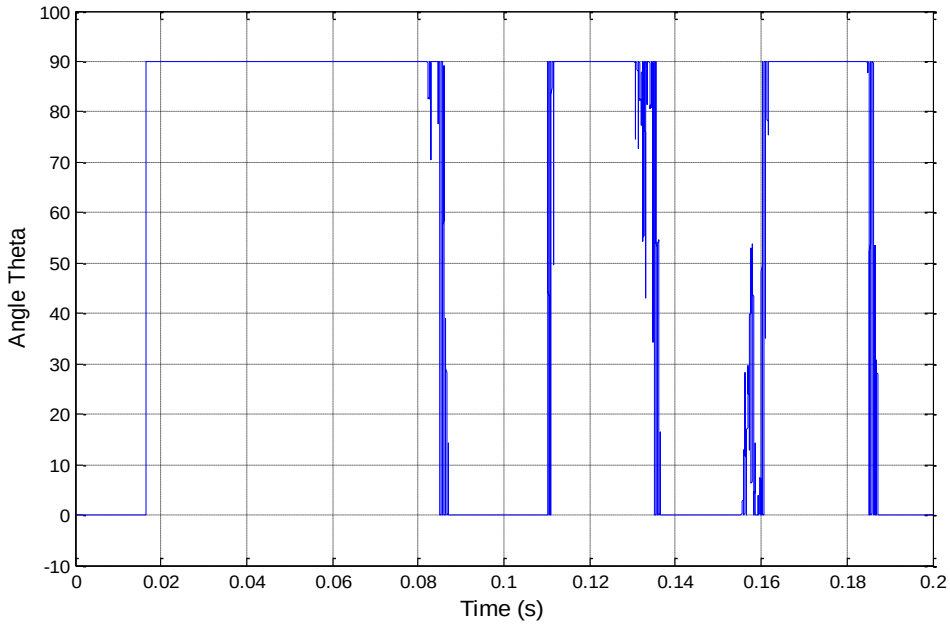

Figure 5.6: Solar Tracker Angle Dynamics

Figure 5.6 shows the dynamics of the solar tracker. The solar tracker angle θ has been plotted with respect to time. It is observed that the PI controller orients the tracker according to the control requirements. An angle of 0^0 indicates the position when the tracker is oriented to receive maximum irradiation producing maximum power. When the

angle is 90^0 the panels are oriented vertical with respect to the incoming solar irradiation direction and hence no power is generated.

5.3 Voltage control using DC-DC Converter

In this work the DC-DC converter used is used for maximum power point tracking (MPPT) besides its usual purpose. The DC-DC converter can also be used for the purpose of controlling the voltage so that the voltage at the PCC can be maintained near to unity. Voltage control using DC-DC converter has many advantages including low cost, no requirement of additional components etc.

The voltage is controlled by controlling the gate signals. The voltage is measured at the PCC and is compared with the reference value of 1 pu. The controller accordingly controls the gate signal such that the voltage at the PCC is maintained at unity. The duty cycle of the converter system varies from 0.67 to 0.92.

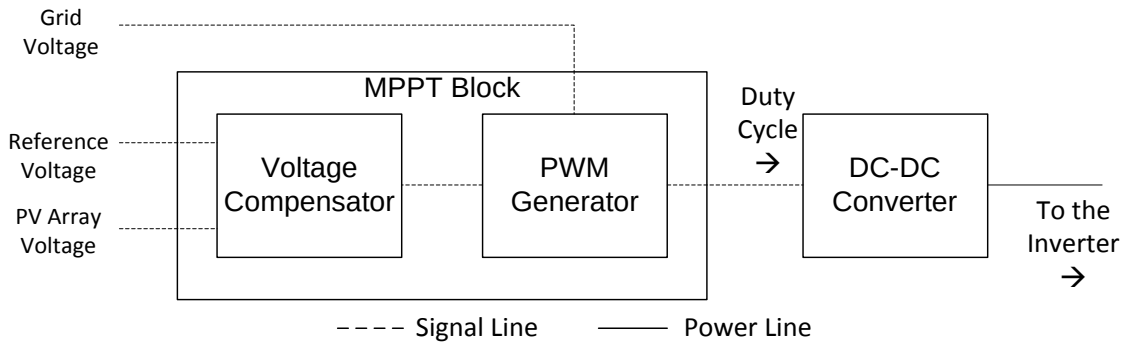

Figure 5.7: Voltage control using DC-DC converter

The power grid system is tested again for different levels of PV penetration with the DC-DC converter voltage control. To analyze its effectiveness in maintaining a voltage level near to 1.00 pu. For a detailed analysis, the PV penetration has been

increased from 30 kW to 110 kW. The following are the results for different scenarios. The PV penetration has been varied from 30 kW to 110 kW.

Table 5.3: Voltage profile at different buses in pu for different levels of PV penetration with DC-DC converter based voltage control methodology

PV Power	Bus-1	Bus-2	Bus-3	Bus-4	Bus-5	Bus-6	Bus-7
30 kW	1.000	0.999	0.999	0.998	0.998	0.995	1.005
50 kW	1.000	0.999	0.997	0.997	0.996	0.990	0.995
70 kW	1.000	0.999	0.998	0.998	0.998	0.995	1.000
90 kW	1.000	1.000	1.001	1.001	1.001	1.010	1.020
110 kW	1.000	1.000	1.001	1.001	1.001	1.010	1.020

Table 5.3 shows the bus voltage profile of the grid system when DC-DC control system is used for voltage control. It can be seen that the voltage level is well below 1.05 pu even at the PCC which is bus-7. This voltage control method is best suitable as it does not require any additional equipment as it is implemented using the existing DC-DC converter.

CHAPTER 6

FAULT ANALYSIS

In order to view the effect of connecting the PV generating unit to the Microgrid, a detailed fault analysis has been carried on different buses. Firstly 3-phase faults are applied and then single-phase faults are applied at buses 2, 6 & 7. The PV power penetration is maintained at the base case of 110 kW at normal loading condition. The following are the output results obtained for each case.

6.1 Three-Phase Fault Analysis

Firstly three-phase faults have been applied at buses 2, 6 & 7 for a duration of 4 cycles, from $t = 0.0333\ s$ to $t = 0.1\ s$.

6.1.1 Fault at Bus-7

A three phase fault is applied at bus-7. According to the topology of the microgrid, it should be noticed that applying fault at bus-7 should have more effect on bus-6. The following are the results.

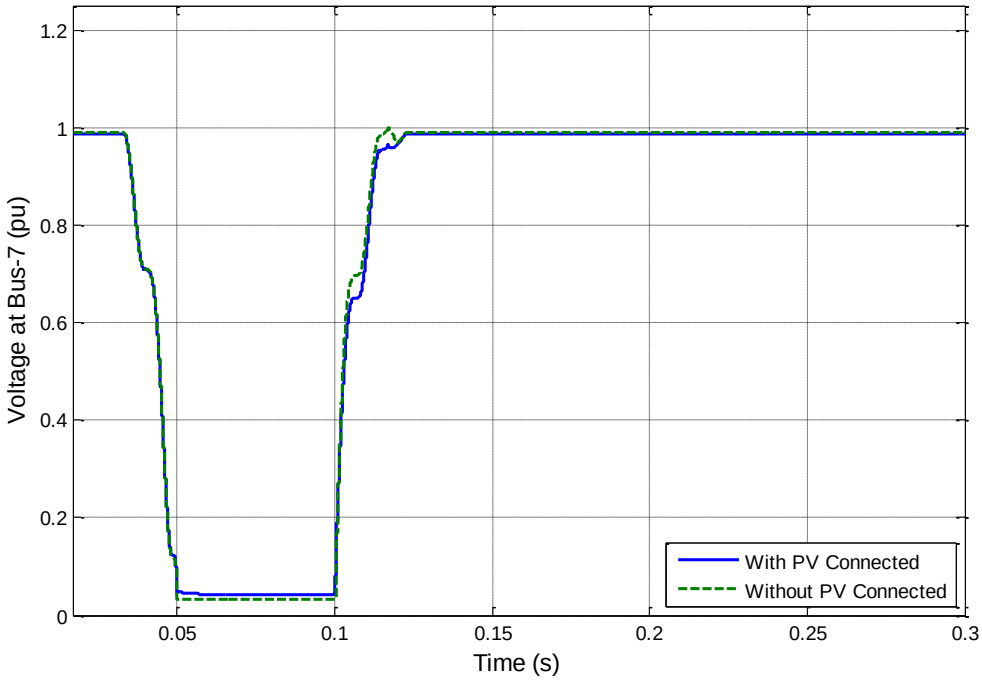

Figure 6.1: Voltage at Bus-7 when a 3-phase fault occurs at Bus-7

Figure 6.1 shows the voltage at bus-7 when a three phase fault occurs at bus-7. It can be observed whether or not the PV system is connected, the voltage heavily decreases during the fault.

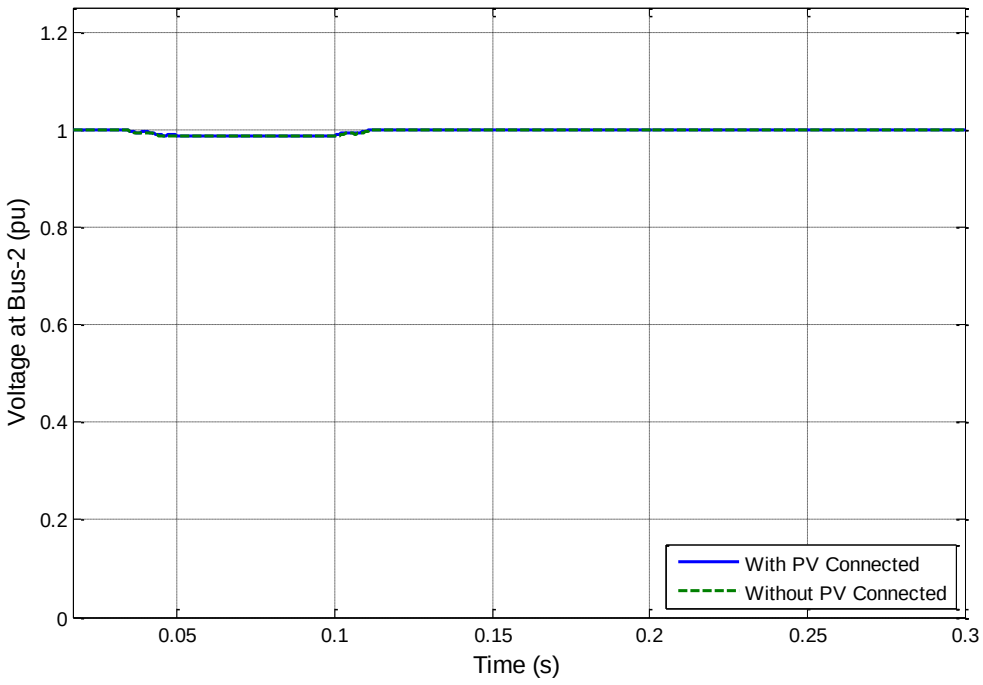

Figure 6.2: Voltage at Bus-2 when a 3-phase fault occurs at Bus-7

During the fault, it can be seen that there is a slight depression in the voltage. Nevertheless, the voltage goes to the normal value when the fault is cleared. As the bus is far away from the fault (which occurs at bus-7) and from the PV generating system, there is almost no difference whether or not PV generating system is connected.

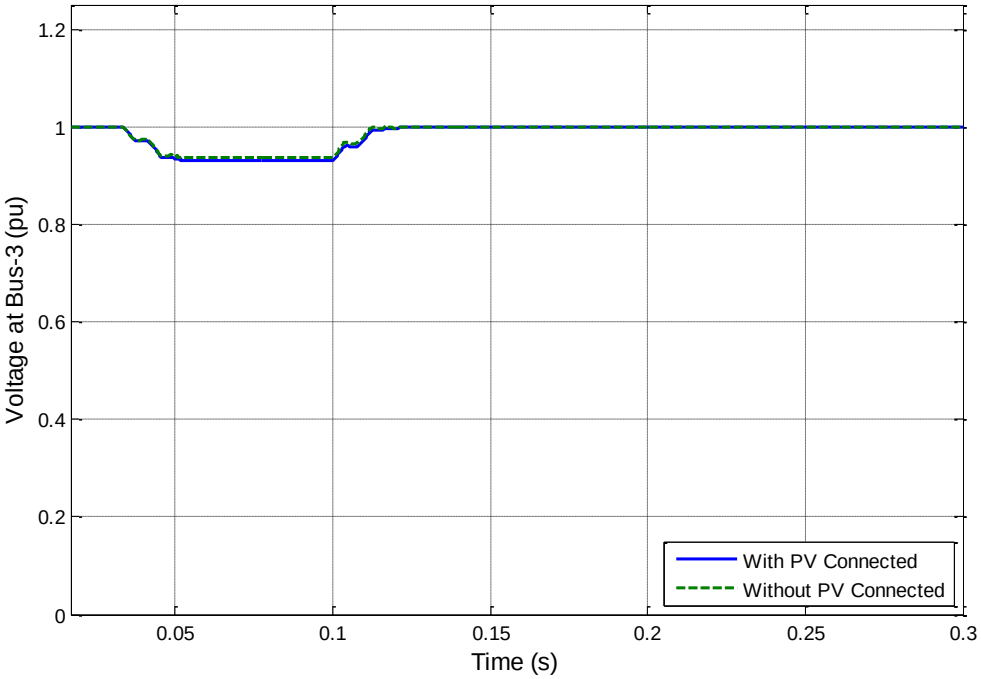

Figure 6.3: Voltage at Bus-3 when a 3-phase fault occurs at Bus-7

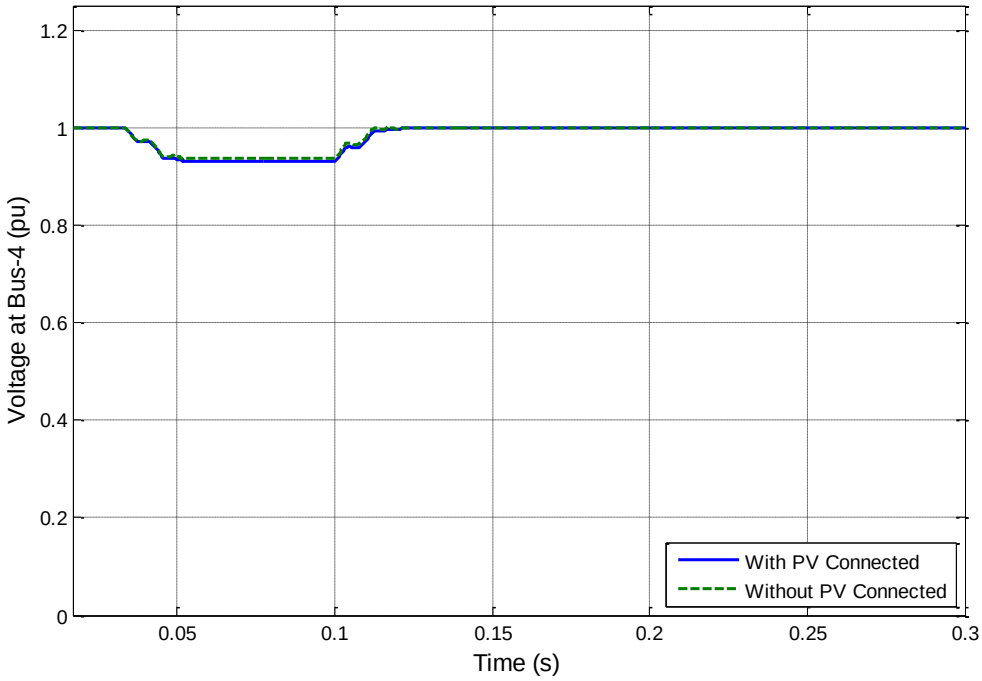

Figure 6.4: Voltage at Bus-4 when a 3-phase fault occurs at Bus-7

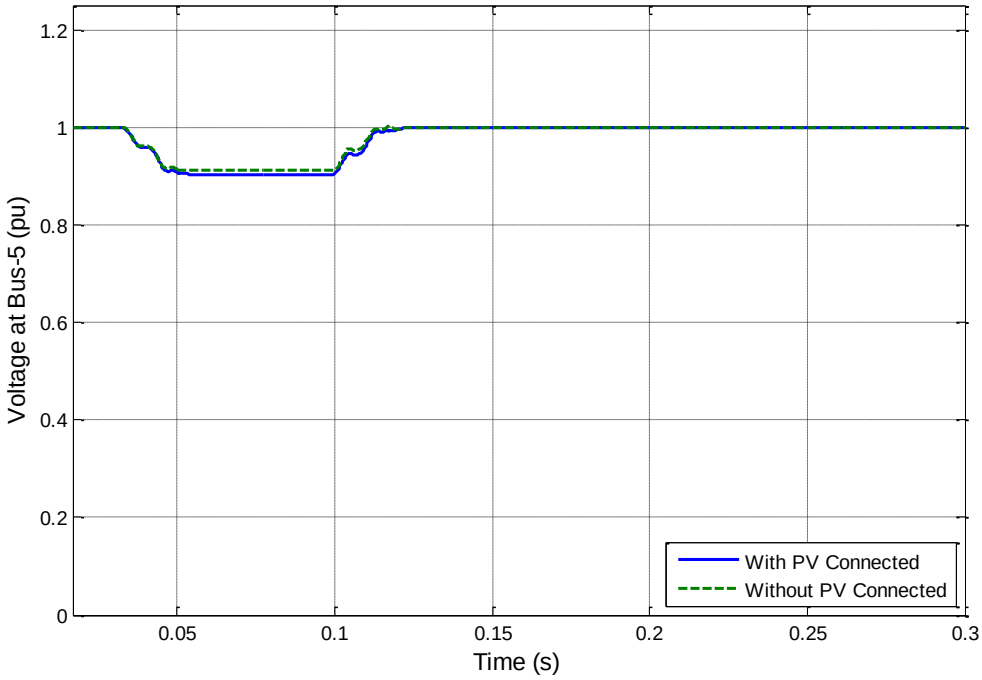

Figure 6.5: Voltage at Bus-5 when a 3-phase fault occurs at Bus-7

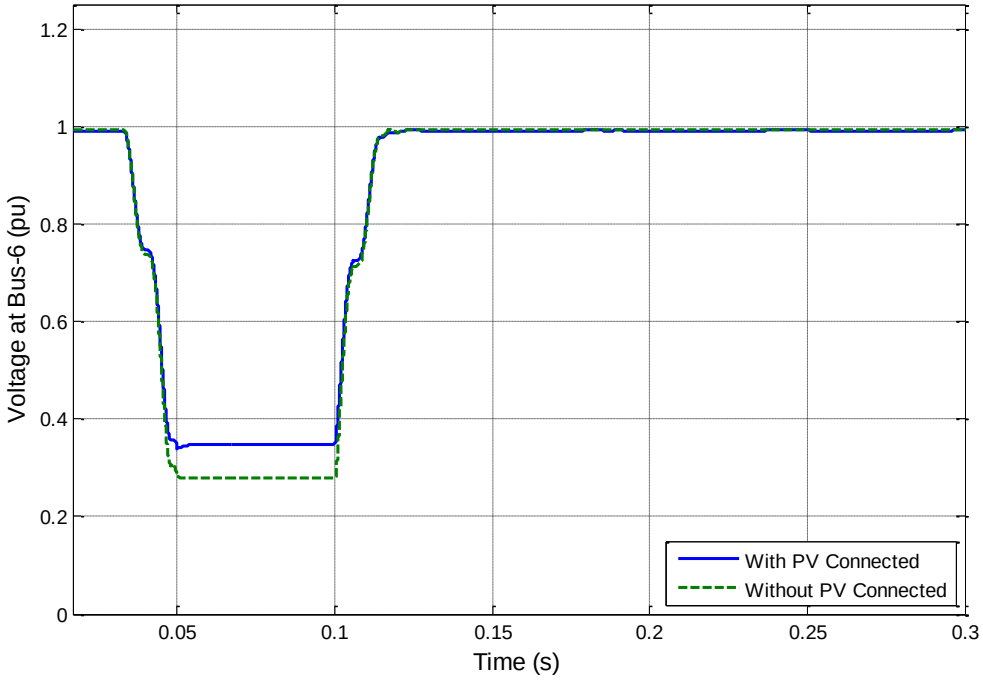

Figure 6.6: Voltage at Bus-6 when a 3-phase fault occurs at Bus-7

From Figure 6.3 to Figure 6.6 it can be seen that nearer the bus to the fault, greater is the voltage depression during the fault. It can be noticed that in the case when PV generating system is connected to the microgrid, during the fault there exists greater voltage due to the injected power from PV generating system into the grid.

6.1.2 Fault at Bus-6

A three phase fault is applied at bus-6. According to the topology of the microgrid, it should be noticed that applying fault at bus-6 should not have much effect on any of the buses except bus-7. The following are the results.

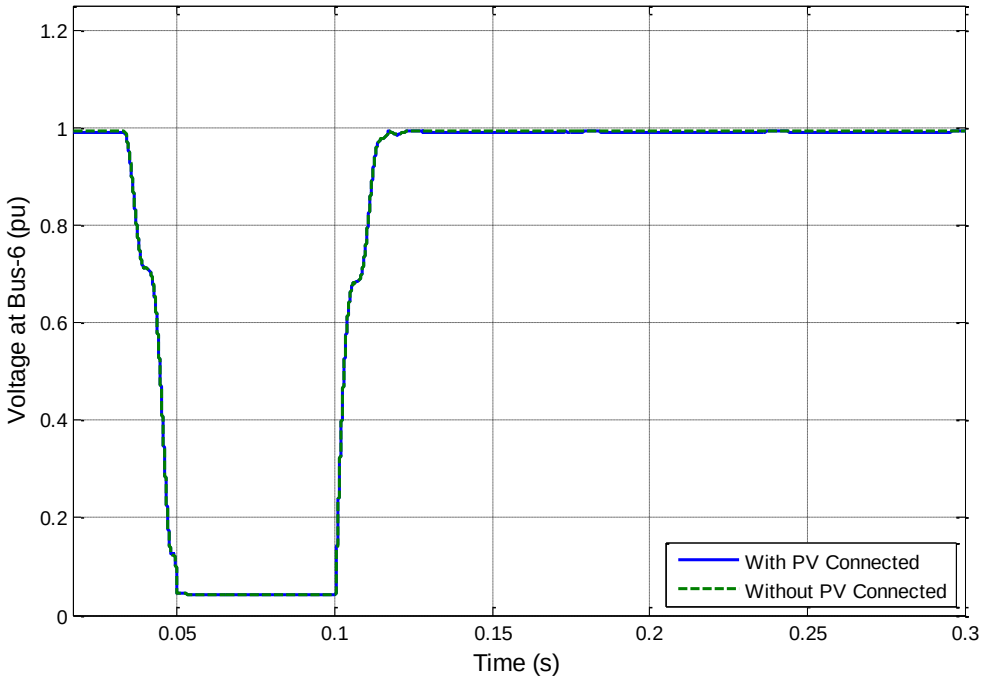

Figure 6.7: Voltage at Bus-6 when a 3-phase fault occurs at Bus-6

Figure 6.7 shows the voltage at bus-6 when a three phase fault occurs at bus-6. It can be observed whether or not the PV system is connected, the voltage heavily decreases during the fault.

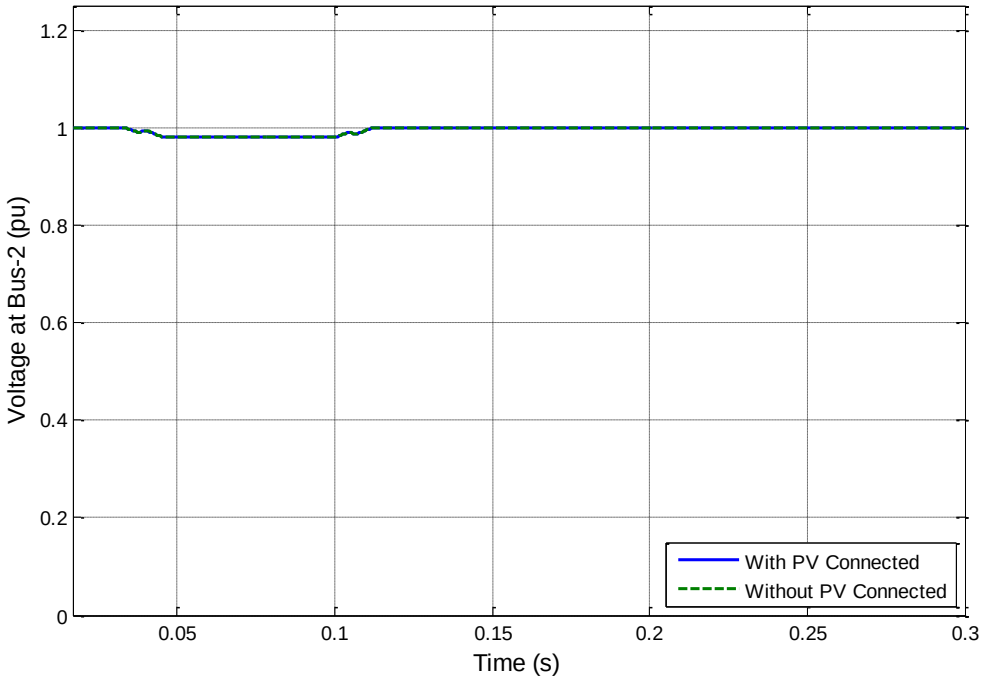

Figure 6.8: Voltage at Bus-2 when a 3-phase fault occurs at Bus-6

During the fault, it can be seen that there is a slight depression in the voltage. The voltage goes to the normal value when the fault is cleared. As the bus is far away from the fault (which occurs at bus-6) and from the PV generating system, there is almost no difference whether or not PV generating system is connected.

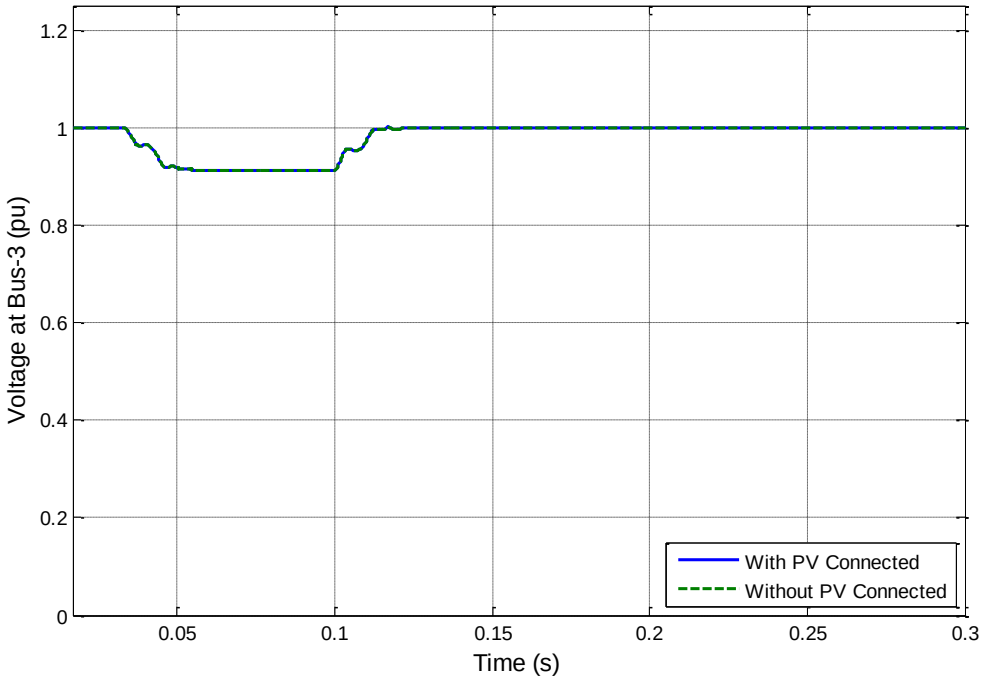

Figure 6.9: Voltage at Bus-3 when a 3-phase fault occurs at Bus-6

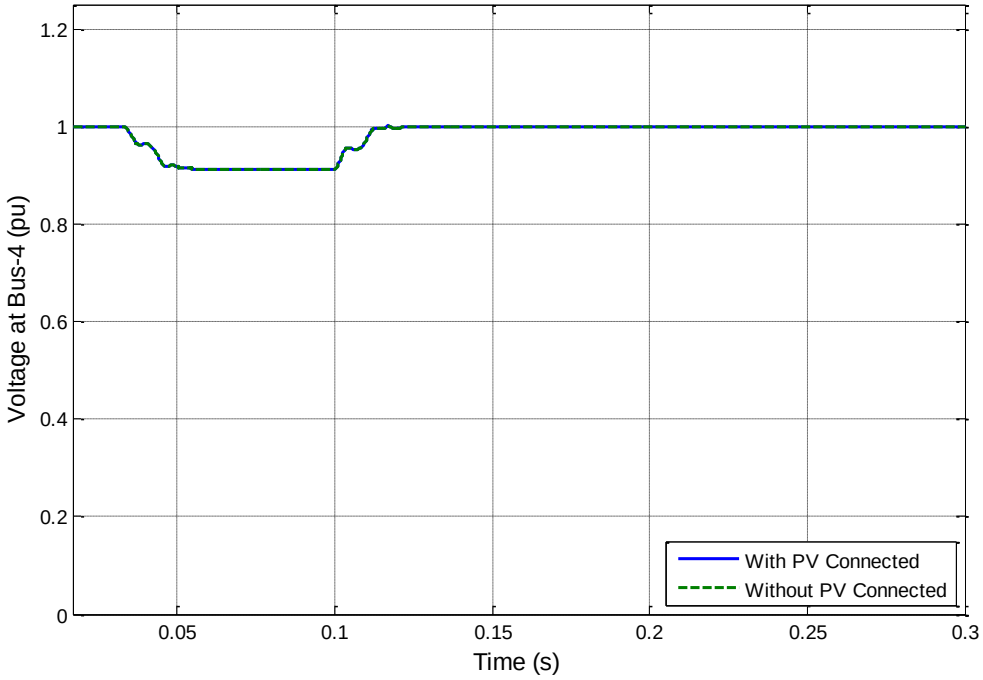

Figure 6.10: Voltage at Bus-4 when a 3-phase fault occurs at Bus-6

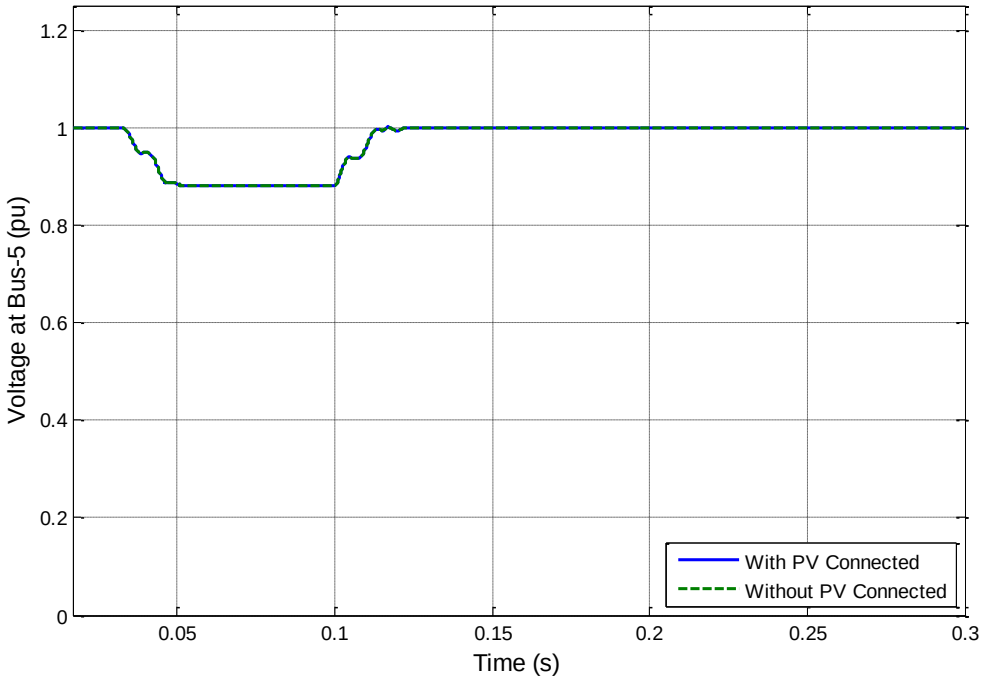

Figure 6.11: Voltage at Bus-5 when a 3-phase fault occurs at Bus-6

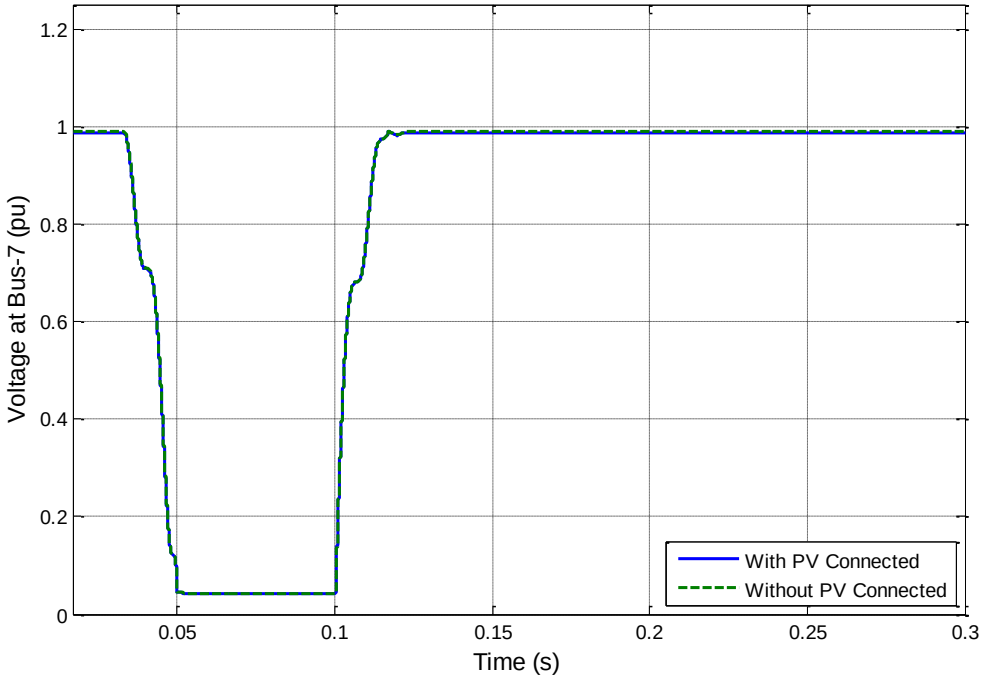

Figure 6.12: Voltage at Bus-7 when a 3-phase fault occurs at Bus-6

From Figure 6.9 to Figure 6.12, it can be seen that nearer the bus to the fault, greater is the voltage depression during the fault.

6.1.3 Fault at Bus-2

A three phase fault is applied at bus-2. According to the topology of the microgrid, it should be noticed that applying fault at bus-2 should have a prominent effect on all the buses except the generator bus.

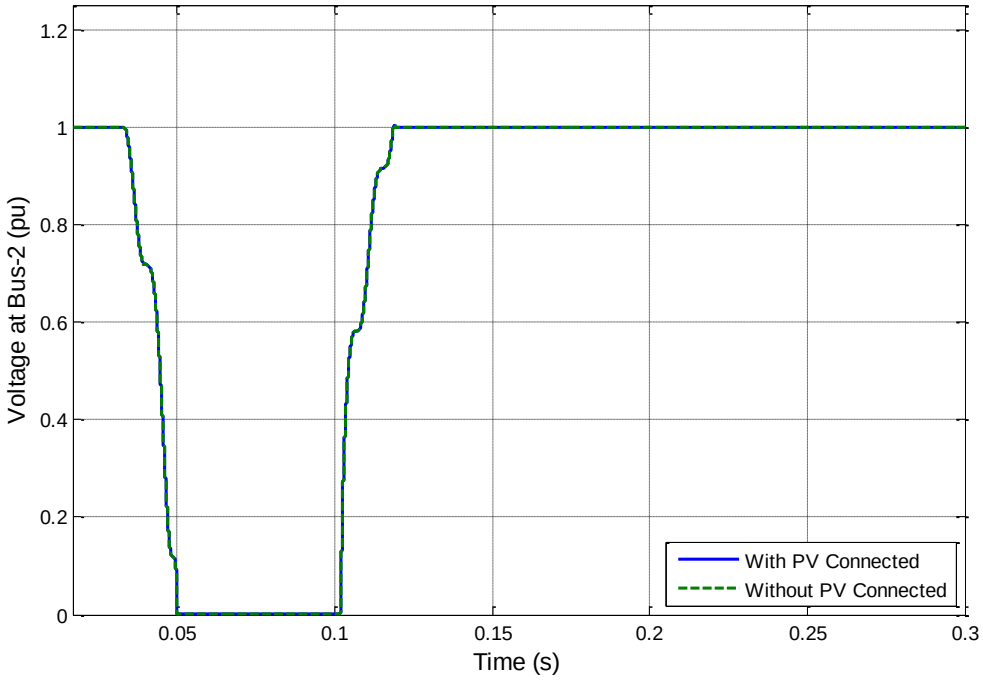

Figure 6.13: Voltage at Bus-2 when a 3-phase fault occurs at Bus-2

In the case of bus-2, the voltage remains zero even when PV is connected.

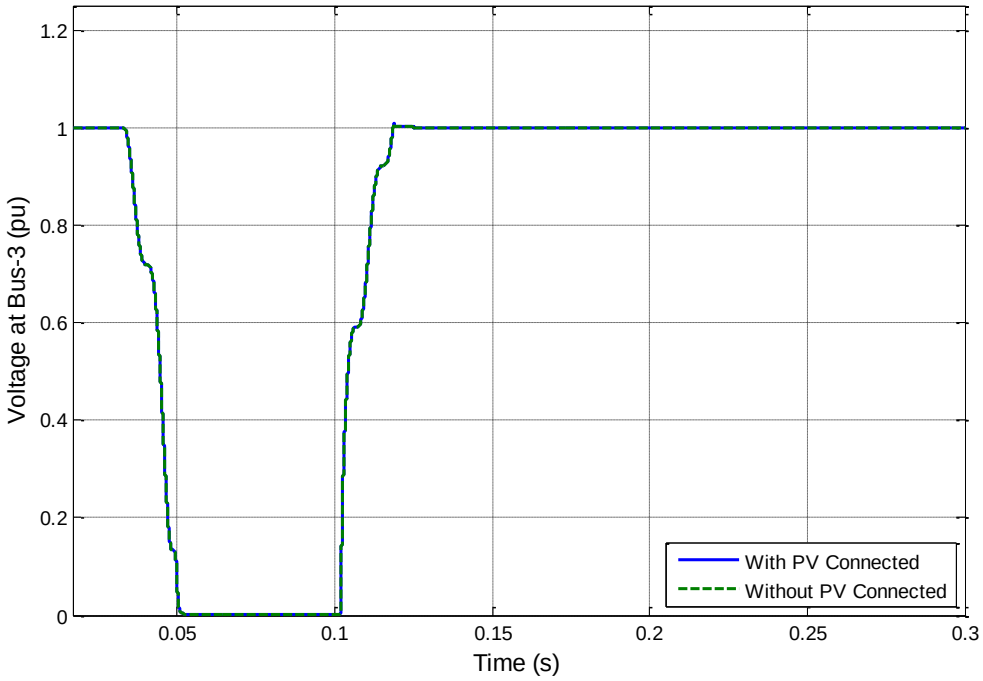

Figure 6.14: Voltage at Bus-3 when a 3-phase fault occurs at Bus-2

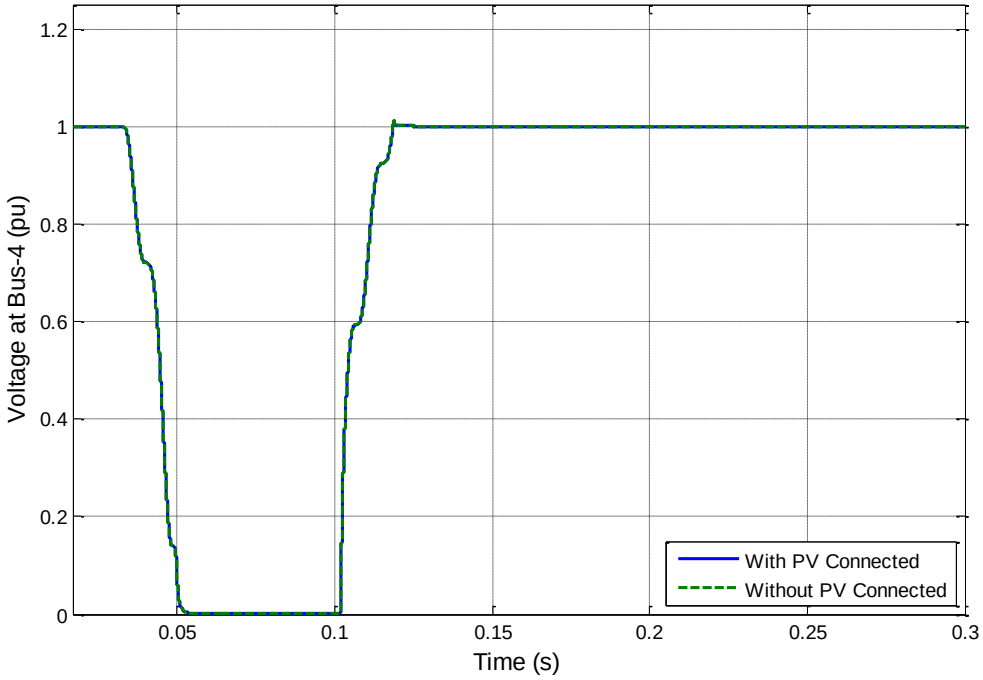

Figure 6.15: Voltage at Bus-4 when a 3-phase fault occurs at Bus-2

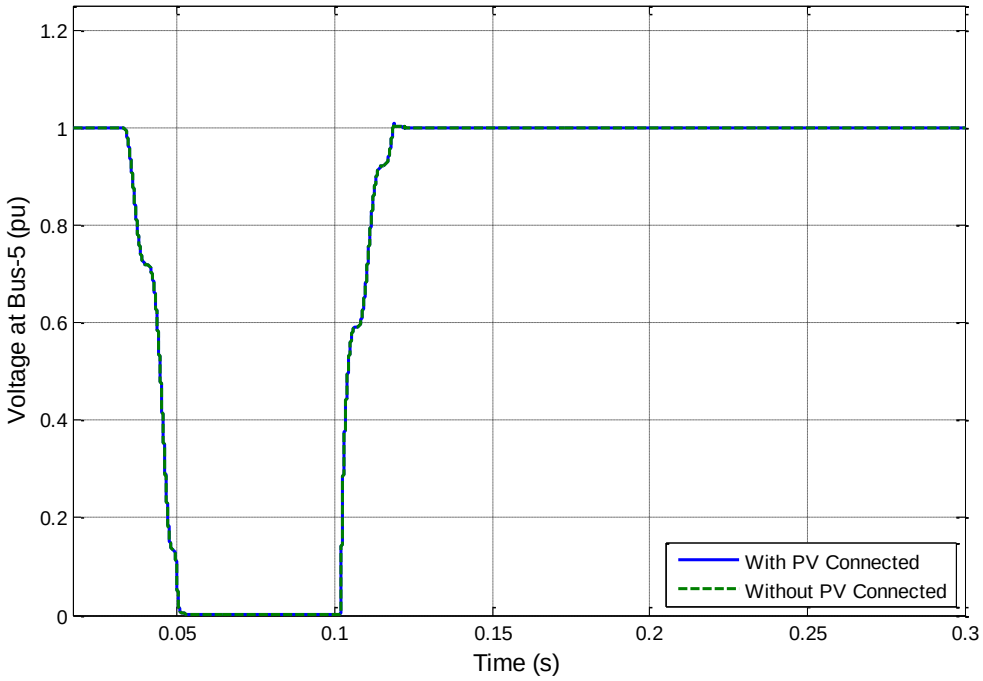

Figure 6.16: Voltage at Bus-5 when a 3-phase fault occurs at Bus-2

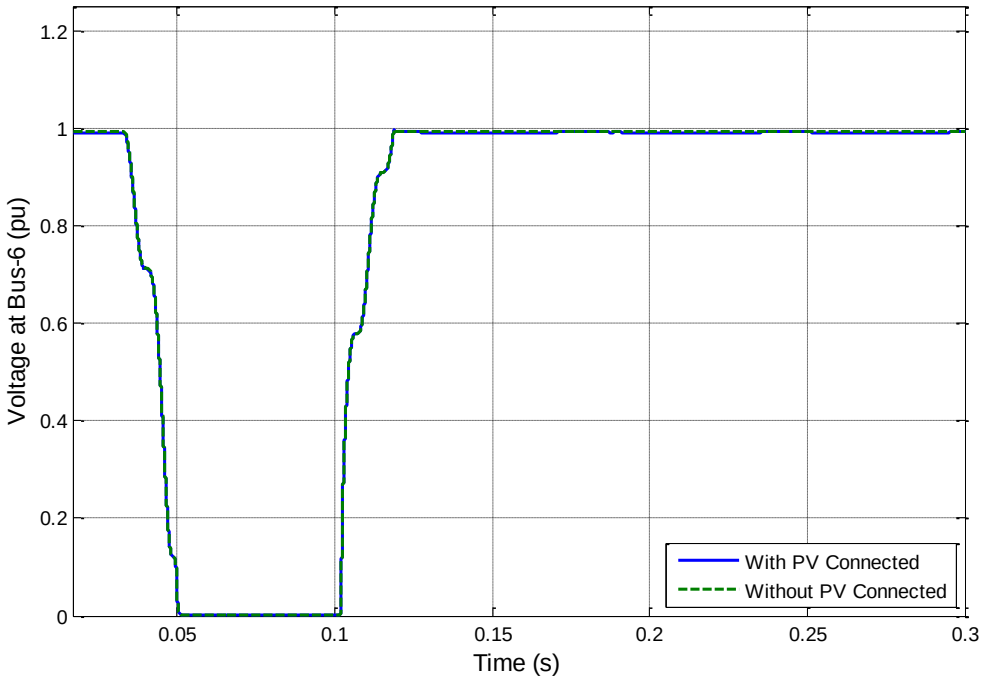

Figure 6.17: Voltage at Bus-6 when a 3-phase fault occurs at Bus-2

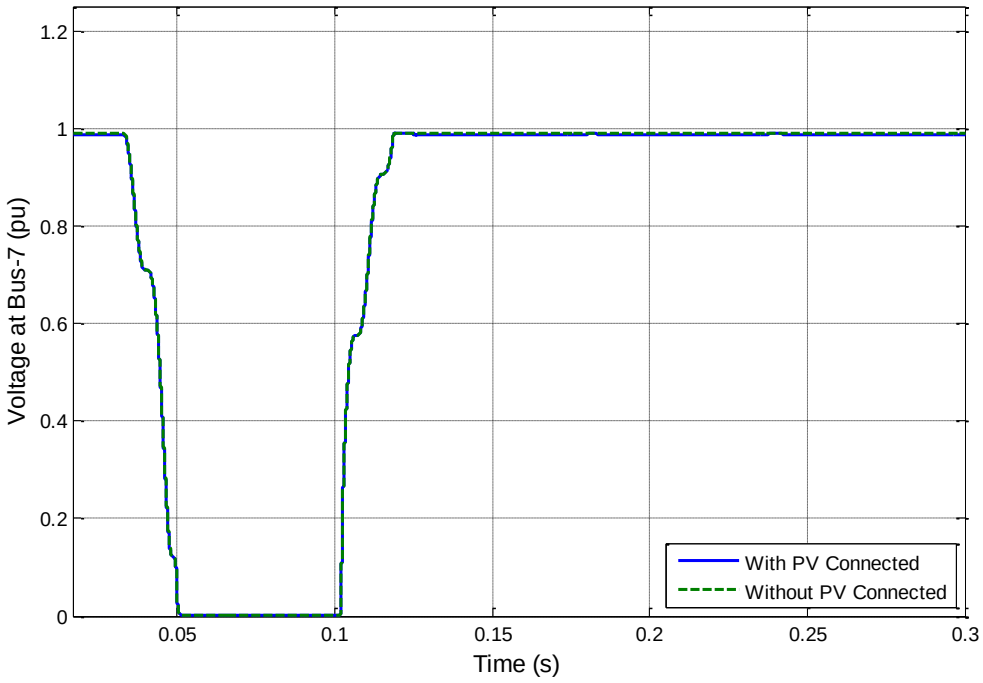

Figure 6.18: Voltage at Bus-7 when a 3-phase fault occurs at Bus-2

The power to all the buses passes through bus-2, therefore when short circuit fault was applied at bus-2, the voltages at bus-3, 4, 5, 6 & 7 decreases. There is no difference in the RMS waveform whether or not the PV system is connected to the grid.

6.2 Single Phase Faults

Single phase faults have been applied at buses 2, 6 & 7 for a duration of 4 cycles, from $t = 0.0333\ s$ to $t = 0.1\ s$.

6.2.1 Fault at bus-7

Single phase fault is applied at bus-7 on phase-A. The following results are obtained.

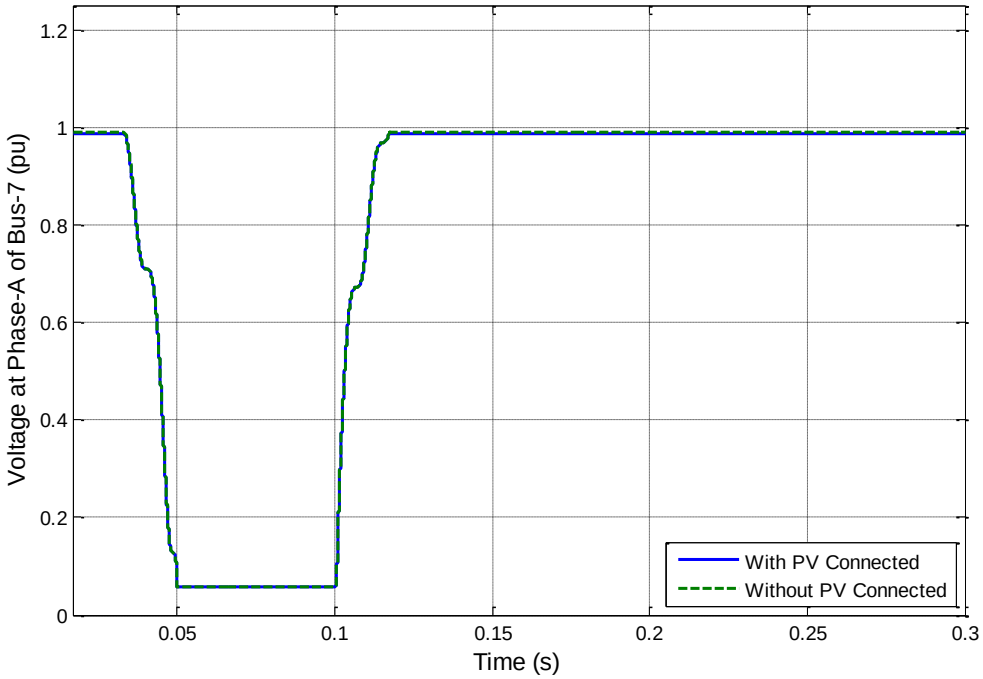

Figure 6.19: Voltage at Phase-A of Bus-7 when a Single-phase fault occurs at Phase-A of Bus-7

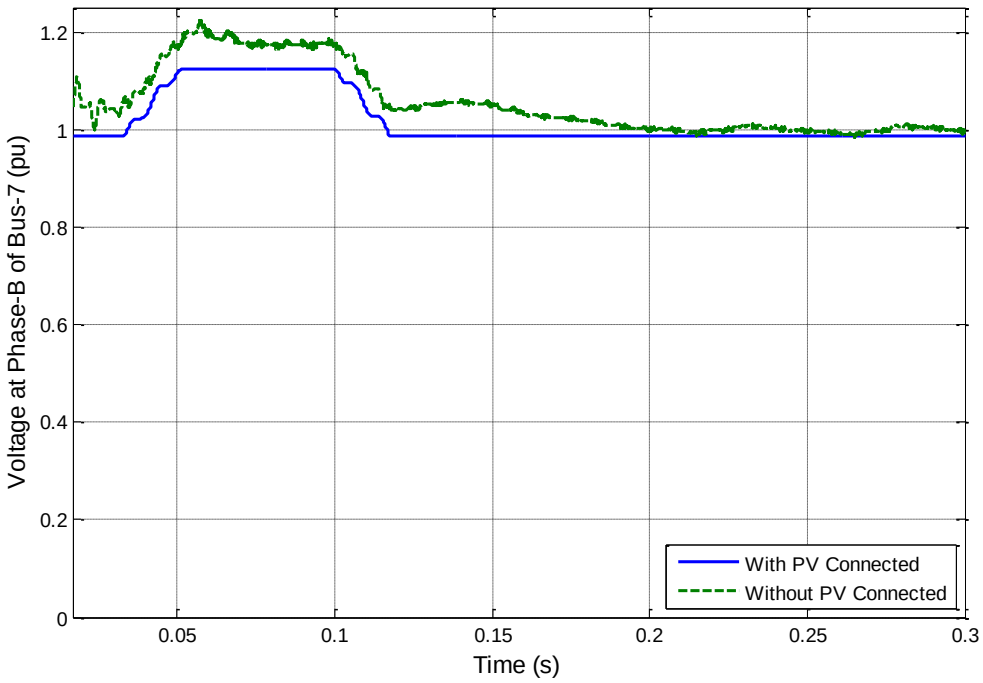

Figure 6.20: Voltage at Phase-B of Bus-7 when a Single-phase fault occurs at Phase-A of Bus-7

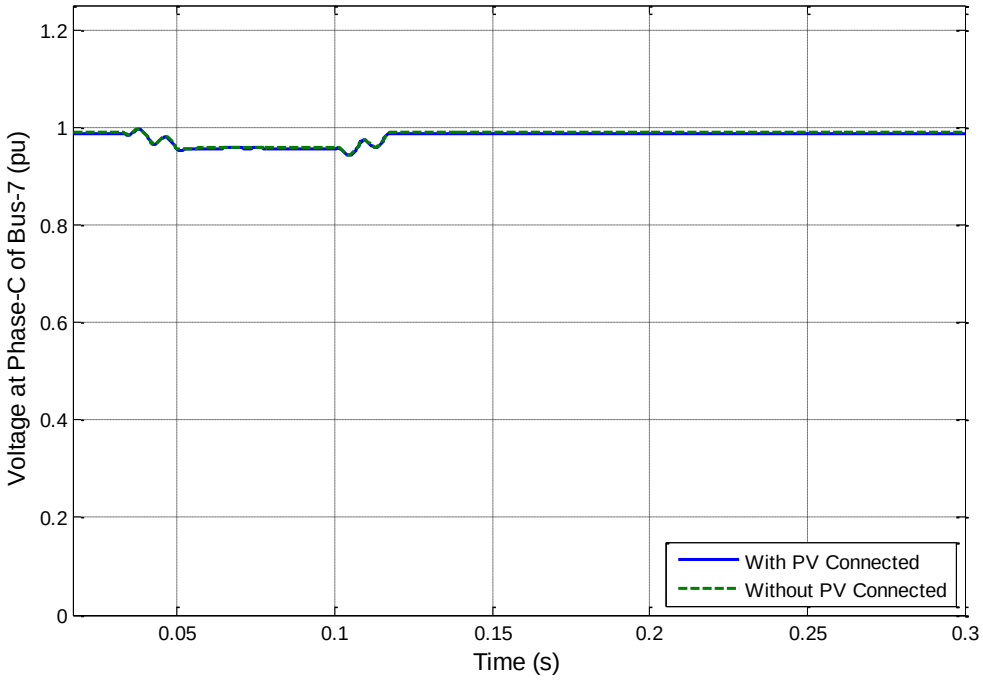

Figure 6.21: Voltage at Phase-C of Bus-7 when a Single-phase fault occurs at Phase-A of Bus-7

Figure 6.19 shows the phase-A of bus-7. As the fault is applied at phase-A, the voltage remains near to zero during the fault. Figure 6.20 and Figure 6.21, it can be noticed that at bus-7, there are high variations in the voltage of phase B & C, but in phase B voltage increases during the fault where as it decreases in phase C during the fault.

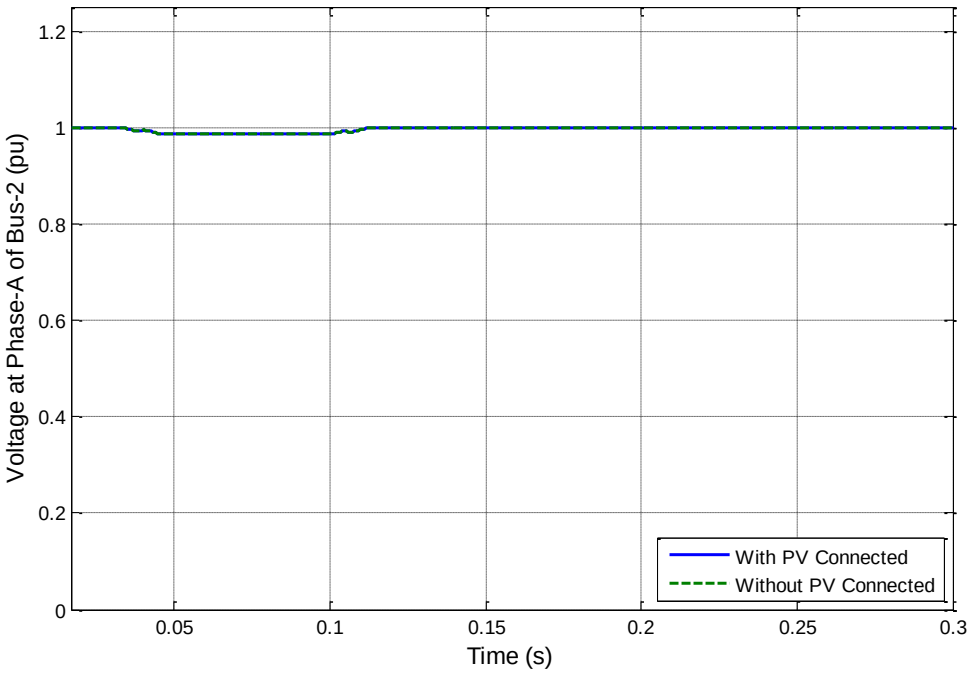

Figure 6.22: Voltage at Phase-A of Bus-2 when a Single-phase fault occurs at Phase-A of Bus-7

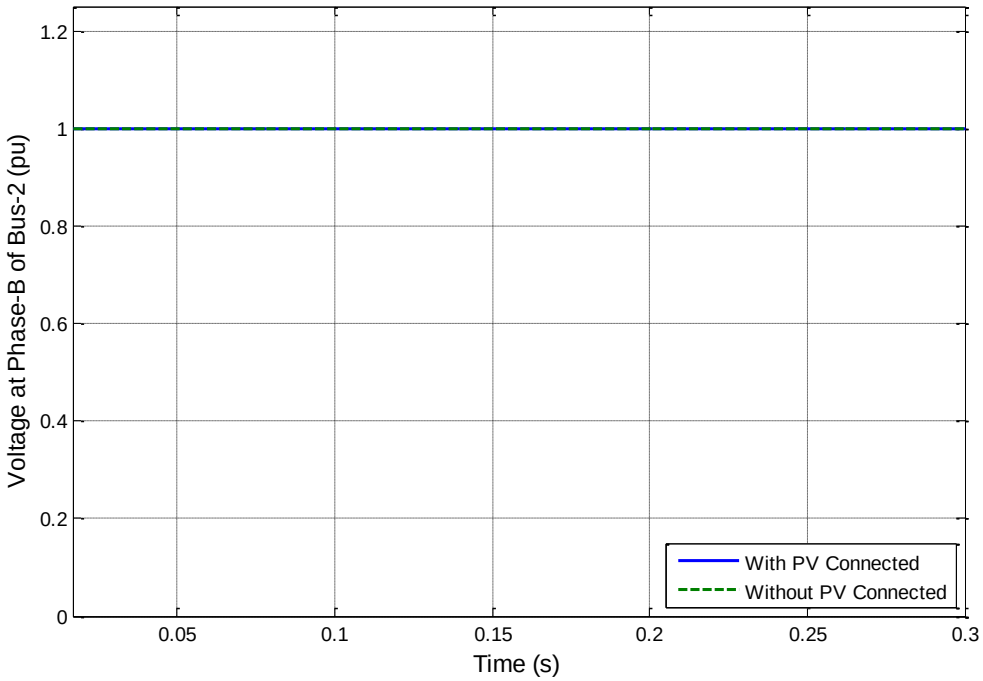

Figure 6.23: Voltage at Phase-B of Bus-2 when a Single-phase fault occurs at Phase-A of Bus-7

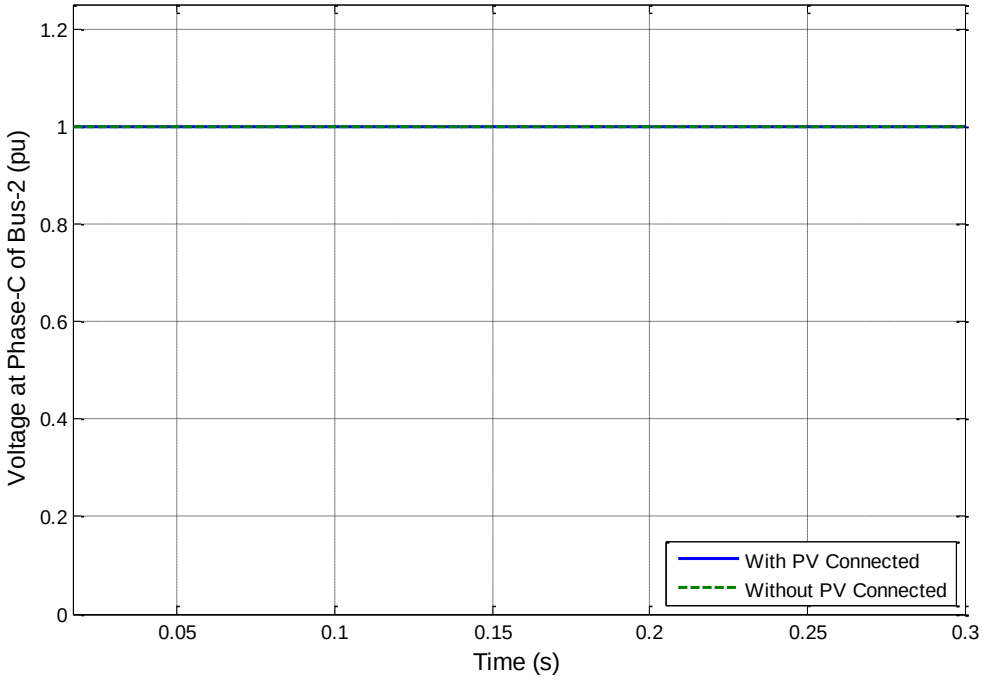

Figure 6.24: Voltage at Phase-C of Bus-2 when a Single-phase fault occurs at Phase-A of Bus-7

From Figure 6.22 to Figure 6.24, it can be noticed that at bus-2, there are no variations of voltage in all the phases when the fault occurs at phase A of bus-7. This is due to the situation of bus-2 such that it has no effects if a short circuit occurs at any bus of the system except the generator bus.

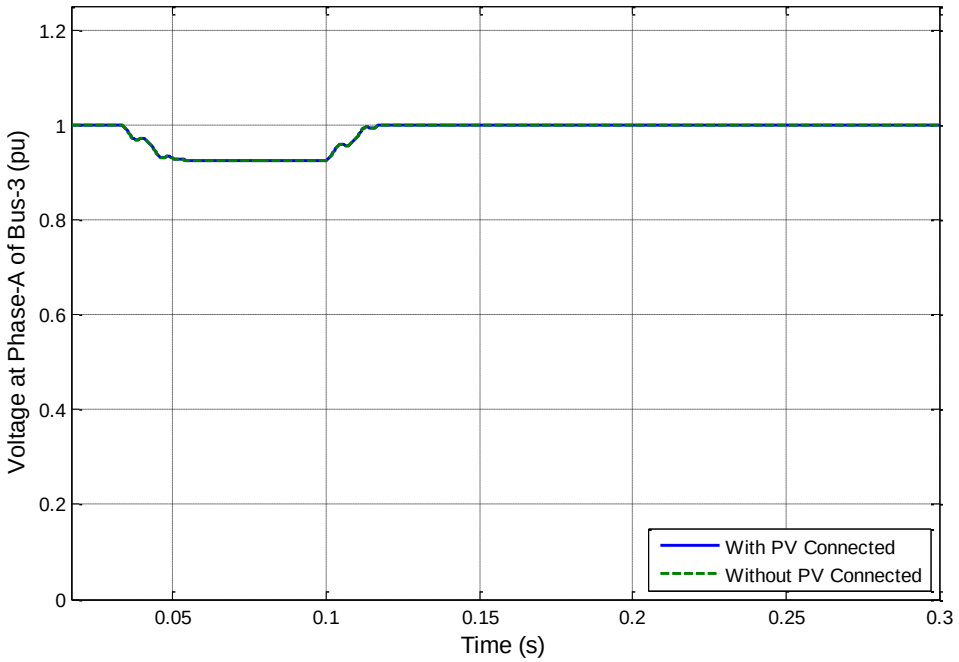

Figure 6.25: Voltage at Phase-A of Bus-3 when a Single-phase fault occurs at Phase-A of Bus-7

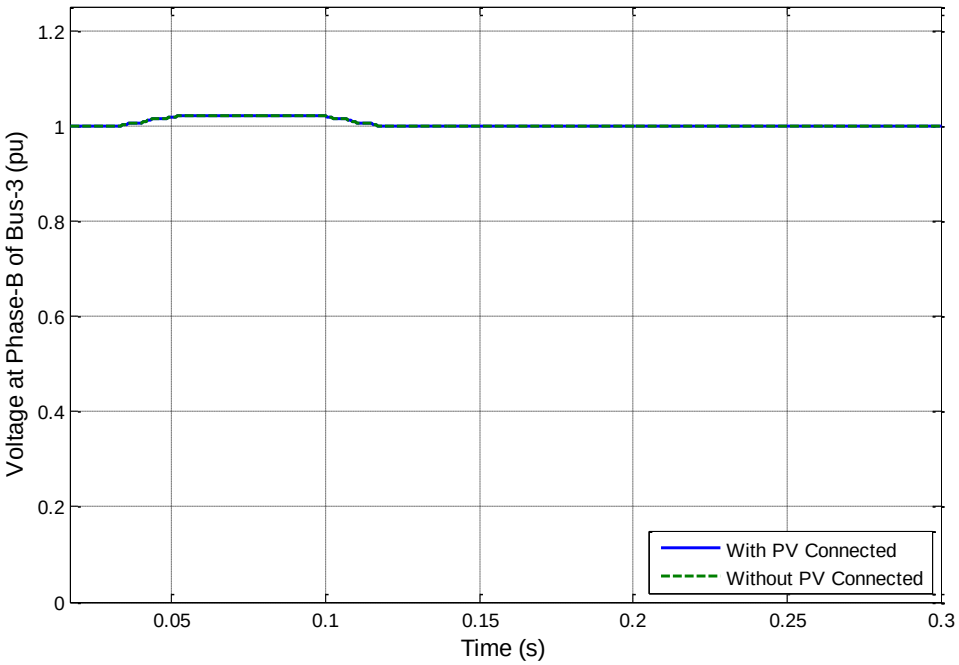

Figure 6.26: Voltage at Phase-B of Bus-3 when a Single-phase fault occurs at Phase-A of Bus-7

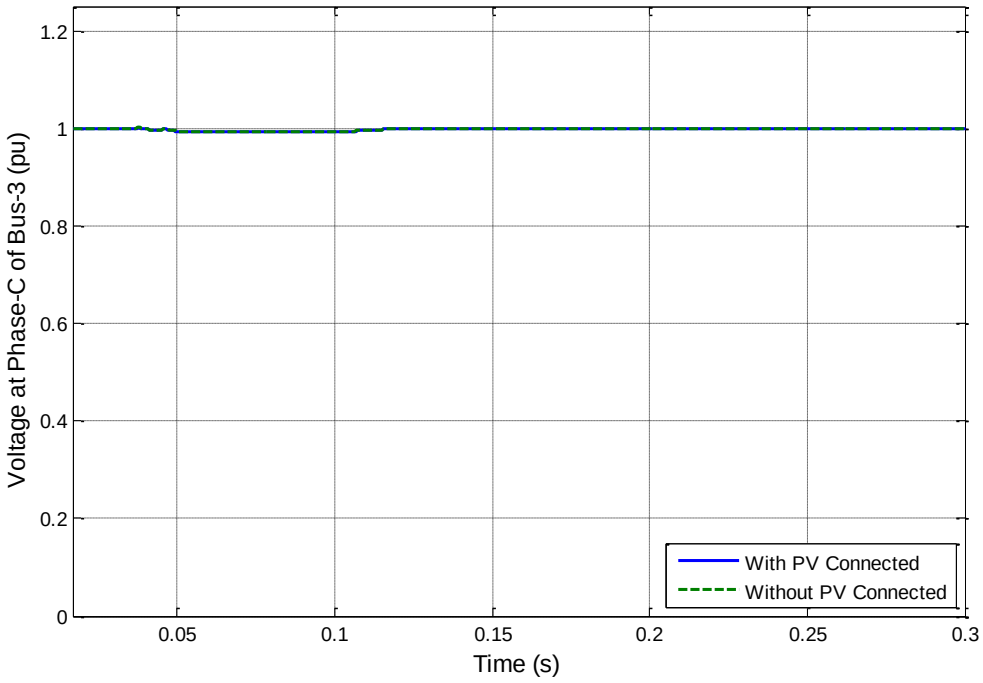

Figure 6.27: Voltage at Phase-C of Bus-3 when a Single-phase fault occurs at Phase-A of Bus-7

From Figure 6.25 to Figure 6.27, it can be noticed that at bus-3, there are little variations in the voltage of all the phases, on the other hand phase-A has the highest variations as the fault occurs at phase-A.

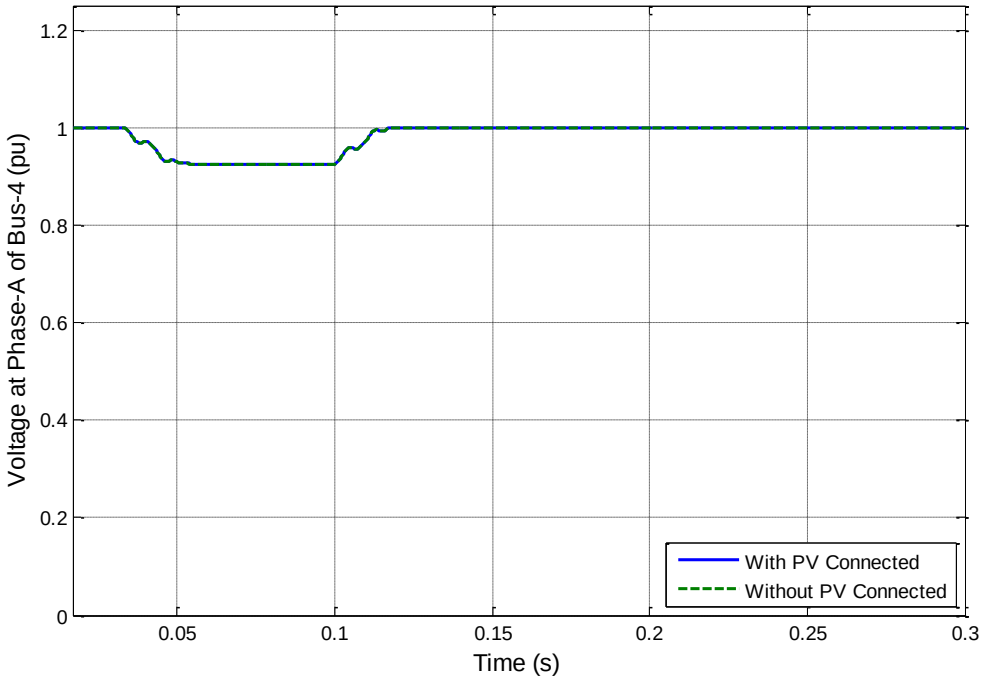

Figure 6.28: Voltage at Phase-A of Bus-4 when a Single-phase fault occurs at Phase-A of Bus-7

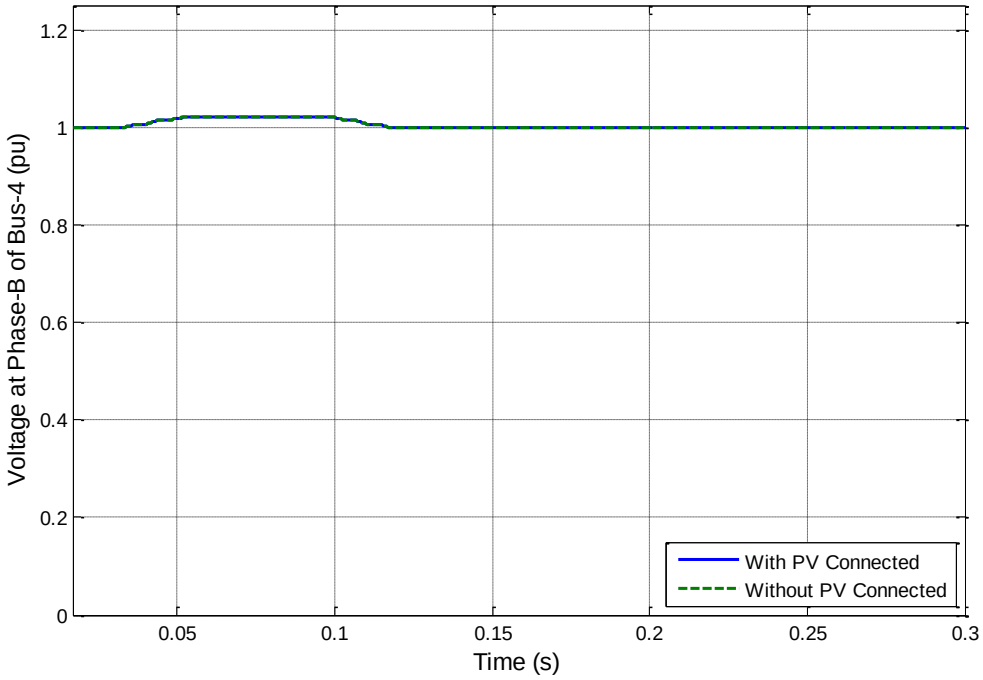

Figure 6.29: Voltage at Phase-B of Bus-4 when a Single-phase fault occurs at Phase-A of Bus-7

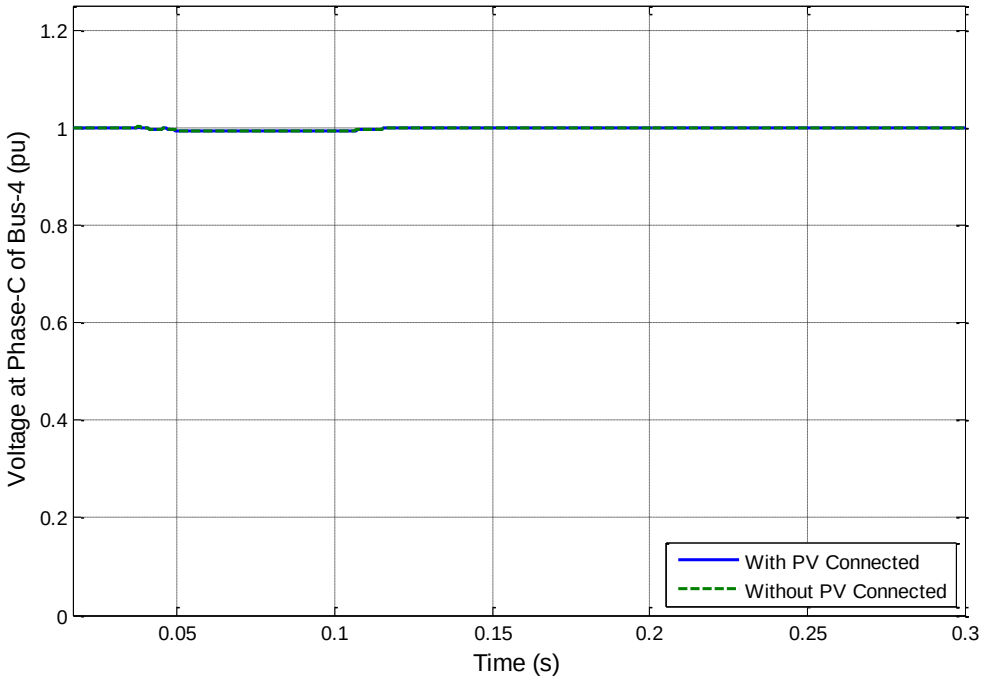

Figure 6.30: Voltage at Phase-C of Bus-4 when a Single-phase fault occurs at Phase-A of Bus-7

From Figure 6.28 to Figure 6.30, it can be noticed that at bus-4, there are little variations in the voltage of all the phases. As the fault occurs at phase-A, it has the highest variations.

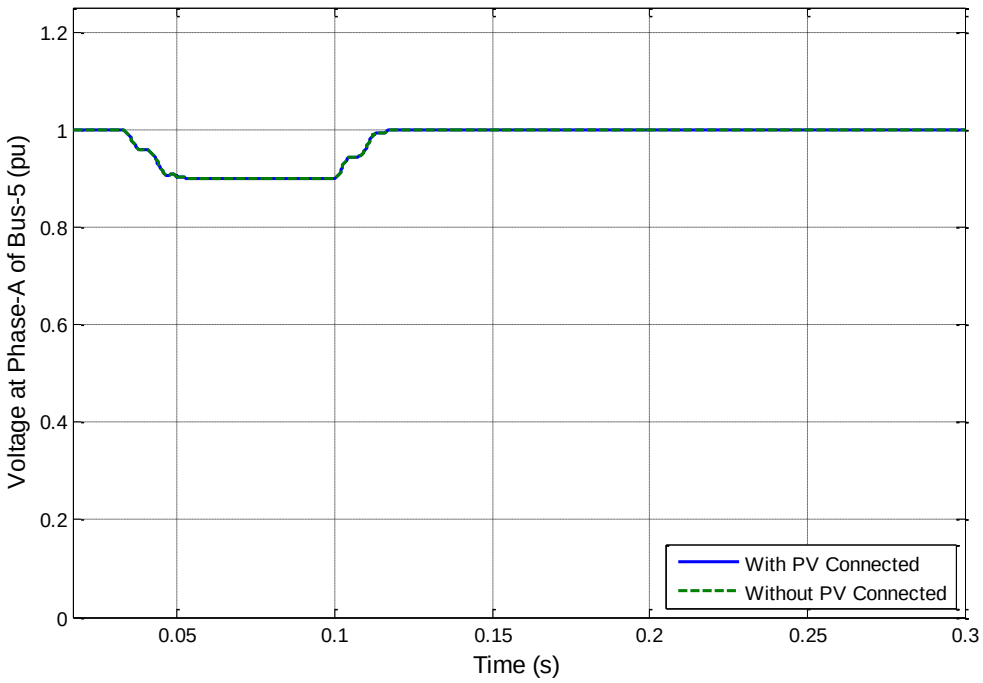

Figure 6.31: Voltage at Phase-A of Bus-5 when a Single-phase fault occurs at Phase-A of Bus-7

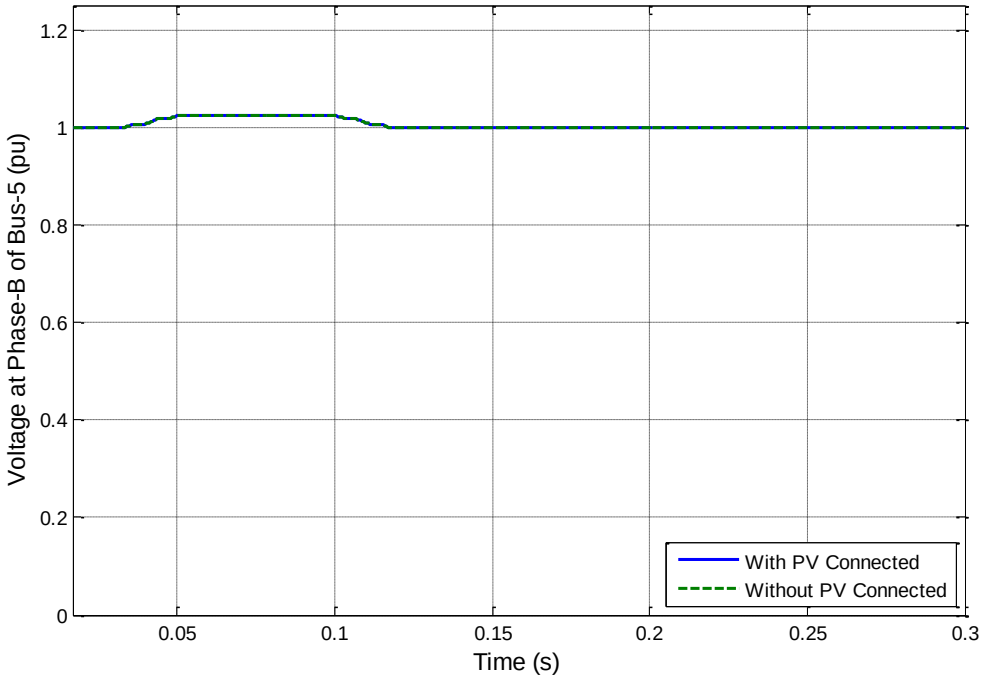

Figure 6.32: Voltage at Phase-B of Bus-5 when a Single-phase fault occurs at Phase-A of Bus-7

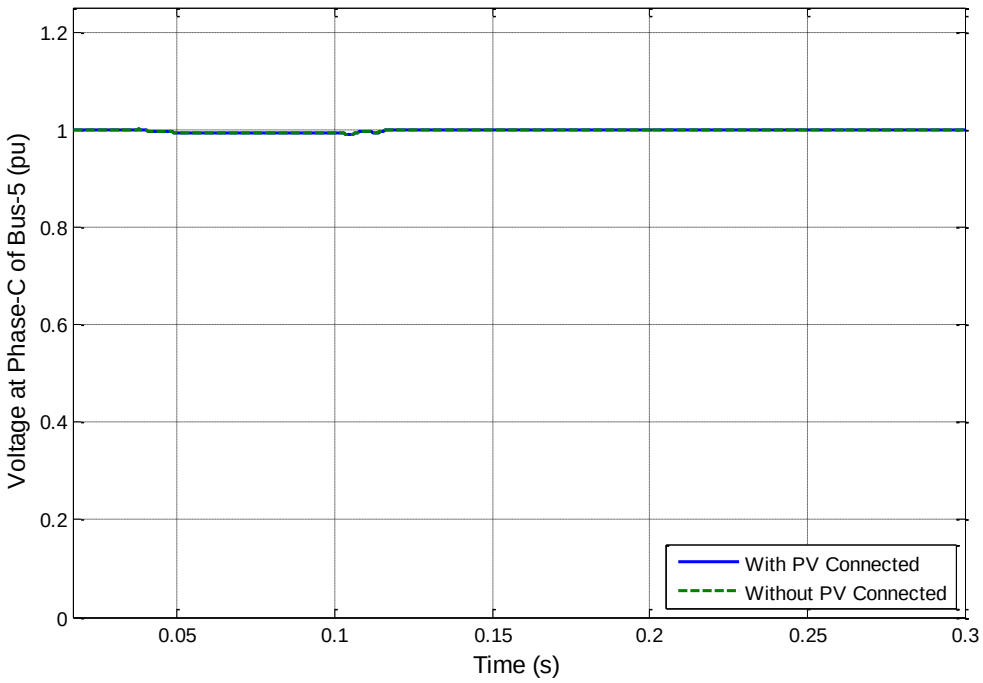

Figure 6.33: Voltage at Phase-C of Bus-5 when a Single-phase fault occurs at Phase-A of Bus-7

From Figure 6.31 to Figure 6.33, it can be noticed that at bus-5, there are little variations in the voltage of phase B & C. Phase-A has the highest variations as the fault occurs at phase-A.

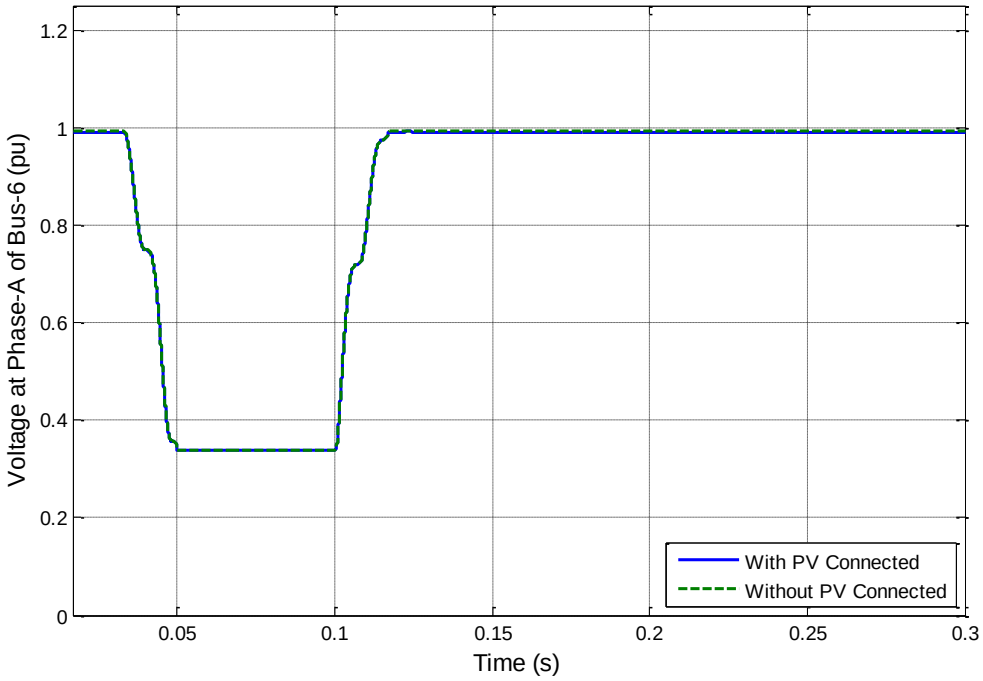

Figure 6.34: Voltage at Phase-A of Bus-6 when a Single-phase fault occurs at Phase-A of Bus-7

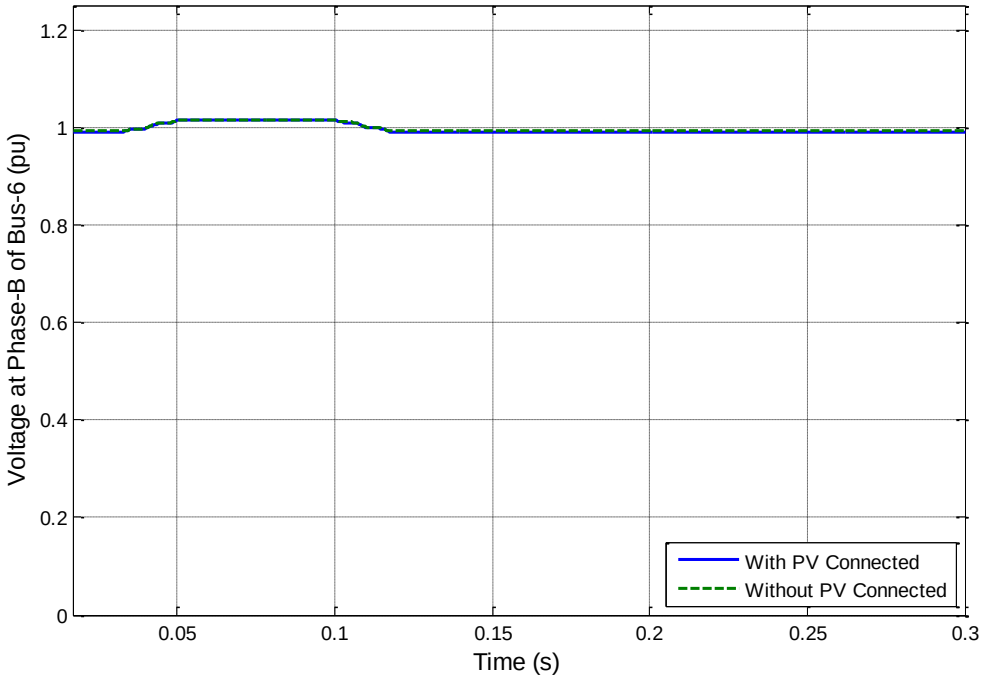

Figure 6.35: Voltage at Phase-B of Bus-6 when a Single-phase fault occurs at Phase-A of Bus-7

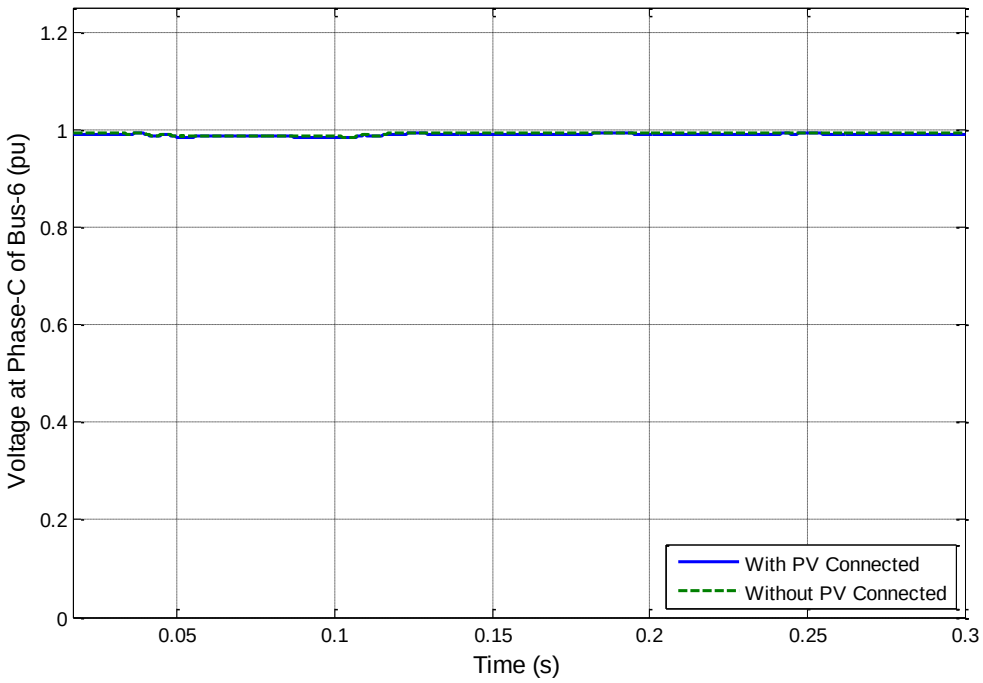

Figure 6.36: Voltage at Phase-C of Bus-6 when a Single-phase fault occurs at Phase-A of Bus-7

From Figure 6.34 to Figure 6.36, it can be noticed that at bus-6, there are variations in the voltage of phase B & C, but there is a significant drop in phase-A.

From Figure 6.19 to Figure 6.36, it can be seen that when the fault is applied at phase A of bus-7, there are little variations at the other phases during the fault. If the voltage waveform of phase A is observed, it can be seen that there is more prominent decreases in the voltage of the buses.

6.2.2 Fault at Bus-6

Single phase fault is applied at bus-6 on phase-A. The following results are obtained.

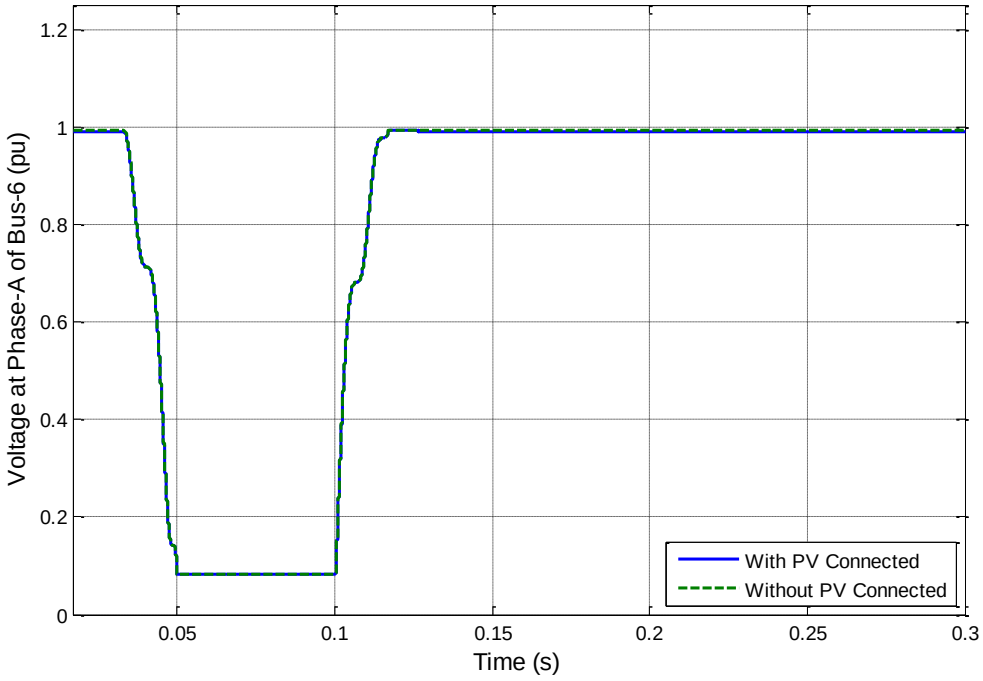

Figure 6.37: Voltage at Phase-A of Bus-6 when a Single-phase fault occurs at Phase-A of Bus-6

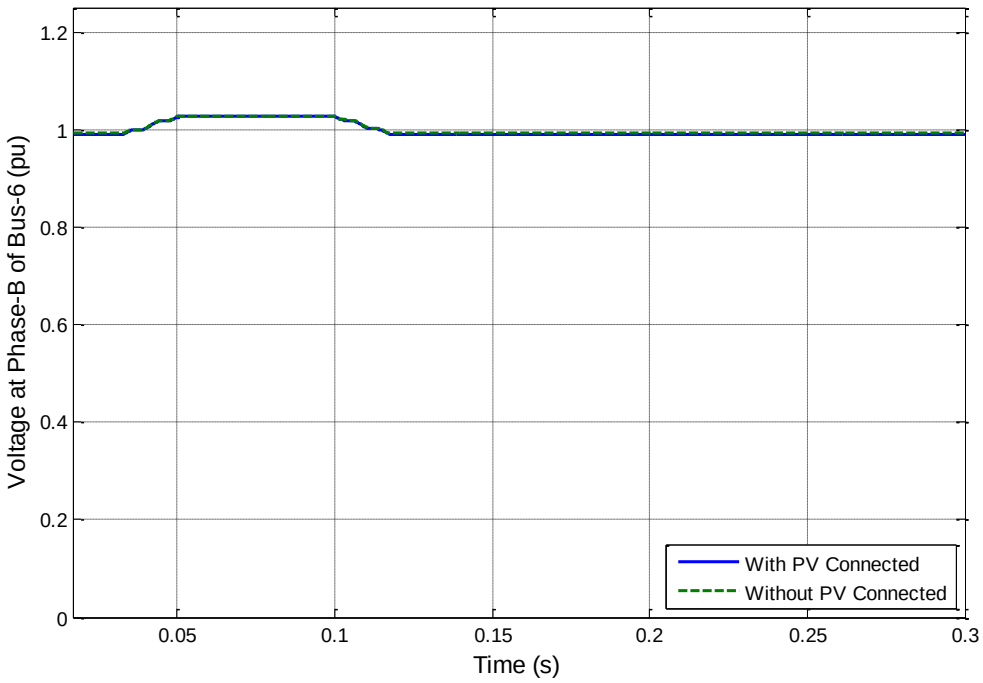

Figure 6.38: Voltage at Phase-B of Bus-6 when a Single-phase fault occurs at Phase-A of Bus-6

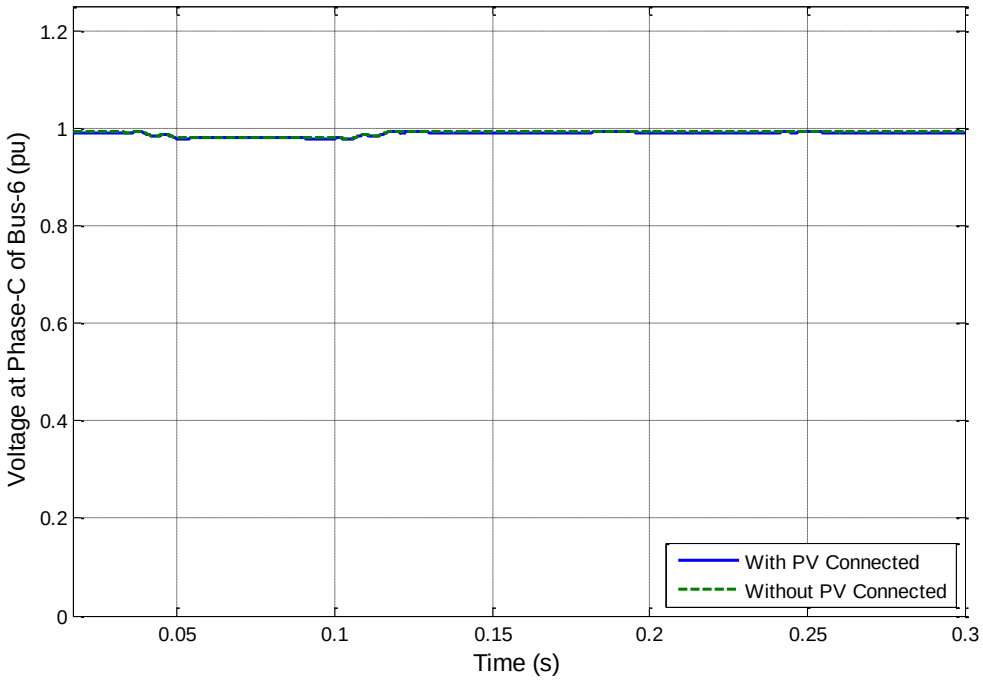

Figure 6.39: Voltage at Phase-C of Bus-6 when a Single-phase fault occurs at Phase-A of Bus-6

From Figure 6.37 to Figure 6.39, it can be noticed that at bus-6, there are variations in the voltage of phase B & C, but in phase B voltage increases during the fault where as it decreases in phase C during the fault. In phase-A, there is a huge drop in the voltage as the fault occurs in phase-A.

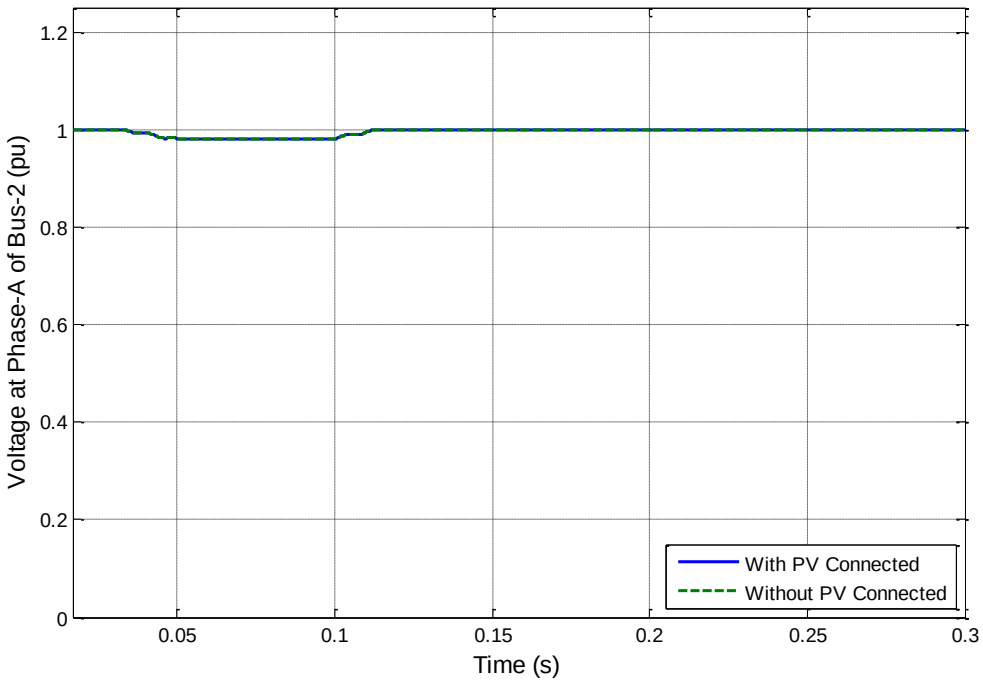

Figure 6.40: Voltage at Phase-A of Bus-2 when a Single-phase fault occurs at Phase-A of Bus-6

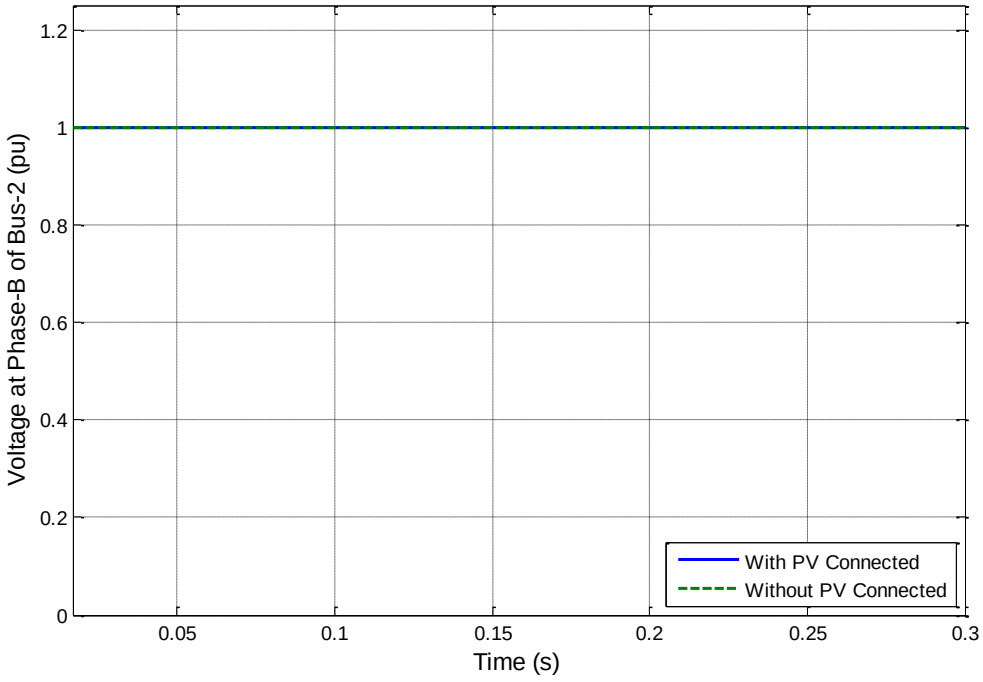

Figure 6.41: Voltage at Phase-B of Bus-2 when a Single-phase fault occurs at Phase-A of Bus-6

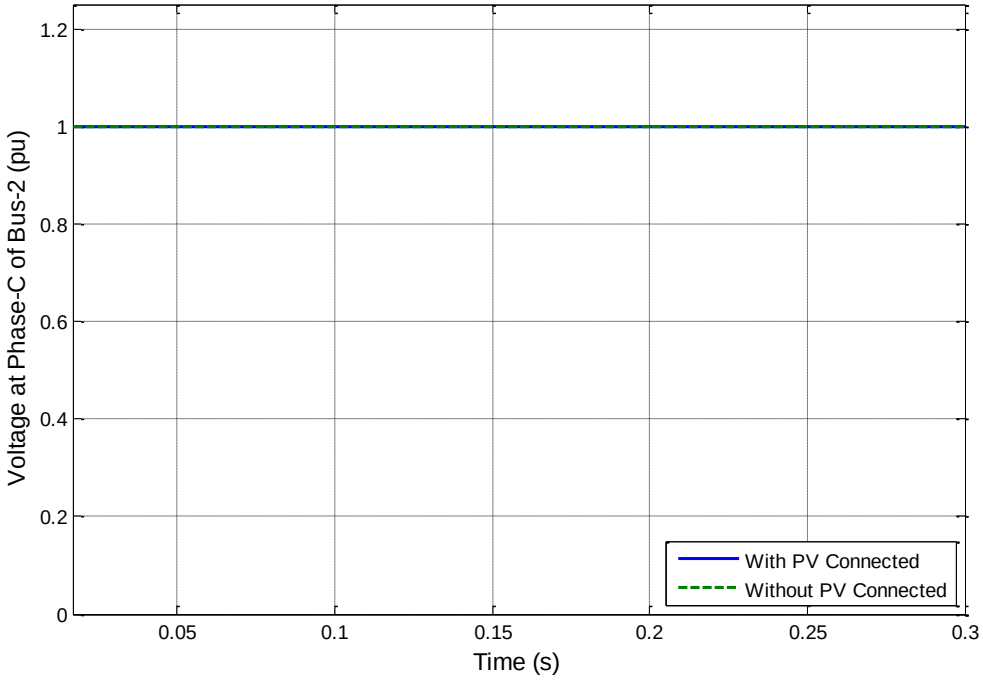

Figure 6.42: Voltage at Phase-C of Bus-2 when a Single-phase fault occurs at Phase-A of Bus-6

From Figure 6.40 to Figure 6.42, it can be noticed that at bus-2, there are no variations of voltage in phase B or C when the fault occurs at phase A of bus-6. This is due to the situation of bus-2 such that it has no effects if a short circuit occurs at any bus of the system except the generator bus. In phase-A, there is a small decrease in the voltage during the fault.

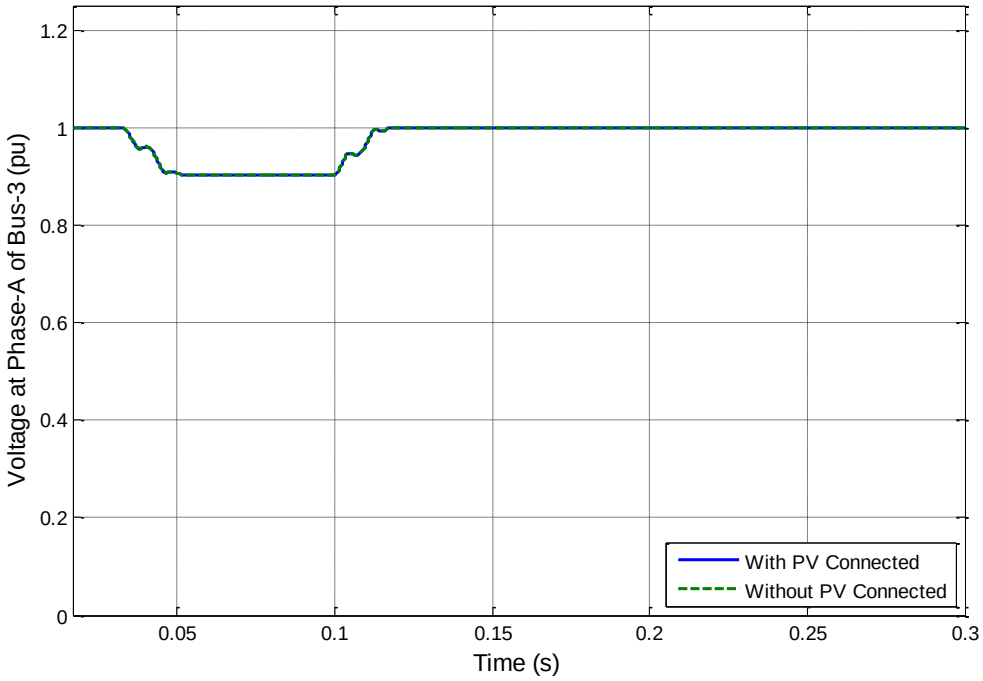

Figure 6.43: Voltage at Phase-A of Bus-3 when a Single-phase fault occurs at Phase-A of Bus-6

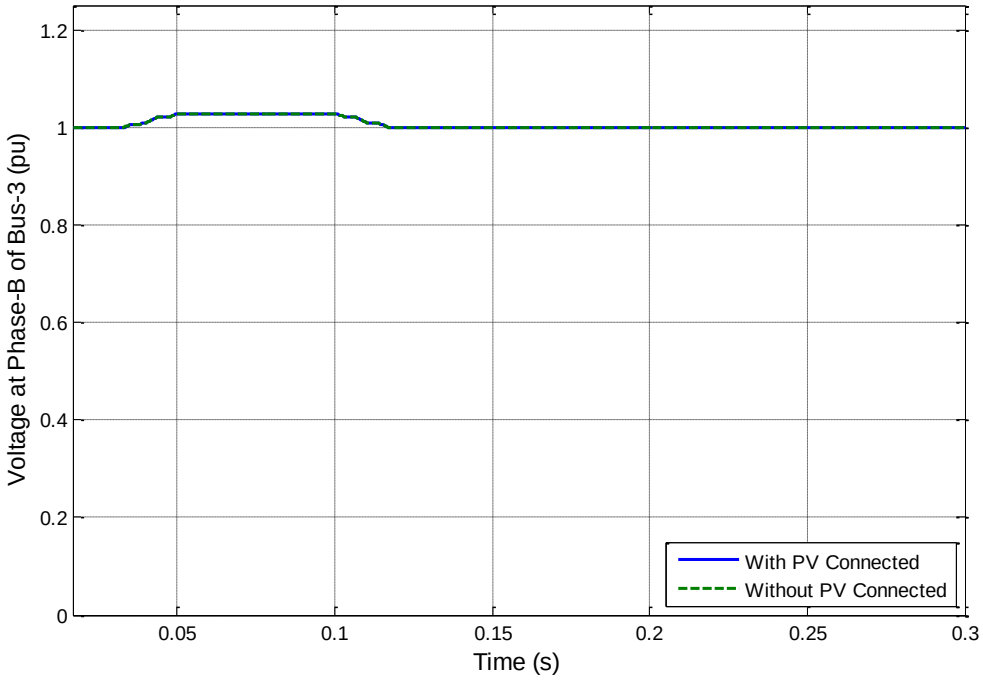

Figure 6.44: Voltage at Phase-B of Bus-3 when a Single-phase fault occurs at Phase-A of Bus-6

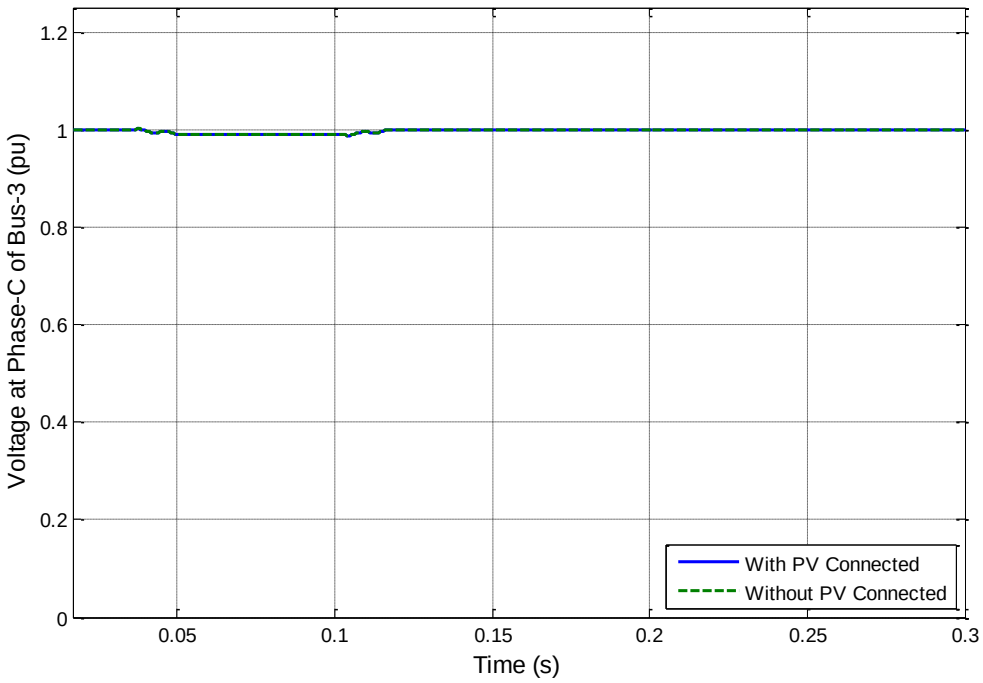

Figure 6.45: Voltage at Phase-C of Bus-3 when a Single-phase fault occurs at Phase-A of Bus-6

From Figure 6.43 to Figure 6.45, it can be noticed that at bus-3, there are little variations in the voltage of phase B & C, but in phase B voltage increases during the fault where as it decreases in phase C during the fault. In phase-A, there is a small decrease in the voltage during the fault.

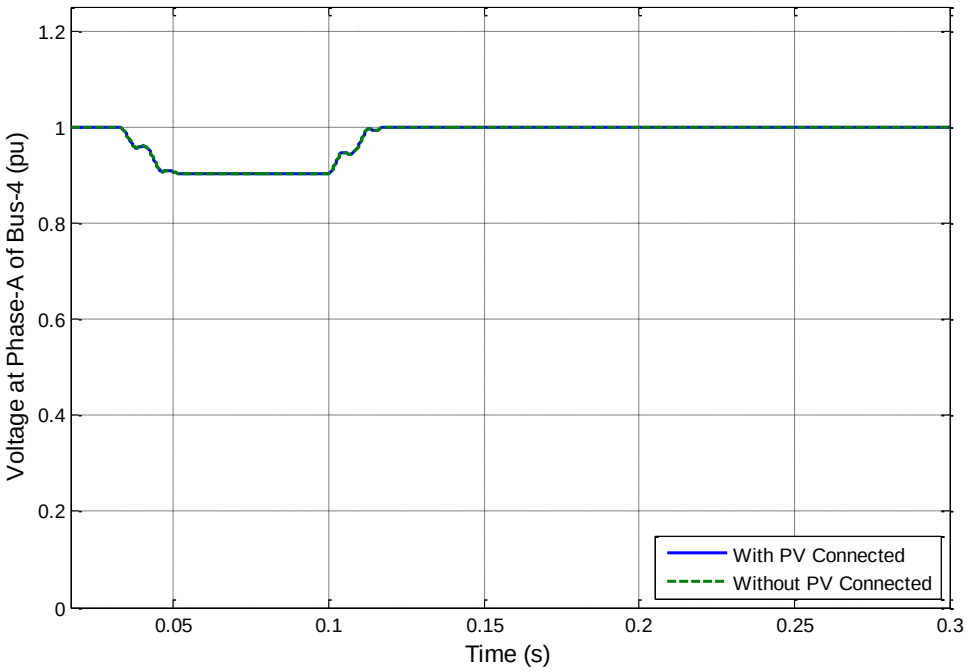

Figure 6.46: Voltage at Phase-A of Bus-4 when a Single-phase fault occurs at Phase-A of Bus-6

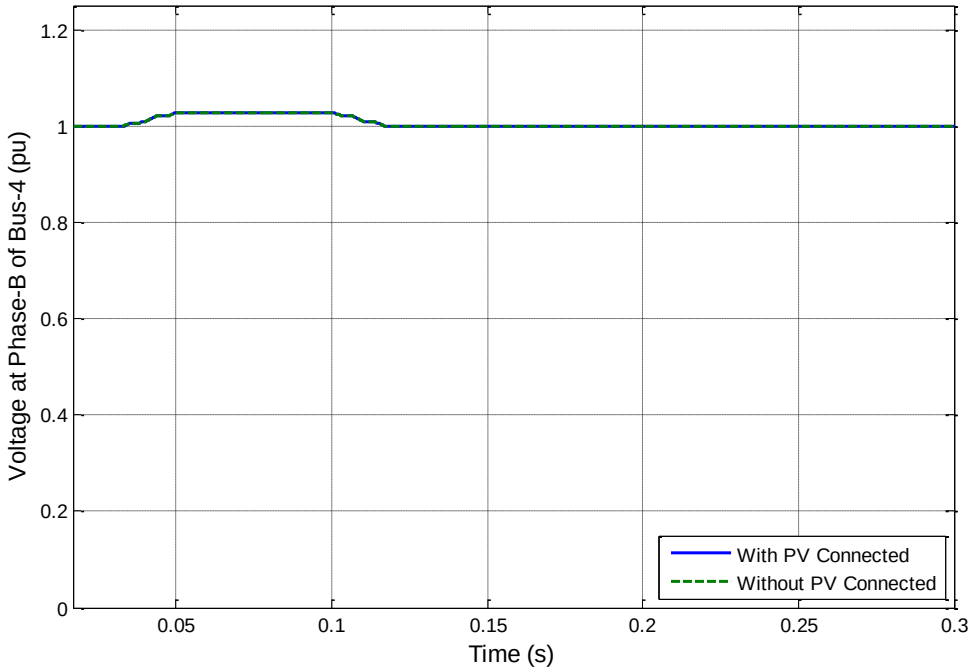

Figure 6.47: Voltage at Phase-B of Bus-4 when a Single-phase fault occurs at Phase-A of Bus-6

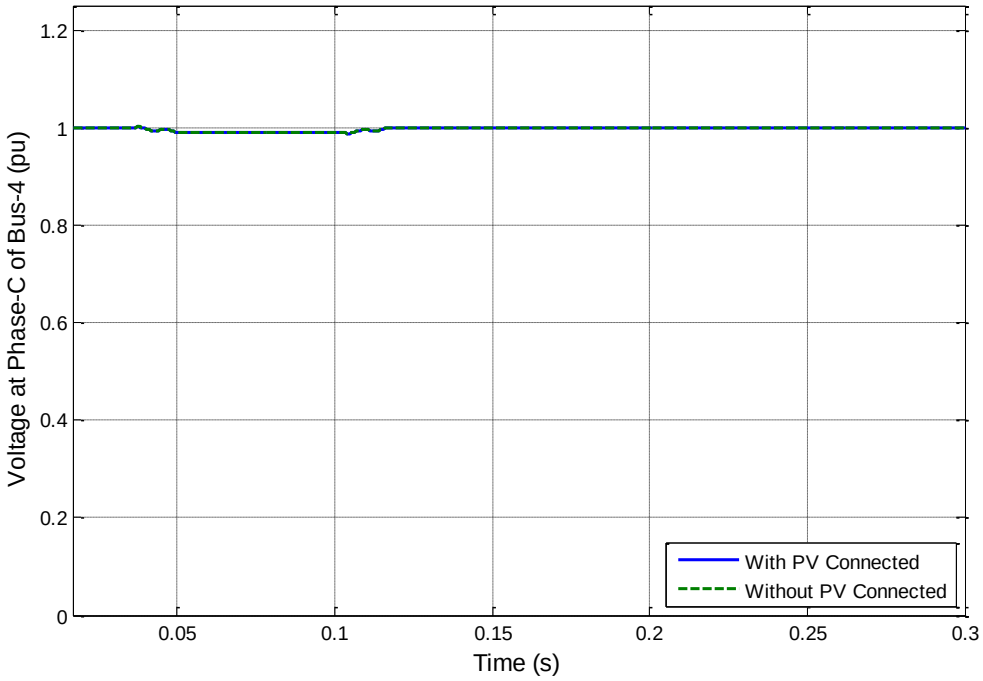

Figure 6.48: Voltage at Phase-C of Bus-4 when a Single-phase fault occurs at Phase-A of Bus-6

From Figure 6.46 to Figure 6.48, it can be noticed that at bus-4, there are little variations in the voltage of phase B & C, but in phase B voltage increases during the fault where as it decreases in phase C during the fault. In phase-A, there is a small decrease in the voltage during the fault.

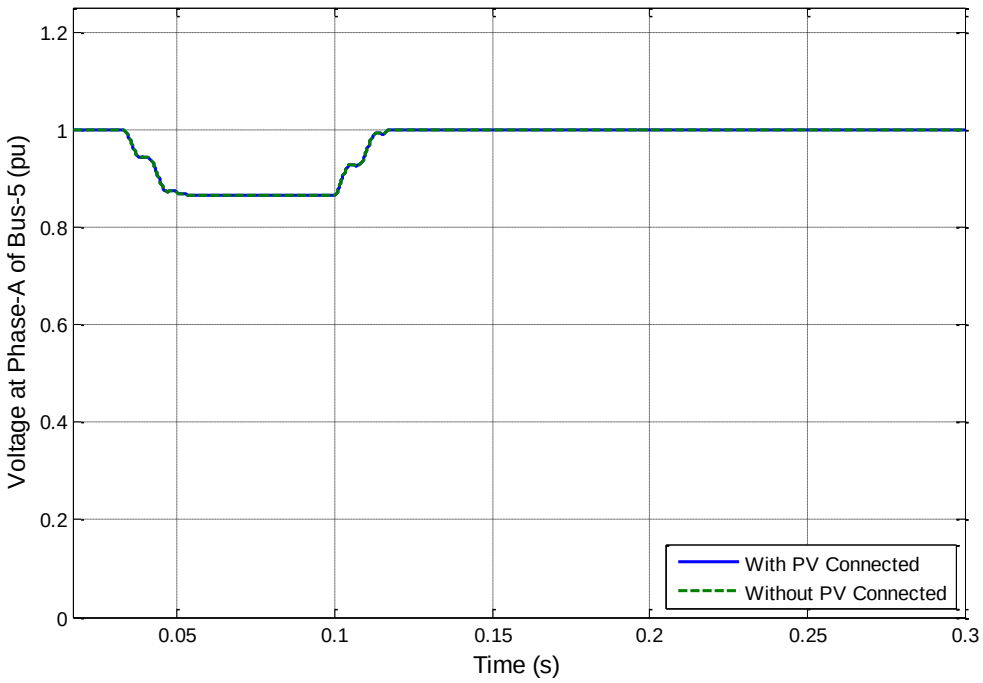

Figure 6.49: Voltage at Phase-A of Bus-5 when a Single-phase fault occurs at Phase-A of Bus-6

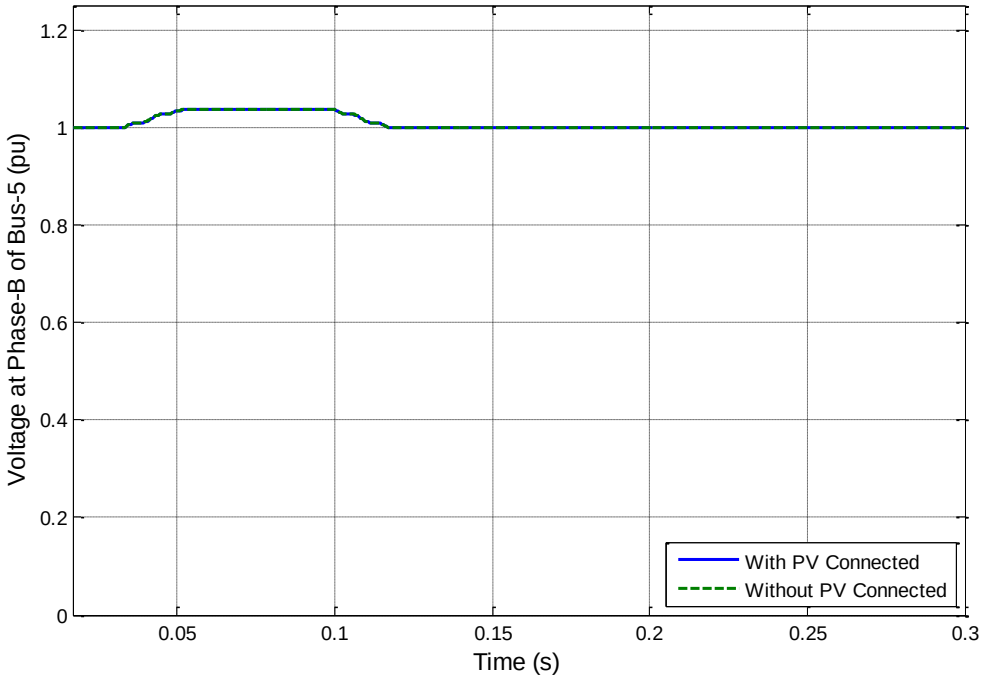

Figure 6.50: Voltage at Phase-B of Bus-5 when a Single-phase fault occurs at Phase-A of Bus-6

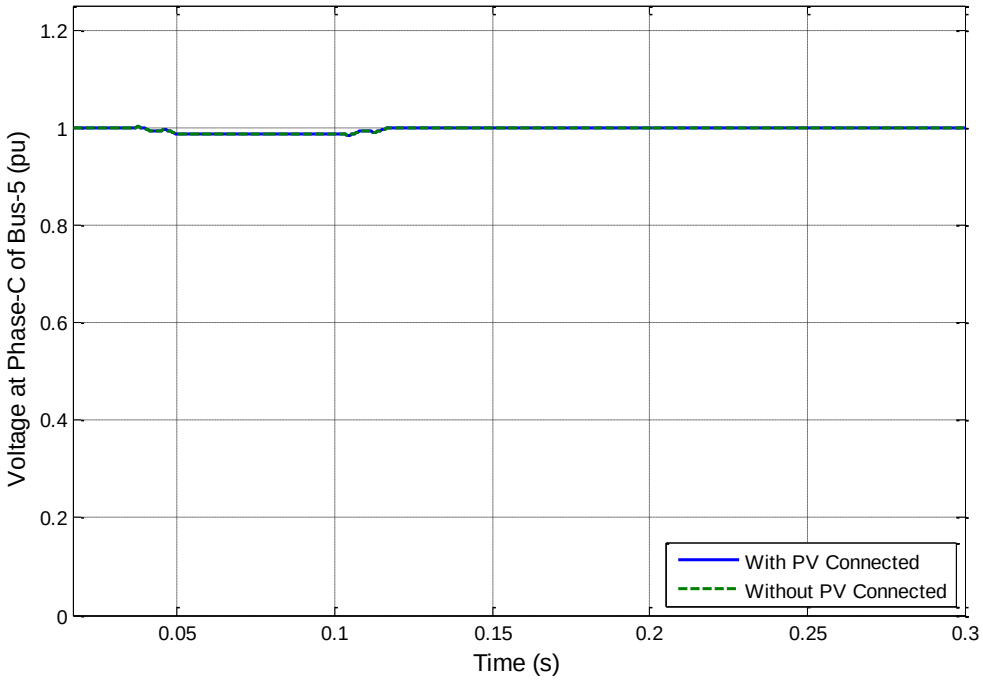

Figure 6.51: Voltage at Phase-C of Bus-5 when a Single-phase fault occurs at Phase-A of Bus-6

From Figure 6.49 to Figure 6.51, it can be noticed that at bus-5, there are little variations in the voltage of phase B & C, but in phase B voltage increases during the fault where as it decreases in phase C during the fault. In phase-A, there is a small decrease in the voltage during the fault.

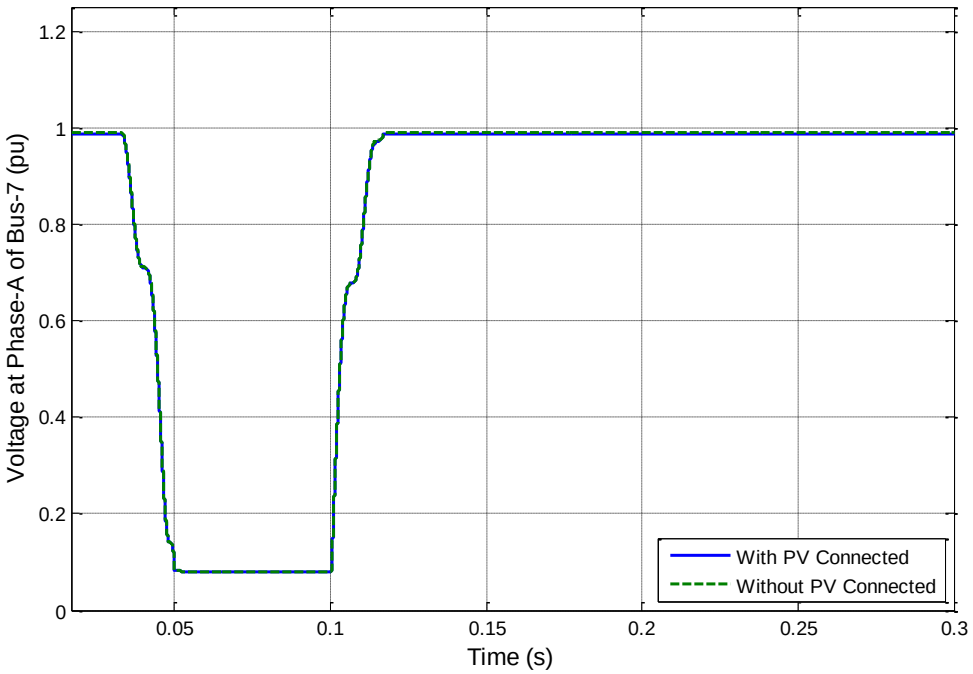

Figure 6.52: Voltage at Phase-A of Bus-7 when a Single-phase fault occurs at Phase-A of Bus-6

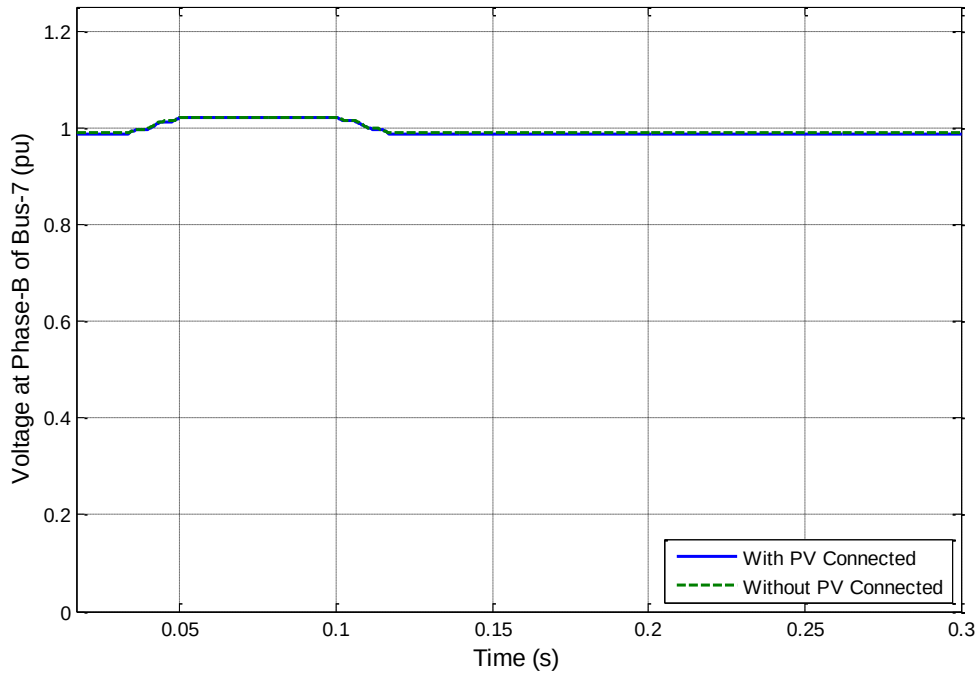

Figure 6.53: Voltage at Phase-B of Bus-7 when a Single-phase fault occurs at Phase-A of Bus-6

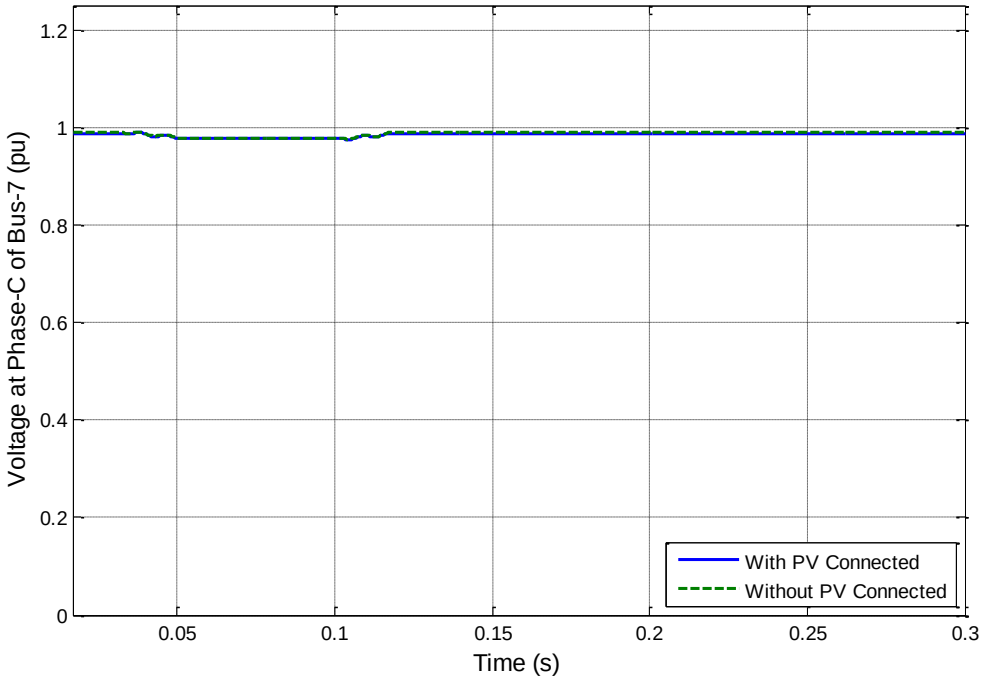

Figure 6.54: Voltage at Phase-C of Bus-7 when a Single-phase fault occurs at Phase-A of Bus-6

From Figure 6.52 to Figure 6.54, it can be noticed that at bus-7, there are some variations in the voltage of phase B & C, but in phase B voltage increases during the fault where as it decreases in phase C during the fault. In phase-A, there is a huge decrease in the voltage during the fault.

From Figure 6.37 to Figure 6.54, it can be seen that when the fault is applied at phase A, there are little variations at the other phases during the fault. If the voltage waveform of phase-A is observed, it can be seen that there is more prominent decreases in the voltage of the buses.

6.2.3 Fault at Bus-2

Single phase fault is applied at bus-2 on phase-A. The following results are obtained.

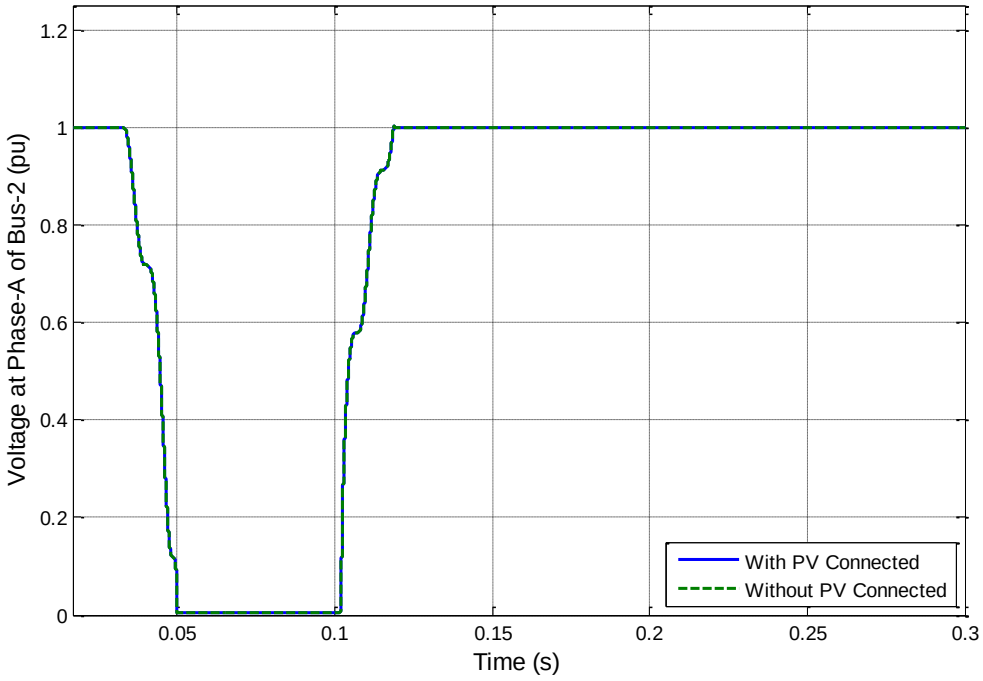

Figure 6.55: Voltage at Phase-A of Bus-2 when a Single-phase fault occurs at Phase-A of Bus-2

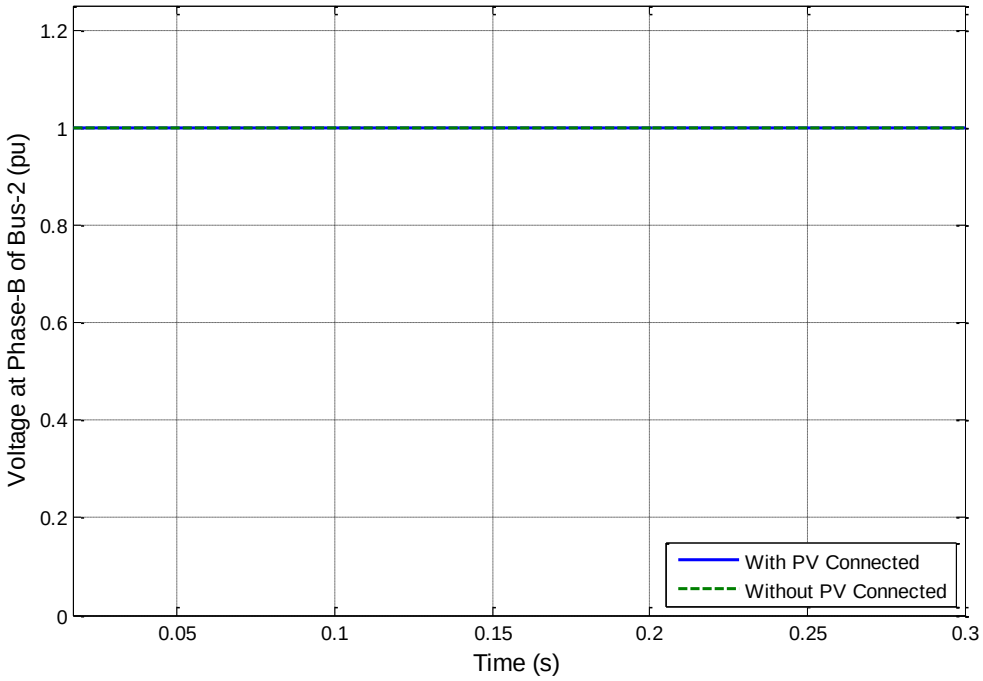

Figure 6.56: Voltage at Phase-B of Bus-2 when a Single-phase fault occurs at Phase-A of Bus-2

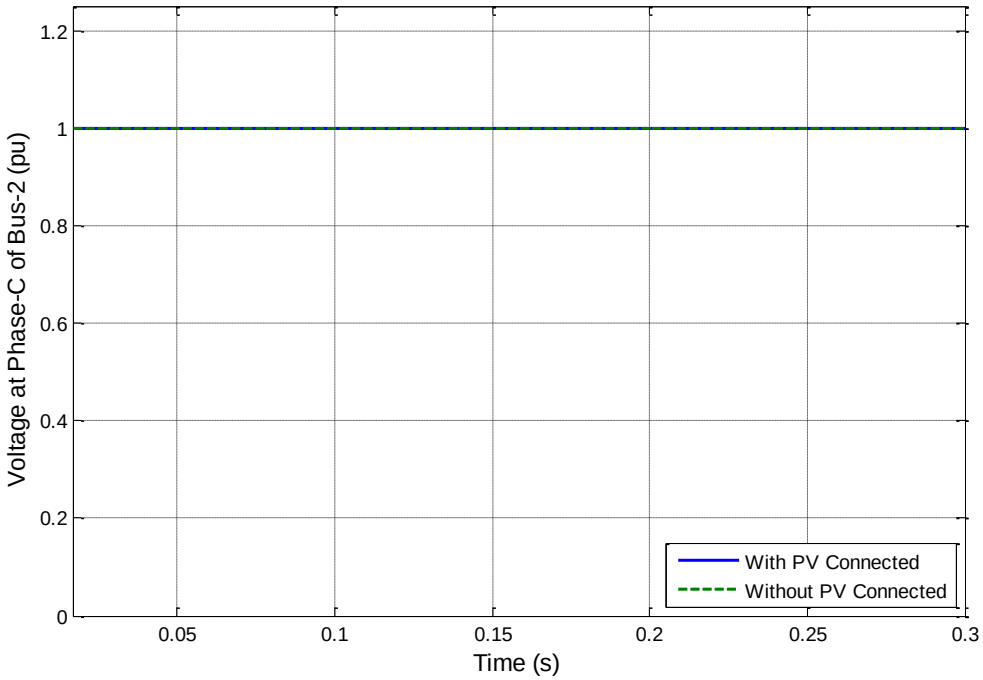

Figure 6.57: Voltage at Phase-C of Bus-2 when a Single-phase fault occurs at Phase-A of Bus-2

From Figure 6.55 to Figure 6.57, it can be noticed that at bus-2, there are almost no variation of voltage in any of the phases B or C although the fault occurs at phase A of bus-2. At phase-A, voltage becomes zero during the fault.

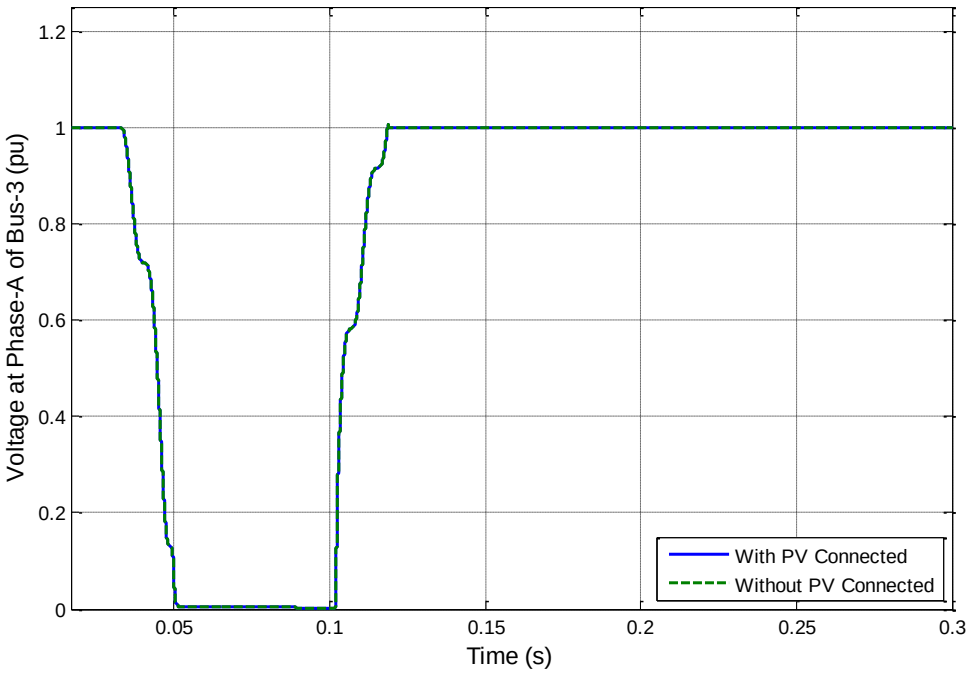

Figure 6.58: Voltage at Phase-A of Bus-3 when a Single-phase fault occurs at Phase-A of Bus-2

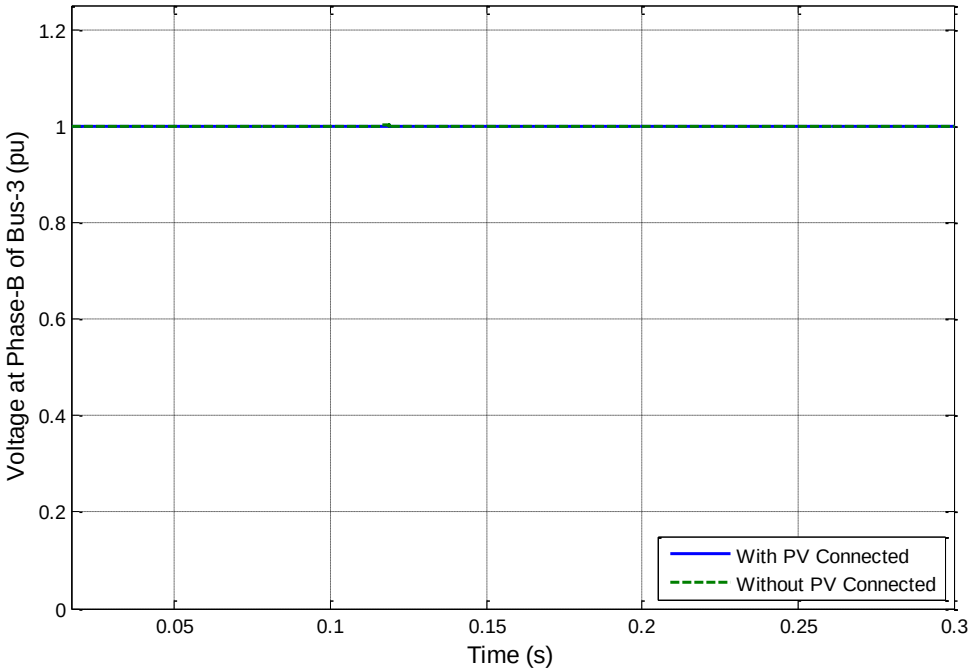

Figure 6.59: Voltage at Phase-B of Bus-3 when a Single-phase fault occurs at Phase-A of Bus-2

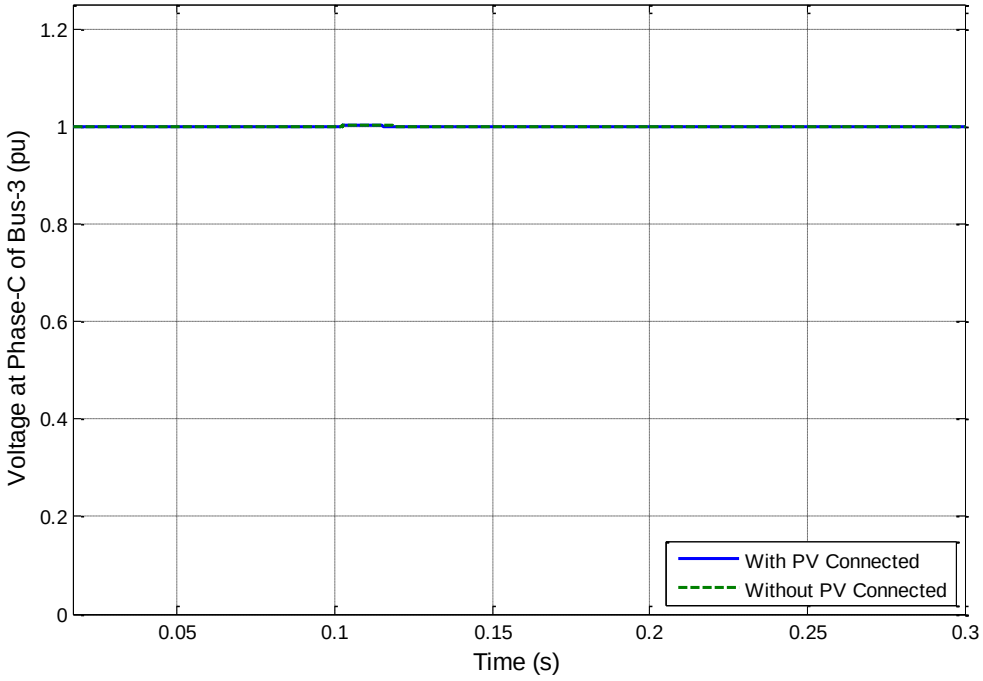

Figure 6.60: Voltage at Phase-C of Bus-3 when a Single-phase fault occurs at Phase-A of Bus-2

From Figure 6.58 to Figure 6.60, it can be noticed that voltage in phase B & C is not affected much, but the voltage at phase-A decreases drastically, as the fault occurs at phase-A.

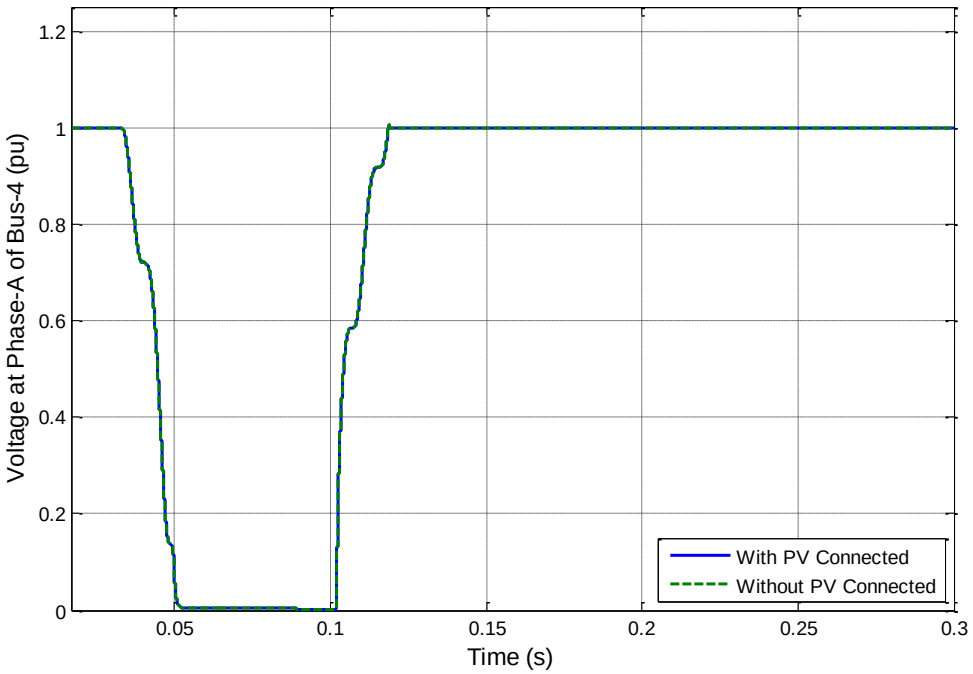

Figure 6.61: Voltage at Phase-A of Bus-4 when a Single-phase fault occurs at Phase-A of Bus-2

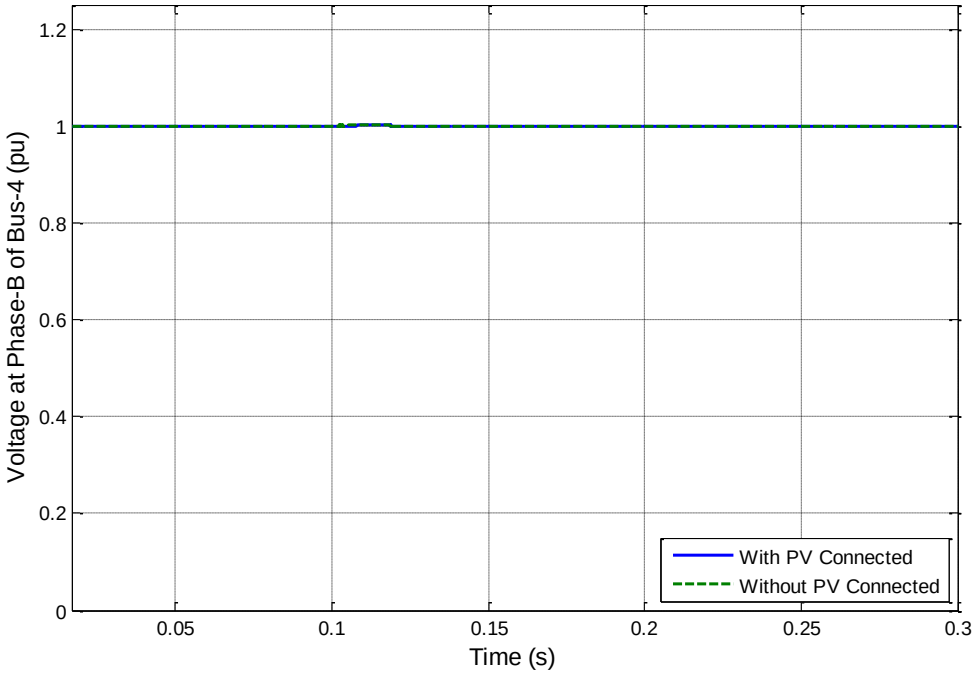

Figure 6.62: Voltage at Phase-B of Bus-4 when a Single-phase fault occurs at Phase-A of Bus-2

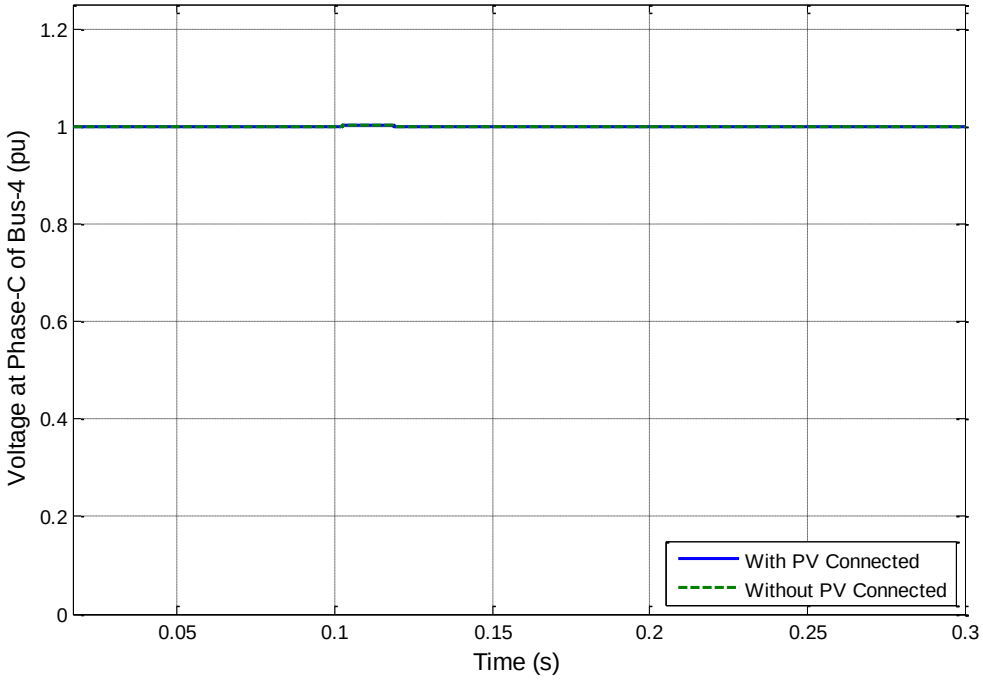

Figure 6.63: Voltage at Phase-C of Bus-4 when a Single-phase fault occurs at Phase-A of Bus-2

From Figure 6.61 to Figure 6.63, it can be noticed that voltage in phase B & C is not affected, but the voltage at phase-A decreases drastically, as the fault occurs at phase-A.

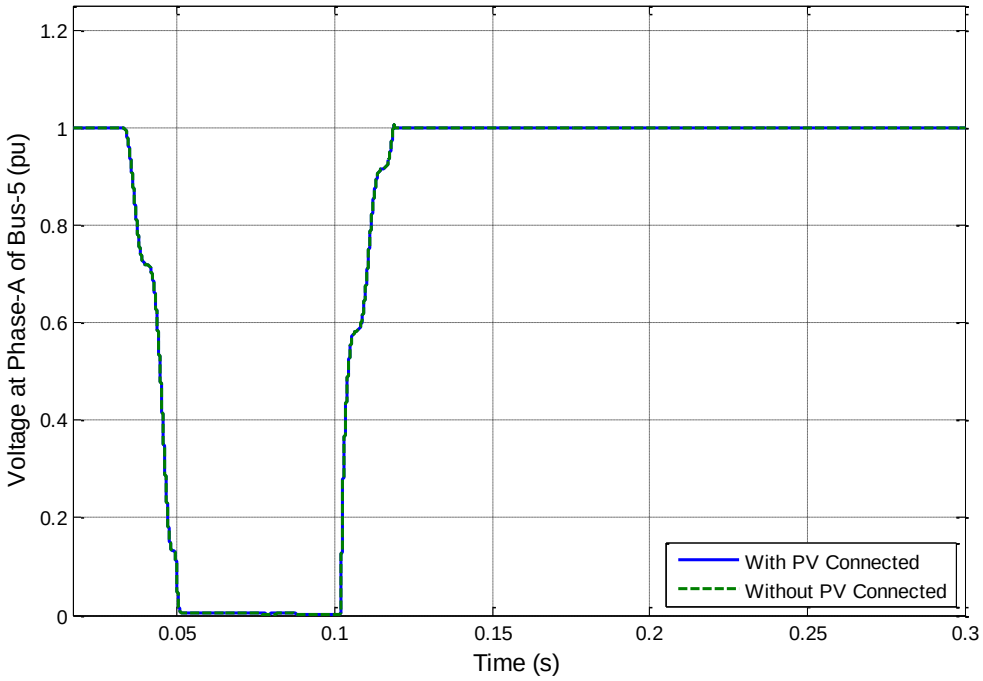

Figure 6.64: Voltage at Phase-A of Bus-5 when a Single-phase fault occurs at Phase-A of Bus-2

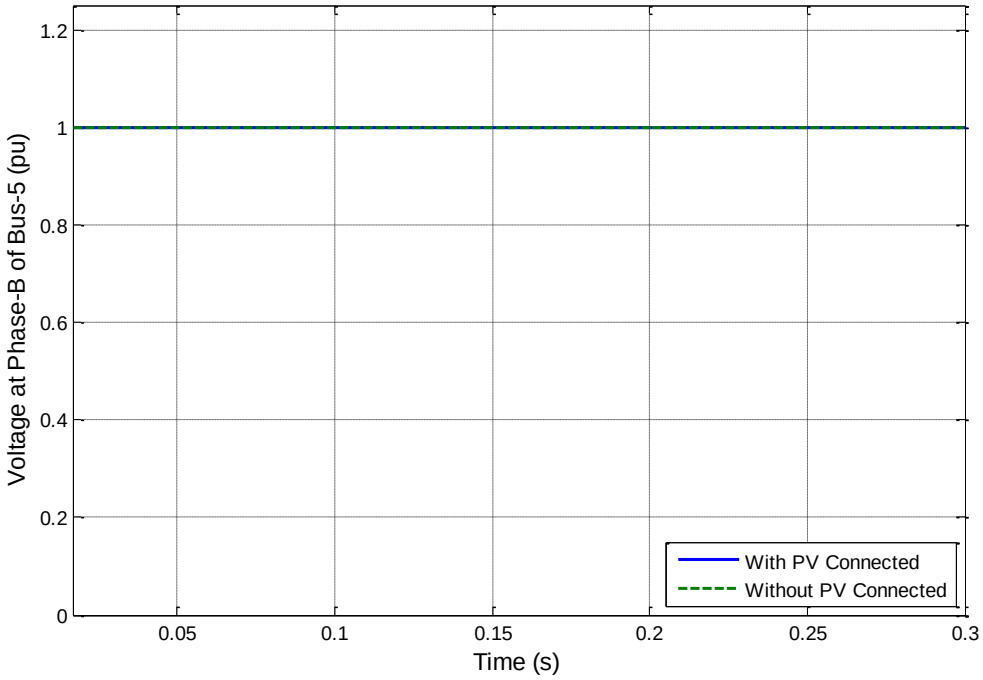

Figure 6.65: Voltage at Phase-B of Bus-5 when a Single-phase fault occurs at Phase-A of Bus-2

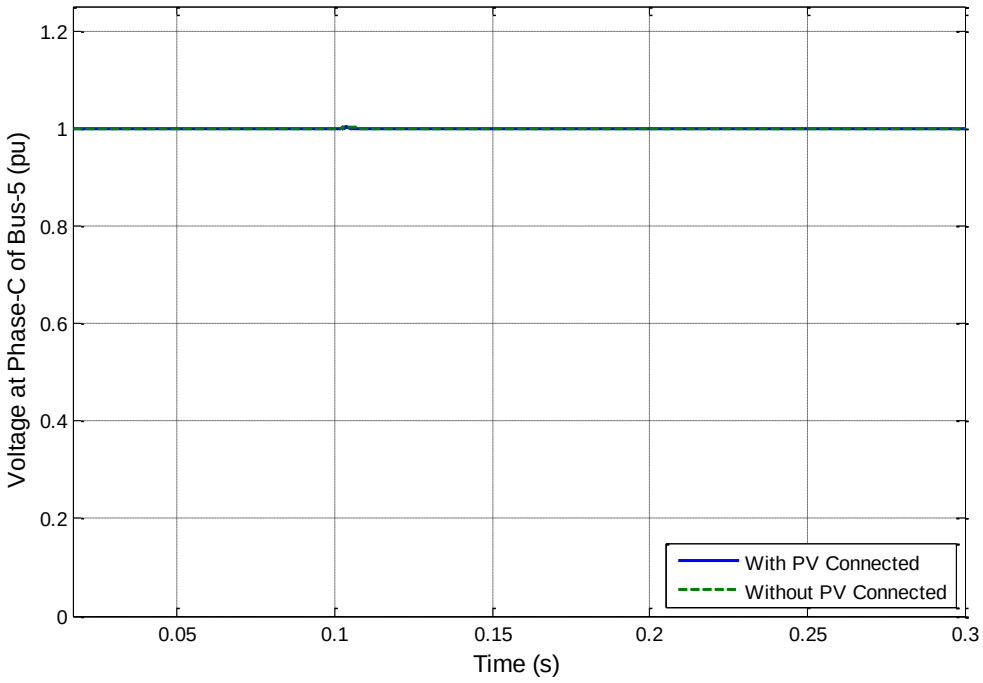

Figure 6.66: Voltage at Phase-C of Bus-5 when a Single-phase fault occurs at Phase-A of Bus-2

From Figure 6.64 to Figure 6.66, it can be noticed that at bus-5, there are almost no variations of voltage in phase B or C, but a prominent decrease of voltage of phase-A as the fault occurs at phase A of bus-2.

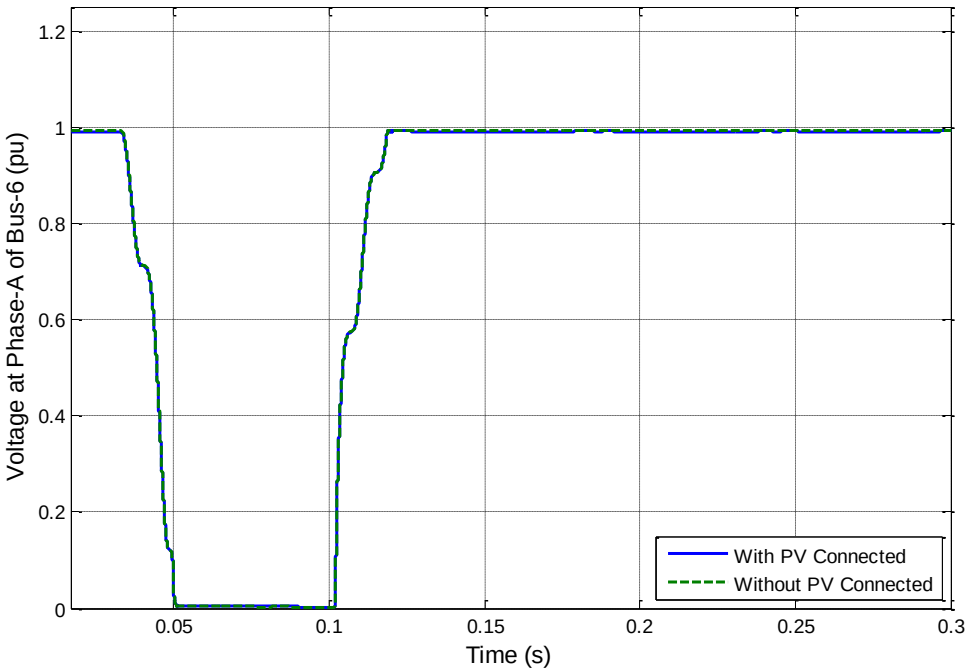

Figure 6.67: Voltage at Phase-A of Bus-6 when a Single-phase fault occurs at Phase-A of Bus-2

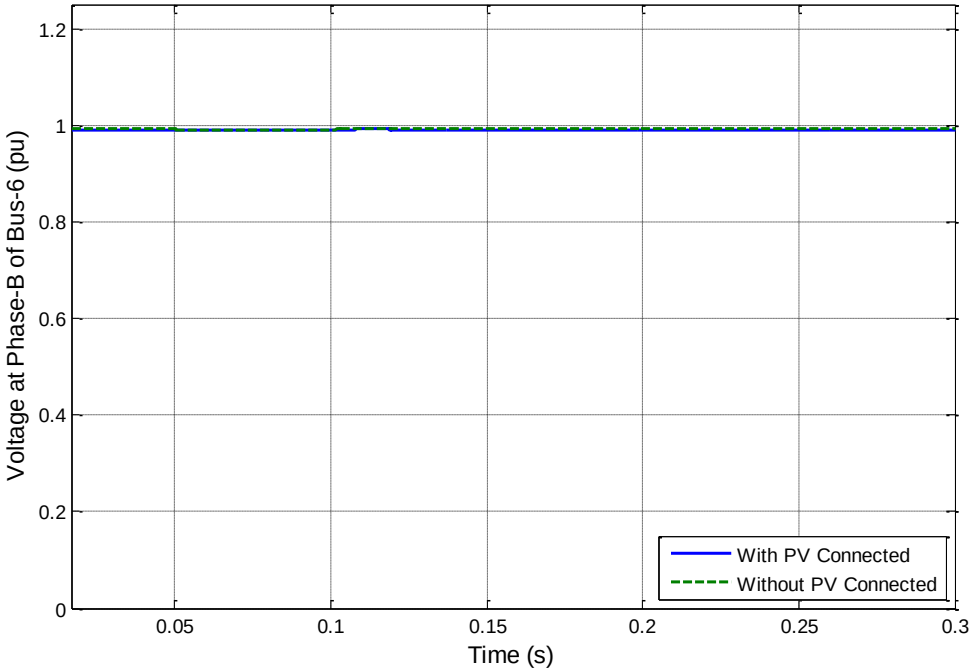

Figure 6.68: Voltage at Phase-B of Bus-6 when a Single-phase fault occurs at Phase-A of Bus-2

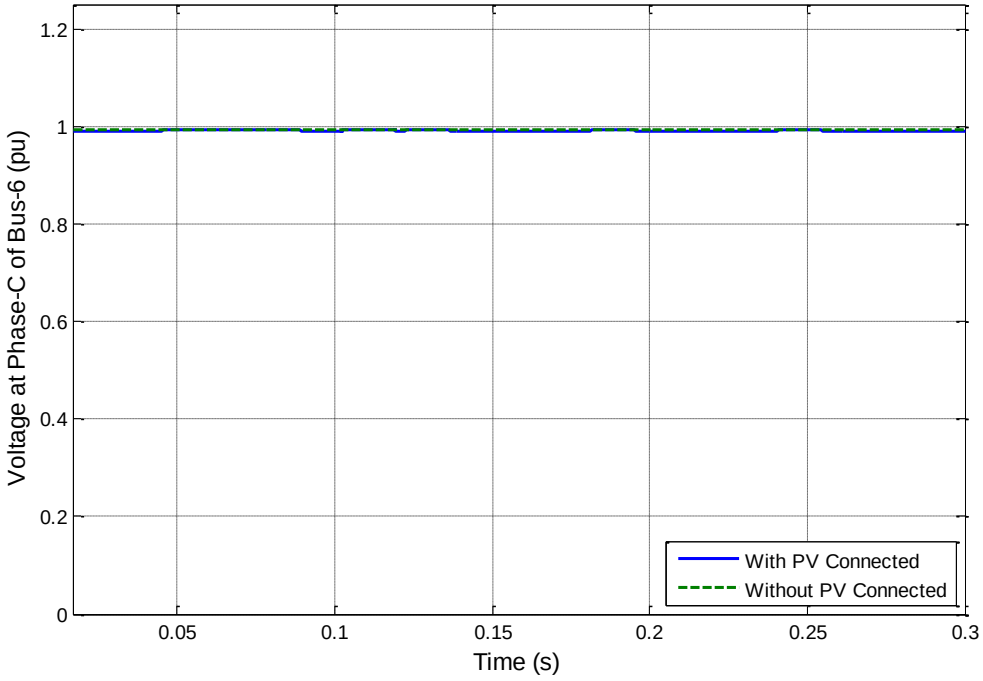

Figure 6.69: Voltage at Phase-C of Bus-6 when a Single-phase fault occurs at Phase-A of Bus-2

From Figure 6.67 to Figure 6.69, it can be noticed that at bus-6, there are slight variations of voltage in phase B or C when the fault occurs at phase A of bus-2. The voltage at phase-A decreases drastically as the fault occurs at phase-A.

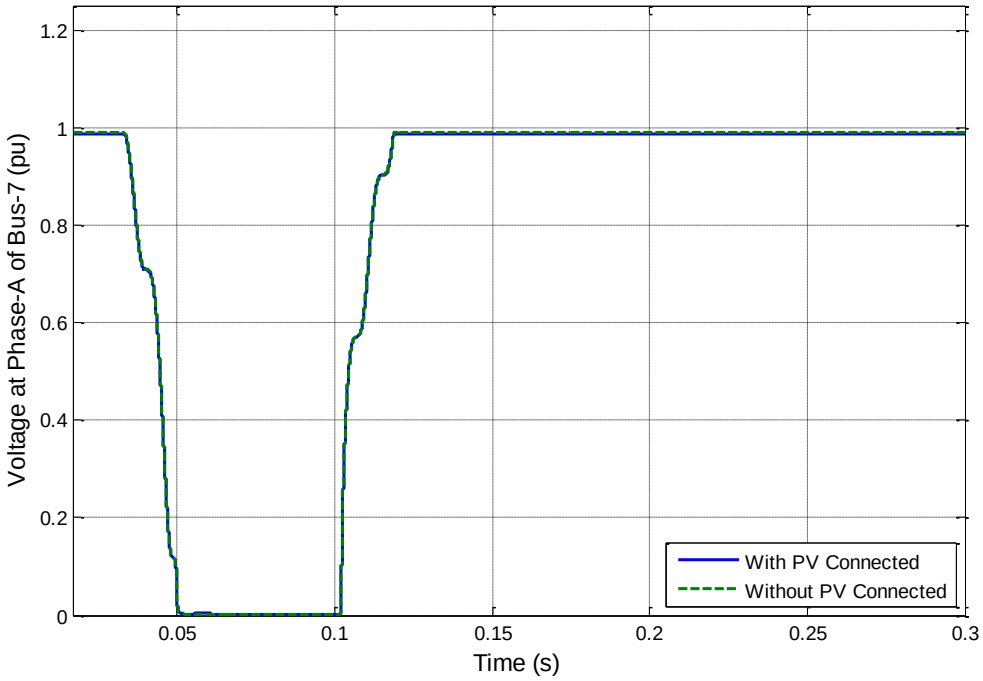

Figure 6.70: Voltage at Phase-A of Bus-7 when a Single-phase fault occurs at Phase-A of Bus-2

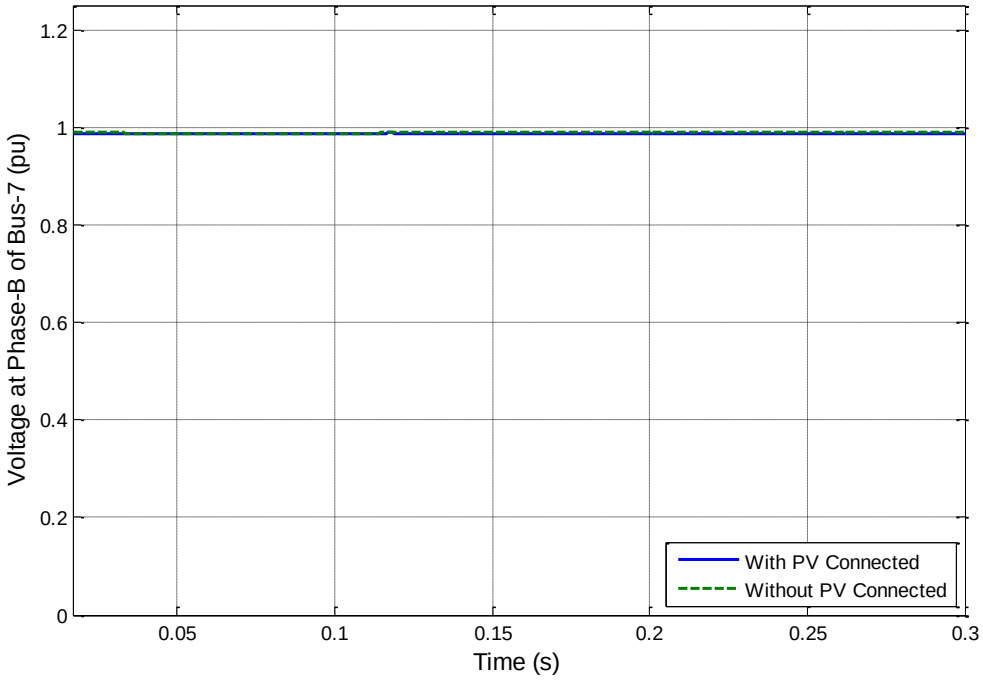

Figure 6.71: Voltage at Phase-B of Bus-7 when a Single-phase fault occurs at Phase-A of Bus-2

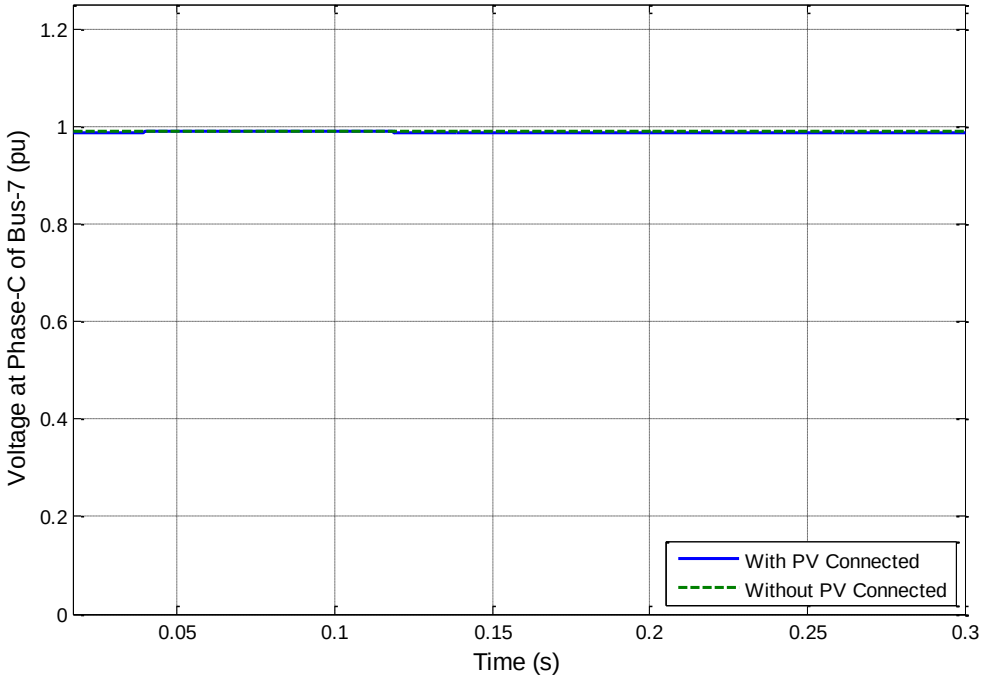

Figure 6.72: Voltage at Phase-C of Bus-7 when a Single-phase fault occurs at Phase-A of Bus-2

From Figure 6.70 to Figure 6.72, it can be noticed that at bus-7, there are a few variations of voltage in phase B or C when the fault occurs at phase A of bus-2. There is a significant voltage drop in phase-A, as the fault occurs at phase-A. In the case when PV is connected, in some cases, some amount of voltage exists at phase-A.

The topology of the Microgrid is such that bus-2 becomes the connecting bus between the generator bus and the other buses. Therefore when a single phase fault is applied at phase-A of bus-2, the voltage at phase-A of all the buses went to zero, but there is negligible effect on other phases. The effect of connecting PV during the fault is that there was still some voltage during the fault in some of the scenarios. This was due to the PV power injection at bus-7.

CHAPTER 7

7.1 Conclusion

From the analysis, the following conclusions are obtained:

- Three voltage control methodologies have been proposed to control the voltage viz. Switch based voltage control and Solar Tracker based voltage control method.
- The solar tracker based voltage control method involving a PI controller gave much better results than the switch based voltage control method.
- A detailed fault analysis has been carried out. The effects of fault occurrence at different buses have been studied. It was noticeable that if a fault occurs at bus-2 then it may cause severe crisis for the entire system owing to its location in between the generator and the entire system.

7.2 Future Work

Owing to the interesting results obtained in this thesis, the following future works are proposed.

- Wind generating system can also be added on one of its buses to see the effect on different buses. The control method proposed in this work can be extended to control voltage at a new PCC of wind.
- Reactive power control can be achieved by controlling the inverter firing angles besides its usual task of synchronizing the PV system with the grid.

APPENDIX

Simulink Models

The Photovoltaic-System

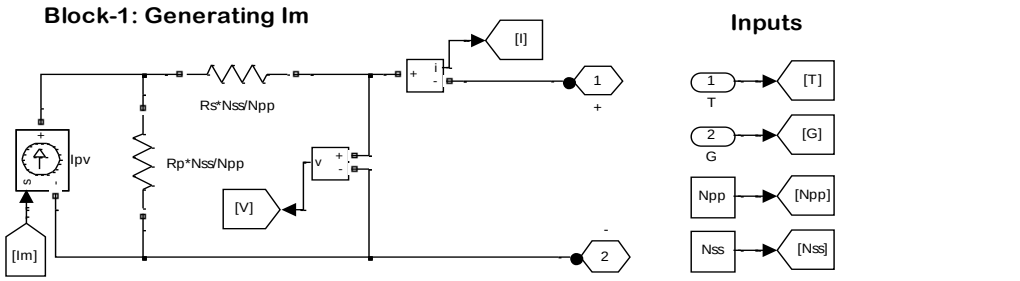

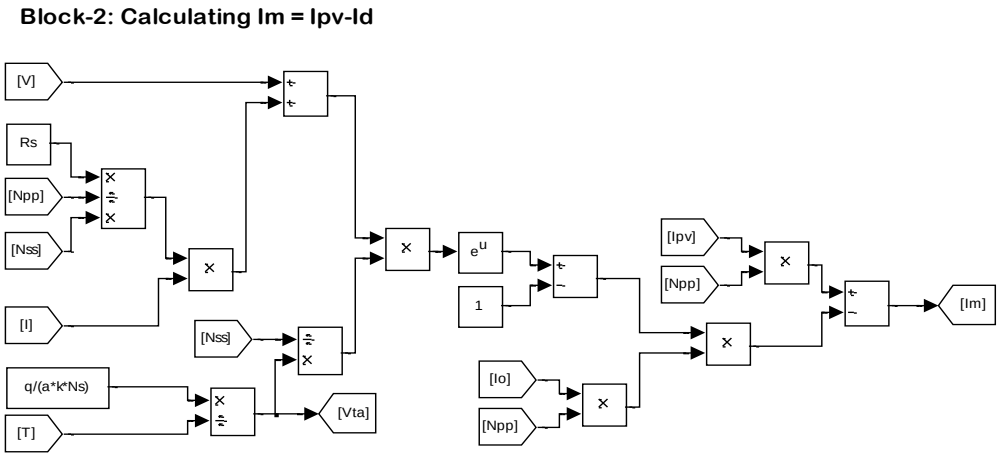

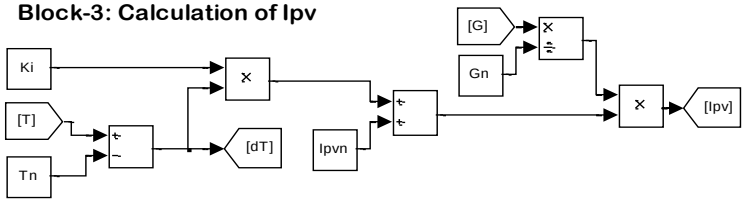

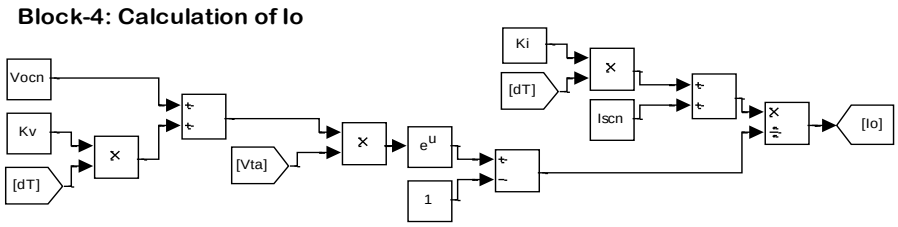

The PV Generation System Block

Block-1: In this block, the PV current is calculated. The block shows the circuit diagram of practical PV cell. The current generated by PV and the diode combination $I_m = I_{pv} - I_d$ is used in the circuit.

Block-2: The generated PV current of the array I_{pv} $\left(N_{ss} \times N_{pp}\right)$ and the diode current I_d are calculated in this block. The corresponding equations of I_{pv} & I_d are:

$$I_{pv} = \left(I_{pv,n} + K_I \Delta T\right) \frac{G}{G_n} \quad (0.1)$$

$$I_d = I_0 \left[e^{\left(\frac{V + R_S I}{V_t a}\right)} - 1 \right] \quad (0.2)$$

Blocks 3 & 4: These blocks calculate the array I_{pv} (for single cell) and I_o. The current I_0 is the diode current given by:

$$I_0 = I_{0,n} \left(\frac{T_n}{T}\right)^3 e^{\left[\frac{qE_g}{ak}\left(\frac{1}{T_n} - \frac{1}{T}\right)\right]} \quad (0.3)$$

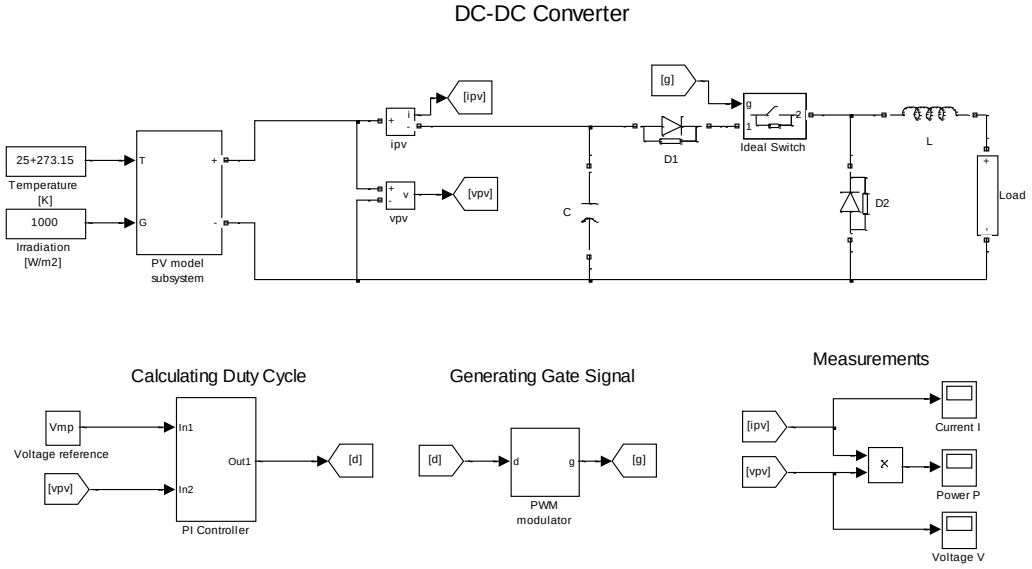

DC-Link of the PV Generating System

Grid Synchronization of PV

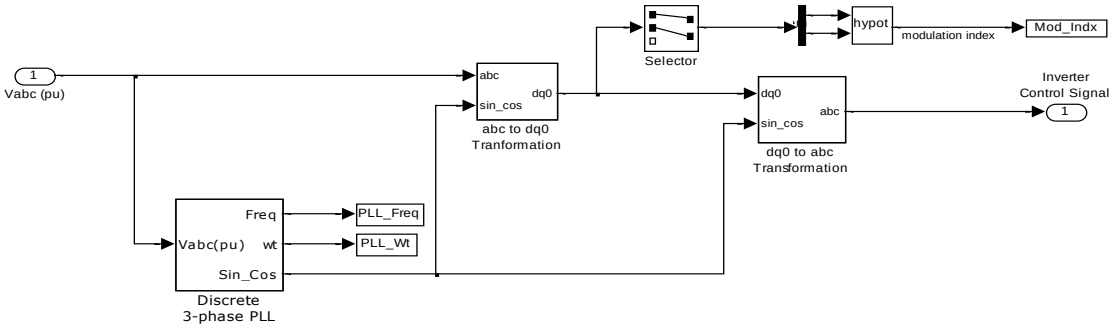

Subsystem for Inverter Synchronization with the Grid

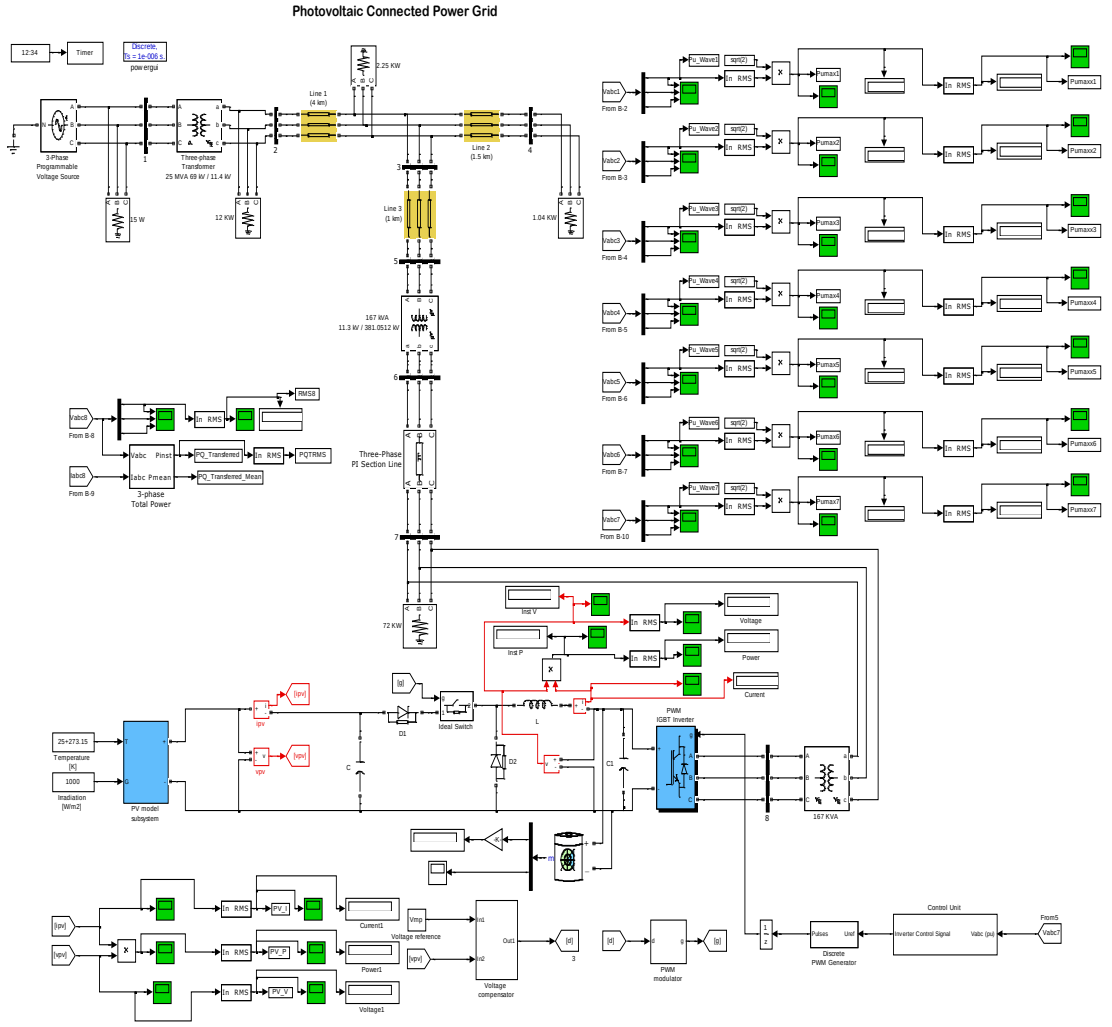

The PV Connected Grid System

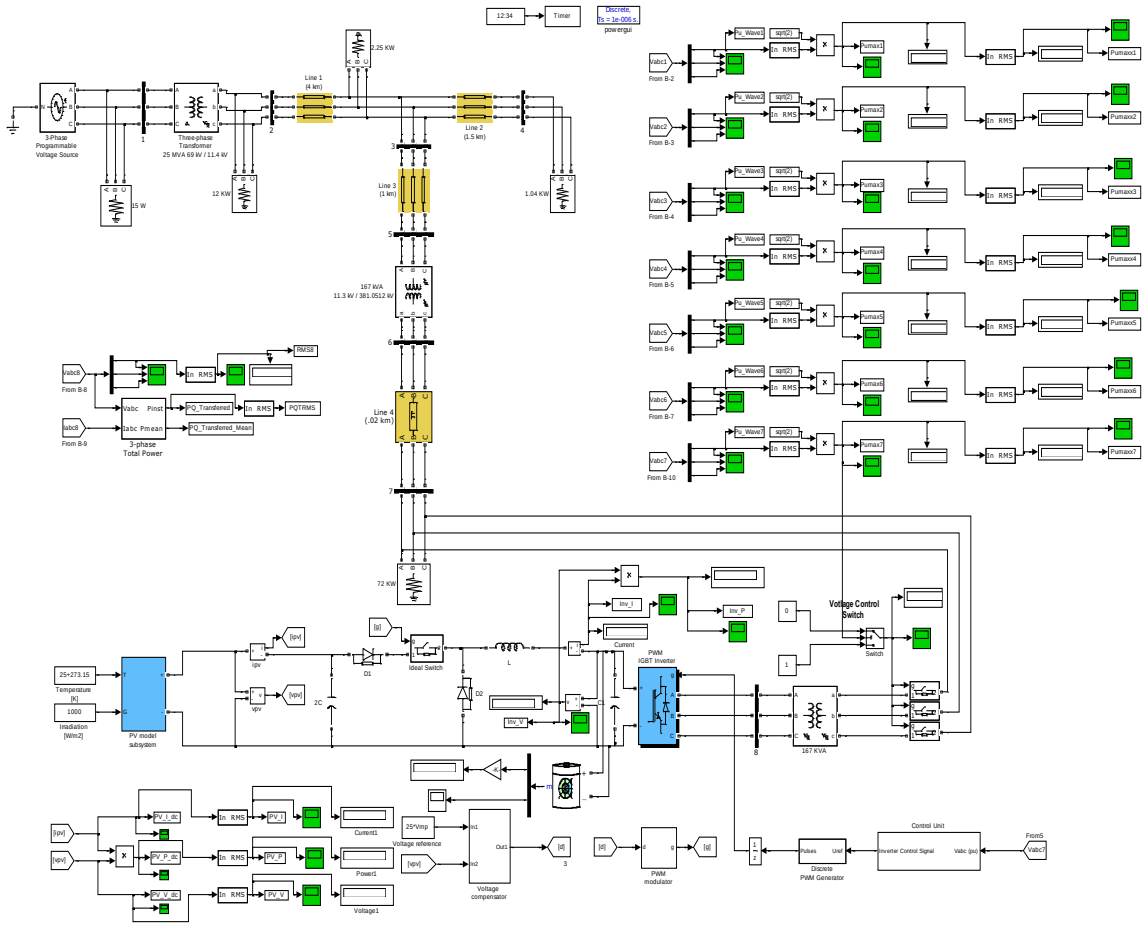

The PV Connected Power Grid Model employing Switch Based Voltage Control

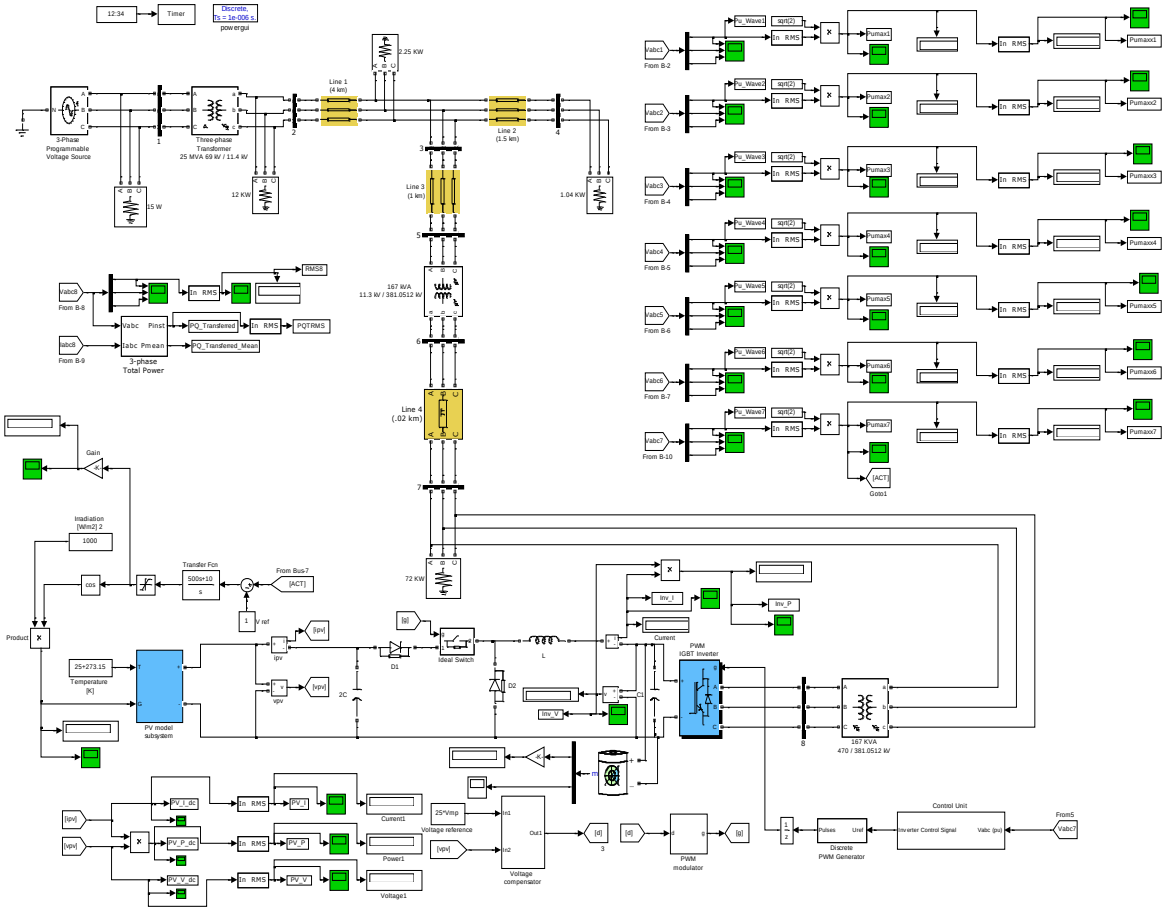

The PV Connected Grid System with Solar Tracker Voltage Control Method

System Parameters

Transformer data summary

Transformer	S (KVA)	X/R	Rated V	R_1 (Ω)	R_2 (Ω)	L_1 (Ω)	L_2 (Ω)
T1	25000	20	3Ø, 69kV/11.4kV	0.866	0.0242	0.047	0.00128
T2	167	5	3Ø, 11.4kV/381.05V	1.103	0.0146	0.0123	1.636 x 10^{-6}

Line impedance summary

Impedance	Type	Length (KM)	Rated V	R(Ω/KM)	X(Ω/KM)
Z1	3C500XP2	4	11.4KV	0.1075	0.1437
Z2	3C500XP2	1.5	11.4KV	0.1075	0.1437
Z3	3C#1XP2	1	11.4KV	0.5426	0.1896
Z4	3C#1XP2	0.02	220V	0.3325	0.0977

Load data Summary

Load	L1	L2	L3	L4
Peak load (KVA)	12.94	2.5	1.16	75
Light load (KVA)	4	1.37	0.63	15

REFERENCES

[1] M. Shahid Ali, "Photovoltaic Systems Modeling and Analysis," MS, Electrical Engineering, King Fahd University of Petroleum and Minerals, Dhahran, Kingdom of Saudi Arabia, 2010.

[2] G. J. R. Villalva M. G., Filho E. R., "Comprehensive Approach to Modeling and Simulation of Photovoltaic Arrays," *Power Electronics, IEEE Transactions on*, vol. 24, pp. 1198-1208, 2009.

[3] C.-S. T. Huan-Liang Tsai, Yi-Jie Su, "Development of Generalized Photovoltaic Model Using MATLAB / SIMULINK," *Proceedings of the World Congress on Engineering and Computer Science, WCECS 2008*, pp. 0-5, October 22 - 24 2008.

[4] G. J. R. Villalva M. G., Filho E. R., "Modeling and circuit-based simulation of photovoltaic arrays," in *Power Electronics Conference, 2009. COBEP '09. Brazilian*, 2009, pp. 1244-1254.

[5] PVeducation.org. (2012). *Solar Radiation on a Tilted Surface*. Available: http://pvcdrom.pveducation.org/SUNLIGHT/MODTILT.HTM

[6] S. J. Smita Shrivastava, R.K. Nema, "Distributed Generation: Technical Aspects of Interconnection," *International Journal on Emerging Technologies*, pp. 1(1): 37-40(2010), 2010.

[7] B. K. a. R. DeBlasio, "Technologies for the New Millennium: Photovoltaics as a Distributed Resource," *IEEE Power Engineering Society (PES) Summer Meeting Seattle, Washington*, 2000.

[8] Y.-K. C. Wu, Ching-Shan; Huang, Yi-Shuo; and Lee, Ching-Yin, "Advanced Analysis of Clustered Photovoltaic System's Performance Based on the Battery-

Integrated Voltage Control Algorithm," *International Journal of Emerging Electric Power Systems*, vol. 10, 2009.

[9] J. H. R. Enslin and P. J. M. Heskes, "Harmonic interaction between a large number of distributed power inverters and the distribution network," *IEEE Transactions on Power Electronics*, vol. 19, pp. 1586-1593, 2004.

[10] D. J. L. Fei Wang, Hendrix M. A. M., Ribeiro P. F., "Modeling and Analysis of Grid Harmonic Distortion Impact of Aggregated DG Inverters," *Power Electronics, IEEE Transactions on*, vol. 26, pp. 786-797, 2011.

[11] B. B. M. Heidenreich, "Impact of Large Photovoltaic Penetration on the Quality of the Supply: A Case Study at the Photovoltaic Noise Barrier in Austria," *19th European Photovoltaic Solar Energy Conference Exhibition and Exhibition*, 2005.

[12] G. L. Canova A., Spertino F., Tartaglia M., "Electrical Impact of Photovoltaic Plant in Distributed Network," in *Industry Applications Conference, 2007. 42nd IAS Annual Meeting. Conference Record of the 2007 IEEE*, 2007, pp. 1450-1455.

[13] G. G. Favuzza S., Spertino F., Vitale G., "Comparison of power quality impact of different photovoltaic inverters: the viewpoint of the grid," in *Industrial Technology, 2004. IEEE ICIT '04. 2004 IEEE International Conference on*, 2004, pp. 542-547 Vol. 1.

[14] A. Girgis and S. Brahma, "Effect of distributed generation on protective device coordination in distribution system," in *Power Engineering, 2001. LESCOPE '01. 2001 Large Engineering Systems Conference on*, 2001, pp. 115-119.

[15] T. O. Y.Ueda, K.Kurokawa, T.Itou2, K.Kitamura, Y.Miyamoto, M.Yokota, H.Sugihara, S.Nishikawa, "Detailed Performance Analysis Results of Grid-Connected Clustered PV Systems in Japan - First 200 System Results of Demonstrative Research on Clustered PV Systems," 2005.

[16] K. K. Ueda Y., Tanabe T., Kitamura K., Sugihara H., "Analysis Results of Output Power Loss Due to the Grid Voltage Rise in Grid-Connected Photovoltaic Power Generation Systems," *Industrial Electronics, IEEE Transactions on*, vol. 55, pp. 2744-2751, 2008.

[17] J. Bratt, "Grid Connected PV Inverters: Modeling and Simulation," Master of Science, Electrical Engineering, San Diego State University, 2011.

[18] K. V. K. R. R. Kiranmayi, M. Vijay Kumar, "Modeling and a MPPT method for Solar Cells," *Journal for Engineering and Applied Sciences*, pp. 128-133, 2008.

[19] S. E. Evju, "Fundamentals of Grid Connected Photo-Voltaic Power Electronic Converter Design," Master of Science in Energy and Environment, Department of Electrical Power Engineering, Norwegian University of Science and Technology, 2007.

[20] C. M. F. Santos, "Optimized Photovoltaic Solar Charger With Voltage Maximum Power Point Tracking," Instituto Superior Tecnico, Universidade Technica de Lisboa, 2008.

[21] F. Hassan and R. Critchley, "A robust PLL for grid interactive voltage source converters," in *Power Electronics and Motion Control Conference (EPE/PEMC), 2010 14th International*, 2010, pp. T2-29-T2-35.

[22] A.-A. O. A. Anani N., Ponnapalli P., Al-Araji S. R., Al-Qutayri M. A., "Synchronization of a single-phase photovoltaic generator with the grid," in *EUROCON - International Conference on Computer as a Tool (EUROCON), 2011 IEEE*, 2011, pp. 1-4.

[23] Y. T. Fujita H., Akagi H., "A hybrid active filter for damping of harmonic resonance in industrial power systems," *Power Electronics, IEEE Transactions on*, vol. 15, pp. 215-222, 2000.

[24] D. Fewson, *Introduction to Power Electronics*: Essential Electronics Series, 1998.

[25] T. T. Chuong, "Distributed Generation Impact on Voltage Stability in Distribution Networks," *GMSARN International Conference on Sustainable Development: Issues and Prospects for the GMS*, 12-14 Nov 2008.

[26] J. C. M. Abeyasekera T., Atkinson D. J., Armstrong M., "Suppression of line voltage related distortion in current controlled grid connected inverters," *IEEE Transactions on Power Electronics*, vol. 20, pp. 1393-1401, 2005.

[27] S. S. W. Mack Grady, "Understanding Power System Harmonics," *IEEE Power Engineering Review*, vol. 21, pp. 8-11, 2001.

[28] B. K. P. Yih-huei Wan, "Factors Relevant to Utility Integration of Intermittent Renewable Technologies," National Renewable Energy Laboratory, Colorado1993.

[29] A. O. Zue, Chandra, A., "Simulation and stability analysis of a 100 kW grid connected LCL photovoltaic inverter for industry," in *Power Engineering Society General Meeting, 2006. IEEE*, 2006, p. 6 pp.

Vitae

Name	:	**Mohammed Khaleel Ahmed**
Nationality	:	Indian
Education	:	**M.S.** (Electrical Engineering, Major: Power Systems), King Fahd University of Petroleum and Minerals, Dhahran, Saudi Arabia. **B.E.** (Electrical Engineering), Muffakham Jah College of Engineering and Technology, Osmania University, Hyderabad, India.
Experience	:	**Research Assistant,** 2 Years 3 Months King Fahd University of Petroleum and Minerals, Dhahran, Saudi Arabia. **Associate Software Engineer,** 1 Year Accenture Services Private Ltd., Hyderabad, India.
Contact	:	+966-590776504, +91-9963379750 mdkhaleel.ahmed86@gmail.com mka_mj@yahoo.com